

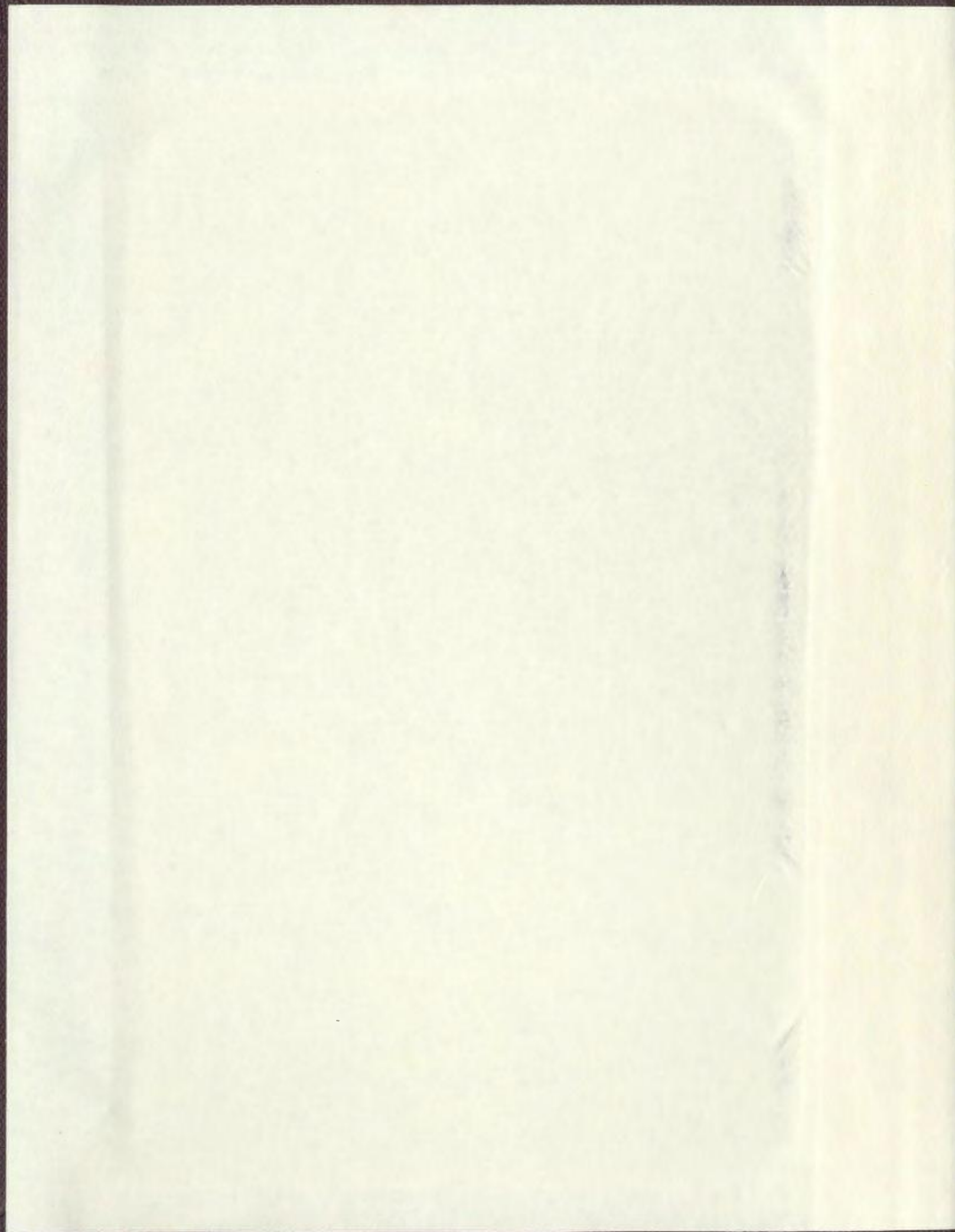
THE PROVENANCE OF LOWER TERTIARY SANDS
FROM THE LABRADOR SHELF

CENTRE FOR NEWFOUNDLAND STUDIES

**TOTAL OF 10 PAGES ONLY
MAY BE XEROXED**

(Without Author's Permission)

JEANNE LOUISE MILLS





National Library
of Canada

Bibliothèque nationale
du Canada

Canadian Theses Service

Service des thèses canadiennes

Ottawa, Canada
K1A 0N4

NOTICE

The quality of this microform is heavily dependent upon the quality of the original thesis submitted for microfilming. Every effort has been made to ensure the highest quality of reproduction possible.

If pages are missing, contact the university which granted the degree.

Some pages may have indistinct print especially if the original pages were typed with a poor typewriter ribbon or if the university sent us an inferior photocopy.

Reproduction in full or in part of this microform is governed by the Canadian Copyright Act, R.S.C. 1970, c. C-30, and subsequent amendments.

AVIS

La qualité de cette microforme dépend grandement de la qualité de la thèse soumise au microfilmage. Nous avons tout fait pour assurer une qualité supérieure de reproduction.

S'il manque des pages, veuillez communiquer avec l'université qui a conféré le grade.

La qualité d'impression de certaines pages peut laisser à désirer, surtout si les pages originales ont été dactylographiées à l'aide d'un ruban usé ou si l'université nous a fait parvenir une photocopie de qualité inférieure.

La reproduction, même partielle, de cette microforme est soumise à la Loi canadienne sur le droit d'auteur, SRC 1970, c. C-30, et ses amendements subséquents.

THE PROVENANCE OF LOWER TERTIARY SANDS
FROM THE LABRADOR SHELF

BY

C JEANNE LOUISE MILLS

A thesis submitted to the School of Graduate
Studies in partial fulfillment of the
requirements for the degree of
Master of Science

Department of Earth Sciences
Memorial University of Newfoundland

December 1991

St. John's

Newfoundland



National Library
of Canada

Bibliothèque nationale
du Canada

Canadian Theses Service Service des thèses canadiennes

Ottawa, Canada
K1A 0N4

The author has granted an irrevocable non-exclusive licence allowing the National Library of Canada to reproduce, loan, distribute or sell copies of his/her thesis by any means and in any form or format, making this thesis available to interested persons.

The author retains ownership of the copyright in his/her thesis. Neither the thesis nor substantial extracts from it may be printed or otherwise reproduced without his/her permission.

L'auteur a accordé une licence irrévocable et non exclusive permettant à la Bibliothèque nationale du Canada de reproduire, prêter, distribuer ou vendre des copies de sa thèse de quelque manière et sous quelque forme que ce soit pour mettre des exemplaires de cette thèse à la disposition des personnes intéressées.

L'auteur conserve la propriété du droit d'auteur qui protège sa thèse. Ni la thèse ni des extraits substantiels de celle-ci ne doivent être imprimés ou autrement reproduits sans son autorisation.

ISBN 0-315-73365-9

Canada

ABSTRACT

The Mesozoic-Cenozoic sedimentary sequence under the Labrador continental shelf is a sand-shale sequence that records the evolution of the Labrador Sea from the rift stage, through the active sea floor spreading stage to the deep-ocean circulation stage. The sediment prism is thick, ranging from 10,000 to 15,000m and contains several sand units that have been targets for petroleum exploration.

Seven of the 31 wells drilled in the Labrador Sea were chosen for this study. Samples of the Paleocene-age Gudrid sand of the Cartwright Formation and Eocene-age Leif sand of the Kenamu Formation were examined.

Study of 37 light fraction grain mounts indicates that the sands are subarkoses and arkoses with middle- to upper-rank metamorphic rocks as dominant sediment sources. Heavy mineral analysis of 55 samples reveals a dominance of those minerals associated with metamorphosed acid plutonic rocks.

Correspondence analysis of the heavy mineral data set generated in this study demonstrates some profound differences in the sands. The Paleocene-age sands are

defined by four factors: (1) Amphibole factor, (2) Kyanite factor, (3) Zircon-Rutile factor, and (4) Epidote factor. The Eocene-age sands are defined by the Staurolite-Garnet-Tourmaline factor. The differences between the groupings of samples is thought to be suggestive of differences in sediment source. The variability in the Paleocene samples likely represents sediment derived from local areas proximal to the site of deposition, while the similarities between the Eocene samples indicate sediment mixing and homogenization.

The principal source rocks for the Tertiary sands from the Labrador Shelf were amphibolite facies metamorphic rocks (particularly kyanite-, garnet-, and hornblende-rich schists and/or gneisses) and acid plutonics (particularly granites and/or granitic gneisses). Basic intrusive rocks were minor contributors. Pre-existing sedimentary rocks and/or paragneisses were present as local sources.

ACKNOWLEDGEMENTS

I would like to thank the former Aquitaine Company of Canada, and its successor Canterra Energy Limited, for allowing this study to be made, and providing the necessary funding, and Dr. N.J. McMillan, now of the Geological Survey of Canada, for initiating this project. Many thanks to Dr. R.N. Hiscott for his advise and constructive criticism throughout this project.

I would also like to take this opportunity to thank the Baffin-Labrador Group (Canterra Energy Limited, Dome Petroleum Limited, Home Oil Limited, Murphy Oil Limited, PanCanadian Petroleum Limited, Petro-Canada, Soquip) and the Labrador Group (Petro-Canada, AGIP Canada Limited, Amerada Minerals Corporation of Canada Limited, Canterra Energy Limited, Gulf Canada Resources Incorporated, Ranchmen's Resources (1976) Limited, Suncor Incorporated) for making available the samples used in this study.

My sincere gratitude goes to Roberta Ellis, a most careful and conscientious laboratory assistant who spent many long hours in sample preparation and Michael Marchand

of Husky Oil (formerly of Canterra Energy Limited) for introducing me to correspondence analysis and assisting me with the technical aspects of that chapter.

Many thanks to Karen Graham and Scott Stoyles of Lomalta Petroleums Ltd.; Karen for her patience during the typing of this manuscript, and Scott for his comments and constructive criticism during the final stages of this project.

A very special thanks goes to Dr. A. Aksu of Memorial University of Newfoundland whose intervention and assistance was fundamental to the completion of this thesis.

TABLE OF CONTENTS

| | page |
|---|------|
| ABSTRACT | ii |
| ACKNOWLEDGEMENTS | iv |
| TABLE OF CONTENTS | vi |
| LIST OF TABLES | ix |
| LIST OF FIGURES | x |
| LIST OF PLATES | xi |
| Chapter 1 INTRODUCTION | |
| 1.1 Purpose | 4 |
| 1.2 Data Source | 5 |
| Chapter 2 REGIONAL GEOLOGY | |
| 2.1 Introduction | 6 |
| 2.2 REGIONAL GEOLOGY: ONSHORE | |
| 2.2.1 Physiography | 6 |
| 2.2.2 Regional Geology | 7 |
| 2.2.3 Precambrian Stratigraphy and Lithology | 8 |
| 2.2.3.1 Nain Province | 10 |
| 2.2.3.2 Makkovik Subprovince | 11 |
| 2.2.3.3 Grenville Province | 12 |
| 2.2.3.4 Churchill Province | 13 |
| 2.2.3.5 Superior Province | 15 |
| 2.2.4 Paleozoic Stratigraphy and Lithology | 15 |
| 2.2.5 Mesozoic and Cenozoic Stratigraphy and Lithology | 17 |
| 2.3 REGIONAL GEOLOGY: OFFSHORE | |
| 2.3.1 Introduction | 19 |
| 2.3.2 Previous Work | 19 |
| 2.3.3 Basement Structure and Morphology | 21 |
| 2.3.4 Stratigraphy and Lithology | 26 |
| 2.3.5 Syn-rift Megasequence | 28 |
| 2.3.5.1 Alexis Formation | 28 |
| 2.3.5.2 Bjarni Formation | 30 |
| 2.3.5.3 Freydis Member | 31 |
| 2.3.6 Drift-Phase Megasequence | 32 |
| 2.3.6.1 Markland Formation | 32 |
| 2.3.6.2 Gudrid Members | 33 |

| | | |
|--|---|----|
| 2.3.6.3 | Lower Gudrid Member | 34 |
| 2.3.6.4 | Cartwright Formation | 35 |
| 2.3.6.5 | Middle Gudrid Member | 36 |
| 2.3.6.6 | Upper Gudrid Member | 37 |
| 2.3.6.7 | Kenamu Formation | 38 |
| 2.3.7 | Post-Rift Megasequence | 41 |
| 2.3.7.1 | Mokami Formation | 41 |
| 2.3.7.2 | Saglek Formation | 42 |
| 2.3.8 | Tectonic Evolution of the Labrador Sea | 43 |
| 2.3.9 | Development of Drainage | 49 |
| Chapter 3 LIGHT FRACTION ANALYSIS | | |
| 3.1 | Introduction | 56 |
| 3.2 | Methodology | 56 |
| 3.2.1 | Laboratory Techniques | 56 |
| 3.2.2 | Apparatus | 57 |
| 3.2.3 | Petrographic Procedures | 58 |
| 3.3 | Results | 60 |
| 3.4 | Characteristics of the Light Fraction | 65 |
| 3.4.1 | Quartz | 65 |
| 3.4.2 | Feldspar | 66 |
| 3.4.3 | Rock Fragments | 66 |
| Chapter 4 HEAVY MINERAL ANALYSIS | | |
| 4.1 | Introduction | 68 |
| 4.2 | Choice of Grain Size | 70 |
| 4.3 | Methodology | 71 |
| 4.3.1 | Laboratory Techniques | 72 |
| 4.3.2 | Apparatus | 72 |
| 4.3.3 | Petrographic Procedures | 72 |
| 4.4 | Results | 73 |
| 4.5 | Mineralogical Characteristics of the Major Heavy Minerals | 76 |
| 4.5.1 | Non-Opaque, Non-Micaceous, Non-Diagenetic Minerals | 76 |
| 4.5.1.1 | Amphibole Group | 76 |
| 4.5.1.2 | Barite | 77 |
| 4.5.1.3 | Epidote Group | 77 |
| 4.5.1.4 | Garnet Group | 78 |
| 4.5.1.5 | Kyanite | 79 |
| 4.5.1.6 | Pyroxene Group | 81 |
| 4.5.1.7 | Rutile | 81 |
| 4.5.1.8 | Staurolite | 82 |
| 4.5.1.9 | Tourmaline | 82 |
| 4.5.1.10 | Zircon | 83 |

| | |
|---|-----|
| 4.5.2 Opaque, Micaceous, Authigenic Minerals | 84 |
| 4.5.2.1 Opaque Minerals | 84 |
| 4.5.2.2 Micaceous Minerals | 84 |
| 4.5.2.3 Authigenic Minerals | 85 |
| Chapter 5 Correspondence Analysis | |
| 5.1 Introduction | 140 |
| 5.2 Interpreting the Results of Correspondence Analysis | 142 |
| Chapter 6 PROVENANCE | |
| 6.1 Introduction | 150 |
| 6.2 Mineralogy | 150 |
| 6.3 Correspondence Analysis | 153 |
| 6.3.1 Amphibole Factor | 157 |
| 6.3.2 Kyanite Factor | 158 |
| 6.3.3 Zircon-Rutile Factor | 158 |
| 6.3.4 Epidote Factor | 160 |
| 6.3.5 Garnet-Staurolite-Tourmaline Factor | 161 |
| 6.4 Discussion | 163 |
| 6.4.1 Paleocene Sands | 166 |
| 6.4.1.1 Karlsefni | 167 |
| 6.4.1.2 Skolp | 167 |
| 6.4.1.3 Snorri | 167 |
| 6.4.1.4 Gudrid | 167 |
| 6.4.1.5 Cartier | 169 |
| 6.4.1.6 Leif | 169 |
| 6.4.1.7 Freydis | 170 |
| 6.4.2 Eocene | 171 |
| 6.4.2.1 Karlsefni | 172 |
| 6.4.2.2 Skolp | 172 |
| 6.4.2.3 Snorri | 173 |
| 6.4.2.4 Gudrid | 173 |
| 6.4.2.5 Cartier | 173 |
| 6.4.2.6 Leif | 174 |
| 6.4.2.7 Freydis | 174 |
| Chapter 7 Conclusions | 177 |
| References | 180 |
| Appendices | |
| Appendix 1: Laboratory Techniques | 192 |
| (1) heavy mineral separation | 192 |
| (2) cleaning heavy liquid | 193 |
| (3) iron oxide stain removal | 194 |
| Appendix 2: Weights of Magnetic Fractions | 195 |

LIST OF TABLES

- Table 2.1 Table of Formations.
- Table 3.1 Results of Light Fraction Analysis.
- Table 4.1 The Provenance of some Common Heavy Minerals.
- Table 4.2 Results of Heavy Mineral Grain Counting.
- Table 5.1 Correspondence analysis on the entire heavy mineral suite with the percentage of the total variance explained.
- Table 5.2 Correspondence analysis on the major heavy mineral suite with the percentage of the total variance explained.
- Table 5.3 Correspondence analysis on the major heavy minerals, excluding amphibole and pyroxene, with the percentage of the total variance explained.

LIST OF FIGURES

- Figure 1.1 Study area and wells sampled.
- Figure 2.1 Structural Provinces of Labrador, Baffin Island and Greenland.
- Figure 2.2 Onshore occurrences of Paleozoic, Mesozoic and Cenozoic rocks.
- Figure 2.3 Diagrammatic cross-section of the Labrador Shelf.
- Figure 2.4 Tectonic elements of the Labrador and southeast Baffin Island shelves.
- Figure 2.5 Cretaceous drainage of North America.
- Figure 2.6 Tertiary drainage of North America.
- Figure 3.1 Classification of the samples studied.
- Figure 3.2 Four variable plot showing the nature of the quartz population in the samples studied.
- Figure 5.1 Paleocene and Eocene Correspondence Analysis of the entire heavy mineral suite.
- Figure 5.2 Paleocene and Eocene Correspondence showing the close association of amphibole and pyroxene.
- Figure 5.3 Paleocene and Eocene Correspondence Analysis of the major heavy mineral suite.
- Figure 5.4 Paleocene and Eocene Correspondence Analysis of the major heavy mineral suite, excluding amphibole and pyroxene.
- Figure 6.1 Paleocene heavy mineral provinces.
- Figure 6.2 Eocene heavy mineral provinces.
- Figure 6.3 Summary of geology and metamorphic facies of Labrador.
- Figure 6.4 Isopach of Cartwright and Kenamu Formations.

LIST OF PLATES

- Plate 4.1: Green to brown pleochroic hornblende with "ragged" terminations.
- Plate 4.2: Typical hornblende exhibiting green to brown-green pleochroic schemes.
- Plate 4.3: Green to green-brown pleochroic hornblende with striations.
- Plate 4.4: Barite, well-rounded with carbonaceous inclusions.
- Plate 4.5: Epidote (var. pistachite), irregular, angular grain.
- Plate 4.6: Epidote (var. pistachite), sub-equant, prismatic grain with "hackly" appearance.
- Plate 4.7: Epidote (var. pistachite), typical barrel-shaped prismatic grain.
- Plate 4.8: Bipyramidal, prismatic epidote.
- Plate 4.9: Epidote showing surface etching.
- Plate 4.10: Sub-prismatic epidote with prominent striations.
- Plate 4.11: Epidote (var. Zoisite), yellow-grey to yellow-brown, sub-angular, sub-prismatic grain.
- Plate 4.12: Ultrablue interference colours of non-ferroan zoisite.
- Plate 4.13: Clinozoisite.
- Plate 4.14: Colourless garnet with conchoidal fracture.
- Plate 4.15: Colourless garnet with "hackly" appearance.
- Plate 4.16: Salmon-pink garnet, elongate, with prominent conchoidal fracture.

- Plate 4.17: Sub-angular, sub-equant salmon-pink garnet.
- Plate 4.18: Red-brown, sub-angular garnet.
- Plate 4.19: Garnet with "hackly" surface texture.
- Plate 4.20: Garnet with "hackly" to "toothed" surface texture.
- Plate 4.21: Embayed, colourless garnet.
- Plate 4.22: Elongate, prismatic, colourless kyanite with right-angle parting.
- Plate 4.23: Kyanite (as Plate 4.22), exhibiting more prominent parting.
- Plate 4.24: Elongate, sub-prismatic, colourless kyanite with prominent parting.
- Plate 4.25: Elongate, sub-prismatic kyanite with abundant carbonaceous inclusions.
- Plate 4.26: Kyanite with abundant carbonaceous material giving the grain a dusty appearance .
- Plate 4.27: Pyroxene (var. augite).
- Plate 4.28: Pyroxene (var. orthopyroxene), sub-equant, sub-angular grain showing the pink of a pink to green pleochroic colour scheme.
- Plate 4.29: Dark yellow-brown, prismatic rutile showing zoning.
- Plate 4.30: Dark red-brown, elongate, angular, fragmented rutile.
- Plate 4.31: Genuiculate rutile twins.
- Plate 4.32: Prismatic staurolite with "swiss cheese-like" texture.
- Plate 4.33: Typical, irregular staurolite grain.
- Plate 4.34: Staurolite without inclusions.

- Plate 4.35: Typical yellow-brown staurolite.
- Plate 4.36: Prismatic, pink to dark blue tourmaline.
- Plate 4.37: Colourless to green and blue pleochroic tourmaline.
- Plate 4.38: Pale pink to green-brown tourmaline.
- Plate 4.39: Pale yellow to yellow-brown tourmaline.
- Plate 4.40: Well rounded tourmaline with pale yellow to yellow-brown and green-brown colours.
- Plate 4.41: Cross-sectional tourmaline.
- Plate 4.42: Well rounded cross-sectional tourmaline.
- Plate 4.43: Tourmaline with over-growths.
- Plate 4.44: Angular zircon with randomly distributed inclusions.
- Plate 4.45: Prismatic zircon with rutile needles and zoning.
- Plate 4.46: Zircon. Enlarged view of Plate 4.45.
- Plate 4.47: Sub-rounded, prismatic zircon with zoning.
- Plate 4.48: Angular, prismatic zircon with zoning.
- Plate 4.49: Euhedral zoned (alternating metamict and unaltered bands) zircon.
- Plate 4.50: Metamict zircon.
- Plate 4.51: Broken prismatic zircon showing striations parallel to the C-axis.
- Plate 4.52: Broken euhedral zircon with striations parallel to the grain edge.
- Plate 4.53: Colourless angular zircon, devoid of inclusions.

CHAPTER 1

INTRODUCTION

The Labrador Sea is a tectonically depressed basin bounded to the west and east by once continuous Precambrian land masses. The basin is floored by deeply subsided oceanic crust, rimmed by a narrow zone of faulted and extended cratonic basement (the cratonic monocline of Balkwill, 1987; Balkwill et al., 1990). The Cenozoic and Mesozoic sediments deposited in the Labrador Basin comprise a terrace prism on the cratonic monocline and a thick blanket on the deep ocean floor. The Lower Tertiary portion of the sediment wedge on the cratonic monocline is the focus of this study.

The clastic sediments of the margin of the Labrador Basin can be divided into three sequences: the lower Cretaceous and lower Upper Cretaceous syn-rift sediments deposited in fault-bounded structures of the cratonic monocline; the Upper Cretaceous to Upper Eocene sequence deposited during active sea floor spreading; and

the Oligocene to Quaternary sequence deposited after the cessation of ocean floor spreading. The syn-rift sedimentary sequence was the subject of a previous provenance study (Higgs, 1977). The provenance of the Paleocene and Eocene sands of the active sea floor spreading sequence is the subject of the present study.

Work in the Labrador Sea began in the mid-1960's with reconnaissance seismic surveys across the continental margin. Recognition of a large sediment prism prompted exploration drilling activity. The first well was spudded in 1971 (Leif E-38) and, to 1990, 31 exploratory wells have been drilled and a regional seismic grid of some 80,000 kilometres of multi-channel seismic has been acquired (Balkwill et al., 1990). Seven wells have been chosen for the current study (Fig. 1.1).

Petrographic and provenance studies are integral parts of basin analysis. The mineralogy, textural maturity and diagenetic history of the sediment package determine the presence and characteristics of hydrocarbon reservoirs. Heavy and light mineral analyses aid in identifying sandstone provenance, source areas, drainage patterns, approximate distance and direction of sediment transport. They also help to delineate hydrocarbon fairways and indirectly provide some indication of the type(s) of organic matter that can be expected in the

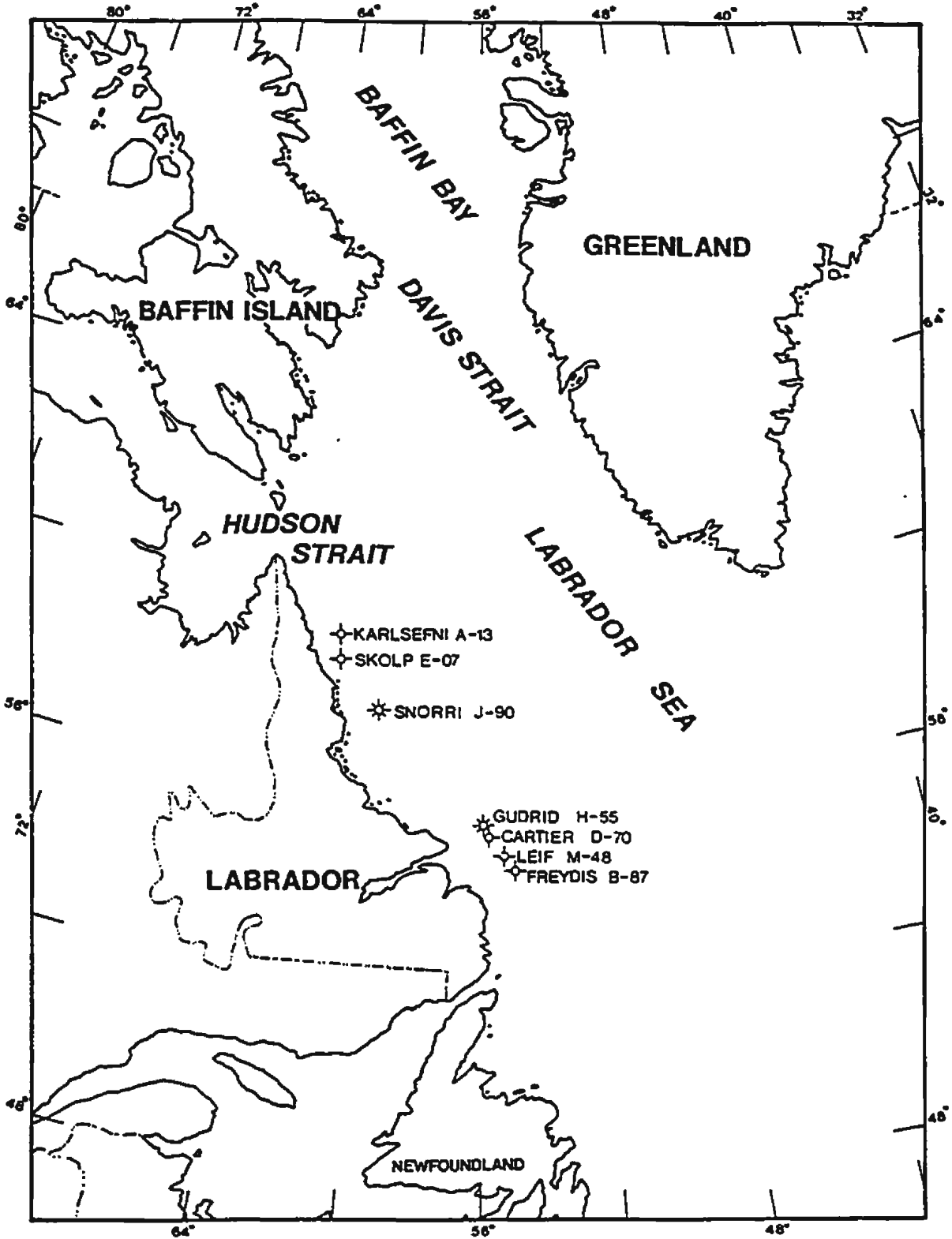


FIGURE 1.1 Study area and wells sampled

basin. With these applications in mind, this thesis describes heavy and light mineral assemblages of selected Lower Tertiary sandstones from the Labrador Shelf.

1.1 Purpose

The purpose of this study is to determine the provenance of the Lower Tertiary sands, particularly the Eocene-age Leif sand and Paleocene-age Gudrid sand, of the Labrador Shelf. Definition of sediment source areas and the delineation of heavy mineral provinces will be examined. To accomplish this, specific tasks needed to be undertaken:

- (1) a thorough understanding of the geography and geology of onshore and offshore areas, and the tectonic and sedimentary history of the Labrador Sea (Chapter 2),
- (2) petrographic analysis of sand samples from drill cuttings. Two techniques were used; viz., light mineral analysis, including defining sand types and potential source rocks based on quartz types (Chapter 3) and heavy mineral analysis (Chapter 4),
- (3) an unbiased, statistical analysis of the results of the heavy mineral analysis (Chapter 5).

1.2 Data Source

Analysis of drill cuttings is the primary thrust of this study. Cuttings were obtained from seven drill holes on the Labrador Shelf (Fig. 1.1). With the exception of Skolp E-07, which was completely sampled, only the Leif and Gudrid sands were sampled. In all, a total of 55 samples were selected for analysis.

Samples for the present study were selected from sand intervals dated micropaleontologically by Eastcan Exploration Ltd. (1975a, 1975b, 1976a, 1976b, 1976c, 1978c) and Total Eastcan Ltd. (1980).

The availability of drill cuttings for sampling was variable and sample quality for some wells was poor because of extensive caving from the poorly indurated upper Tertiary sediments. The samples used in this study were obtained from the Atlantic Geoscience Centre storage. These samples were dry and required special steps in sample treatment before mineral separations could be done (see Appendix 1: Sample Treatment).

CHAPTER 2

REGIONAL GEOLOGY

2.1 Introduction

Because of the nature of this study, an understanding of the regional onshore geology is required so that conclusions concerning source rock areas can be made. A comprehensive understanding of the tectonic evolution and sedimentary history of the Labrador Shelf is also necessary.

This chapter is composed of two main parts: regional onshore geology and regional offshore geology. The development of drainage in Tertiary-age eastern Canada is also discussed with implications for offshore sedimentary deposition outlined.

2.2 REGIONAL GEOLOGY: ONSHORE

2.2.1 Physiography

The Labrador Sea and Baffin Bay are bounded by enormous areas of Precambrian crystalline rocks. The

coastlines of Labrador and Baffin Island form the eastern edge of a westward-tilted Tertiary erosion surface. The coast is rugged, incised by canyons and fiords. The northern coast of Labrador is mountainous with summits rising abruptly from the sea. Elevations of the uplands are 600m above sea level (south of 57 degrees N) to 1000 to 1500m above sea level (57 degrees N to 79 degrees N). The Precambrian surface was dissected by stream erosion after late Tertiary uplift (McMillan, 1973), but the physiographic development was subsequently interrupted by the onset of Pleistocene continental glaciation (Greene, 1974). At its maximum development, the Wisconsinan ice sheet is believed to have covered all of northern Labrador (the Ungava Peninsula), extending to the edge of the continental shelf (Ives, 1957; Greene, 1974).

The coasts of Labrador and southern Baffin Island (to 70 degrees N) are fringed by an array of islands, or skaegaard, (McMillan, 1973 which are rounded knobs of hard crystalline rock formed by severe glacial erosion (Embleton and King, 1971).

2.2.2 Regional Geology

The continental land masses surrounding the Labrador Sea and Baffin Bay consist primarily of Precambrian crystalline and gneissic rocks of the Canadian

and Greenland Shields. These shield areas were once a continuous land mass, sharing similar tectonic elements, lithologies and age (Bridgwater et al., 1973, Fig. 2.1). Offshore seismic reflection studies along the Labrador coast indicate an eastward prograding sedimentary wedge derived from a land source to the west. A similar sedimentary wedge has been recognized along the Greenland coast prograding westward. By Tertiary time, the width of the Labrador Sea and the presence of a mid-ocean ridge system in the central part of the basin suggest sediment input from Greenland was restricted to that continental margin. Descriptions of the regional onshore geology will therefore be confined to Labrador and Baffin Island.

2.2.3 Precambrian Stratigraphy and Lithology

Accounts of the general geology of Labrador and Baffin Island are found in Bridgwater et al. (1973), Douglas (1970), Greene (1974), Price and Douglas (1972), and Taylor (1981). From these summaries it is apparent that gneisses, chiefly granitic gneisses, are the predominant rock type of the Canadian Shield. Supracrustal rocks of both sedimentary and volcanic origins are present, lying unconformably on the older gneisses. Mafic gneisses are also present.

Labrador straddles four of the seven structural

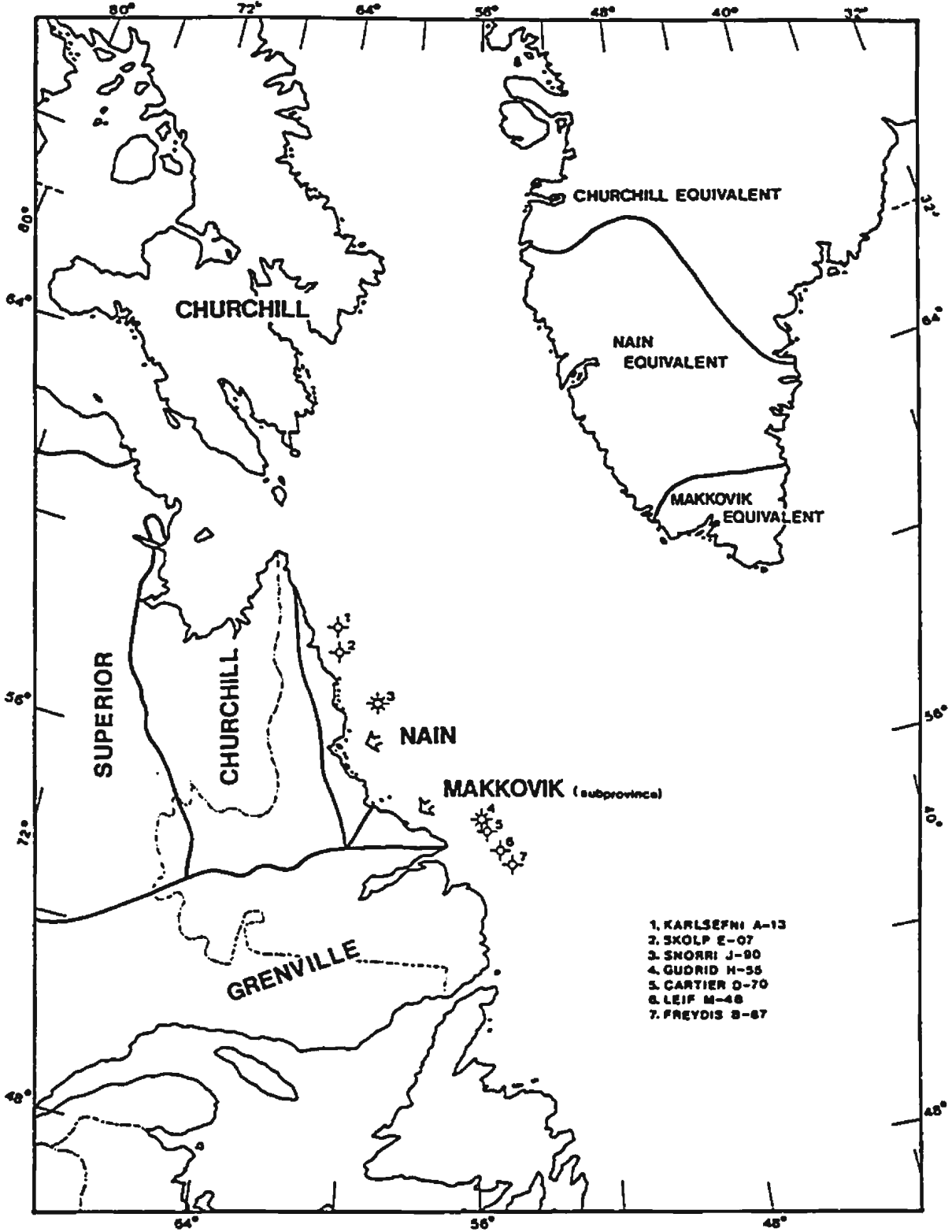


FIGURE 2.1 Structural Provinces of Labrador, Baffin Island and Greenland

provinces of the Canadian Shield (Fig. 2.1): Nain Province, Superior Province, Churchill Province and Grenville Province. The provinces are defined on the basis of age of deformation and structural grain or foliation of the rocks. With the exception of the Superior Province, each of these provinces, and the Makkovik Subprovince of the Nain Province, border the Labrador Sea and/or Baffin Bay.

2.2.3.1 Nain Province

The Nain Province, and the Makkovik Subprovince, form the coastline of much of Labrador (Fig. 2.1). Bounded to the west by an extensive mylonite zone and large adameillite and anorthosite post-tectonic plutons (Taylor, 1981), the Nain Province is mainly composed of products of the late Archean Kenoran orogeny and consists of foliated and banded granitic and granodioritic gneisses with occurrences of agmatite, migmatite and pegmatite dykes. Metasedimentary rocks occur, as do ultrabasic rocks, including peridotite, pyroxenite and amphibolite rocks.

The Archean basement rocks are unconformably overlain by supracrustal rocks of predominantly metasedimentary origins i.e. slate and argillite, with less common dolomitic sandstone, limestone, conglomerate, quartzite and greywacke (Knight and Morgan, 1977, 1981; Morgan, 1975, 1979). Diabase and amphibolite sills are

present.

Paleohelikian (Elsonian Event) anorthosite and adamellite batholiths underline much of the southern part of the Nain Province and were emplaced about 1400Ma, post-dating all orogenic activity (Taylor, 1981).

Structural trends in the Nain Province are chiefly northward. Metamorphic grade in the Archean rocks is predominantly amphibolite facies, but local granulite facies, commonly retrograded to amphibolite facies, also occurs (Taylor, 1981). The Aphebian rocks are generally greenschist facies with some rocks in the greenschist-amphibolite transitional facies.

2.2.3.2 Makkovik Subprovince

The Makkovik Subprovince lies to the southeast of the Nain Province (Fig. 2.1). Its northern boundary with the Nain is defined by the limit of significant Hudsonian deformation and the southern boundary by Grenvillian deformation (Wardle and Bailey, 1981). The subprovince is dominated by thick metamorphosed silicic tuffs, breccias, and rhyolite, with lesser amounts of metasedimentary rocks, primarily quartzites and feldspathic quartzites, with still smaller amounts of limestone, greywacke and metapelites (Taylor, 1981). This sequence lies unconformably on the Archean gneissic terrain. The unconformity was destroyed

by later Hudsonian tectonism; the structures of the basement and the supracrustal rocks are now conformable (Taylor, 1981). Extensive plutonic activity occurred in this subprovince as evidenced by the emplacement of the Big Bight Gabbro followed by the silicic Strawberry Intrusives.

Near the Grenville Front, metasedimentary gneisses are the major rock type. Olivine-bearing gabbros also occur along this boundary.

Much of the Makkovik Subprovince has been metamorphosed to greenschist facies. Style of deformation is relatively simple with structures (fold, faults and cleavage) trending northeast-southwest (Wardle and Bailey, 1981).

2.2.3.3 Grenville Province

The Grenville Province lies to the south and southwest of the Makkovik Subprovince. The boundary is a zone of retrograde metamorphism several kilometres wide in which metamorphic grade decreases northward (Stevenson, 1970). The Province is underlain primarily by gneissic granitic rocks, migmatite and large intrusive plutons in the northeast; extensive areas of paragneiss along the northern boundary; and large areas of paragneiss including quartzite, carbonate, lime-silicate rocks and rare conglomerate in the south (Taylor, 1981). These

metasedimentary gneisses grade into granitic gneiss and migmatite (Taylor, 1981).

Paleohelikian intrusive rocks belonging to the adamellite-anorthosite suite seen in the Nain Province are also present. In the Grenville, these Elsonian intrusives have been metamorphosed and tectonized during the Grenvillian Orogeny, which has altered the ages of older rocks to approximately 1000Ma.

Metamorphic grade of the Grenville Province has been summarized by Bourne (1978). Essentially, the Grenville is a terraine of predominantly high grade metamorphism. Recognizable greenschist, transitional greenschist-amphibolite and lower amphibolite rocks collectively underlie less than five percent of the province, with the remainder of the province composed of upper amphibolite facies, undivided amphibolite and granulite facies and some unmetamorphosed post-Grenvillian intrusions.

Gross structural trends in the Grenville Province are easterly in the northern part of the province and northeasterly elsewhere (Taylor, 1981).

2.2.3.4 Churchill Province

The Churchill Province lies to the west of the Nain Province and north of the Grenville Province. The

province is defined on the basis of major Hudsonian deformation. There are two major subdivisions in the Churchill Province: the western Labrador Trough, consisting of little deformed Aphebian sedimentary and volcanic rocks, lying unconformably on the rim of the Superior Province (Wardle and Bailey, 1981); and the eastern zone uniform leucocratic, garnet-rich quartzofeldspathic gneisses (Ryan, Martineau, Korstgaard and Lee, 1984). Granitoid batholiths occur in the axial zone of the province (Wardle and Bailey, 1981).

The Churchill/Nain boundary is an extensive mylonite zone in part obscured by large post-tectonic adamellite and anorthosite plutons. The western boundary with the Superior Province is a major unconformity with little deformed rocks resting on granulitic gneisses. The Churchill/Grenville boundary is marked by the Grenville Front in which the granulites of the Churchill Province exhibit retrograde metamorphism and have been converted to amphibolite facies.

The Churchill Province underlies the central portion of Labrador and all of Baffin Island. In Labrador, structural trends are dominantly northwest-southeast (Wardle and Bailey, 1981). Regional structural trends on Baffin Island are inconsistent: northwest, north, northeast and other directions are generally common (Taylor, 1981).

Metamorphic grade ranges from granulite to unmetamorphosed sedimentary rocks.

2.2.3.5 Superior Province

The Superior Province is dominated by Archean age pyroxene-bearing granulitic gneisses and acid intrusives (Greene, 1974; Fahrig, 1967; Frarey, 1961; Stockwell, 1963, 1964). As the Grenville Front is approached to the south, the Superior granulites exhibit retrograde metamorphism and have been converted to amphibolite facies. The eastern boundary of the Superior Province is a marked unconformity with the Aphebian sedimentary and volcanic rocks of the Churchill Province resting on the Superior Massif.

2.2.4 Paleozoic Stratigraphy and Lithology

Occurrences of essentially undeformed Paleozoic age rocks are found along the southeast coast of Labrador (Fig. 2.2). The Lower Cambrian sequence comprises an eastward thickening wedge of sedimentary rocks (quartz arenite, arkose, shale and limestone) with minor mafic volcanic rocks, collectively termed the Labrador Group (Schuchert and Dunbar, 1934).

As a group, these rocks lie unconformably on Grenville basement gneisses, and extend beyond the northwestern limit of Appalachian deformation. The

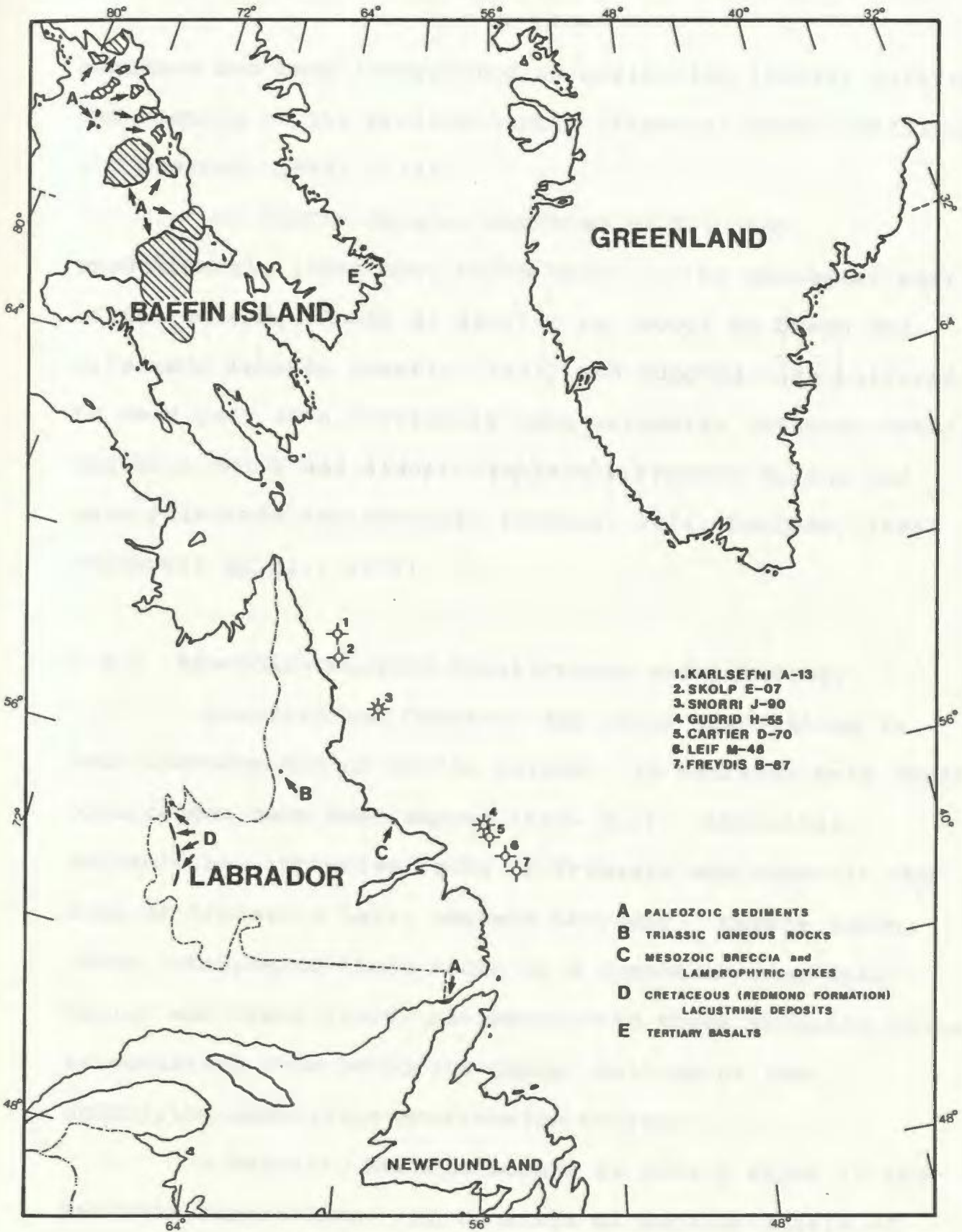


FIGURE 2.2 Onshore occurrences of Paleozoic, Mesozoic and Cenozoic rocks

sequence has been interpreted as reflecting initial rifting and opening of the proto-Atlantic (Iapetus) Ocean (Williams and Stevens, 1969; 1974).

On Baffin Island, Cambrian to Silurian, predominantly limestone, rocks occur in the southeast part of the island. Rocks of similar age occur on Devon and Ellesmere Islands (Austin, 1973) and together are believed to be a part of a previously more extensive cratonic cover sequence which was almost completely removed during the Late Paleozoic and Mesozoic (Greene, 1974; Poulsen, 1966; Stockwell et al., 1970).

2.2.5 Mesozoic-Cenozoic Stratigraphy and Lithology

Mesozoic and Cenozoic age rocks are limited in both Labrador and on Baffin Island. In Labrador only three occurrences have been mapped (Fig. 2.2). Andesitic volcanic and intrusive rocks of Triassic age occur in the area of Mistastin Lake, western Labrador. Currie (1968; 1969) interpreted these rocks as a composite ring dyke. Taylor and Dence (1969) re-interpreted these volcanic rocks as resulting from meteorite impact melting of the underlying adamellite-anorthosite terrane.

A Mesozoic breccia occurs at Ford's Bight in the Makkovik Subprovince. It consists of angular clasts of various igneous and metamorphic rocks and subrounded

quartzite clasts, and is cut by lamprophyric-carbonatite dykes (King and McMillan, 1975). These alkaline intrusives, dated at 129Ma, are similar to those in Greenland (162Ma) and northeast Newfoundland, and are thought to be related to the opening of the Labrador Sea (King and McMillan, 1975).

The Cretaceous Redmond Formation is a sequence of lacustrine clays containing Late Cretaceous plant fossils and redeposited iron formation rubble that occurs in fault-bounded depressions in the Labrador Trough, western Labrador (Blais, 1959; Fig. 2.2).

Mesozoic and Cenozoic sedimentary and volcanic rocks are preserved in several locations on Baffin Island (Fig. 2.2) and other nearby islands. Up to 3000m of Cretaceous and Tertiary marine and continental clastics (sandstones, conglomerates and shales) occur on Bylot Island and Cape Dyer (Austin, 1973; Berkhout, 1973; Beh, 1975, McMillan, 1973). An isolated outcrop of Tertiary (Paleogene) freshwater swamp or marginal marine limestone led Andrews et al. (1972) to infer a warm climate for the region during that time. This outcrop occurs at 730m above present sea level, indicating there was considerable Neogene geomorphological activity, particularly vertical post-depositional movements with associated river downcutting.

Paleogene (Danian) basalt lava flows overlie Precambrian and/or Cretaceous-Tertiary deltaic clastics near Cape Dyer (Austin, 1973; Beh, 1975; McMillan, 1973; Wilson and Clarke, 1965; Fig. 2.2). The 450m thick basalt is chemically and stratigraphically similar to the 7500m thick sequence in west Greenland, with both considered to be remnants of a once continuous basalt plateau (Clarke and Upton, 1971).

2.3 REGIONAL GEOLOGY: OFFSHORE

2.3.1 Introduction

The Cretaceous-Tertiary sedimentary succession on the Labrador Shelf is not exposed on land. Descriptions of the regional geology are based on seismic reflection studies with lithologic control provided by the 31 exploratory wells. A regional seismic grid of approximately 80,000 line kilometres of multi-channel reflection seismic data has provided information concerning crustal geology, basement morphology, evolution of the Labrador Sea and Baffin Bay and the timing of events in relation to the overall evolution of the North Atlantic Ocean.

2.3.2 Previous Work

Work in the Labrador Sea began in 1954 when the

Dominion Observatory produced airborne magnetometer surveys. During the period 1965 - 1969, the Atlantic Geoscience Centre of the Geological Survey of Canada conducted reconnaissance seismic surveys across the Labrador continental margin, demonstrating the existence of a large sedimentary wedge. The Centre has continued to carry out studies, primarily concerned with Quaternary sediments, and since 1971, extensive investigations of the bedrock geology and surficial sediments of the Southeast Baffin Shelf have been undertaken.

The first permits to explore for petroleum in the Labrador Sea were issued in 1966. Reflection seismic studies, aeromagnetic surveys and bottom sampling led to the first well, Leif E-38, in 1971. Since then, 31 wells have been drilled on the Labrador, Baffin Island and Greenland continental shelves.

Geophysical interpretations of the geology of the Labrador Basin include Grant (1972; 1975; 1980; 1982), Srivastava (1978; 1985), Srivastava et al. (1981), Roots and Srivastava (1984), Keen (1979), Keen and Hyndman (1979), Royden and Keen (1980), Hinz et al. (1979). "Fixist" hypotheses for the evolution of the Labrador Basin presented by Kerr (1967), Umpleby (1979), and Grant (1980) have been refuted. It is generally accepted as proven that plate-tectonic extension and spreading has occurred in the

Labrador Basin. Authors, including LePichon et al. (1971), Laughton (1972), van der Linden (1975), Kristofferson (1978), and Srivastava (1978) provide abundant evidence supporting the plate-tectonic theory.

The sediments of the Labrador Shelf terrace prism and its petroleum potential have been described by McMillan (1973b), McWhae and Michel (1975), Cutt and Laving (1977), Umpleby (1979), Rashid et al. (1980), McWhae et al. (1980), Klose et al. (1982), Meneley (1986), Balkwill (1987), and Balkwill et al. (1990).

The stratigraphic nomenclature was defined by Umpleby (1979) on the basis of well cuttings. McWhae et al. (1980) refined Umpleby's lithostratigraphic units with the introduction of seismic-stratigraphic sequences. Balkwill (1987) and Balkwill et al. (1990) have used additional wells and seismic definition to further refine the formations defined by McWhae et al. (1980; Table 2.1). Figure 2.3 illustrates the stratigraphic relationships recognized on the Labrador Shelf.

A comprehensive series of maps pertaining to the geology, geophysics, and hydrocarbon potential of the Labrador Shelf was co-ordinated by Bell (1989).

2.3.3 Basement Structure and Morphology

In 1977, The Geological Survey of Canada, Map 1400

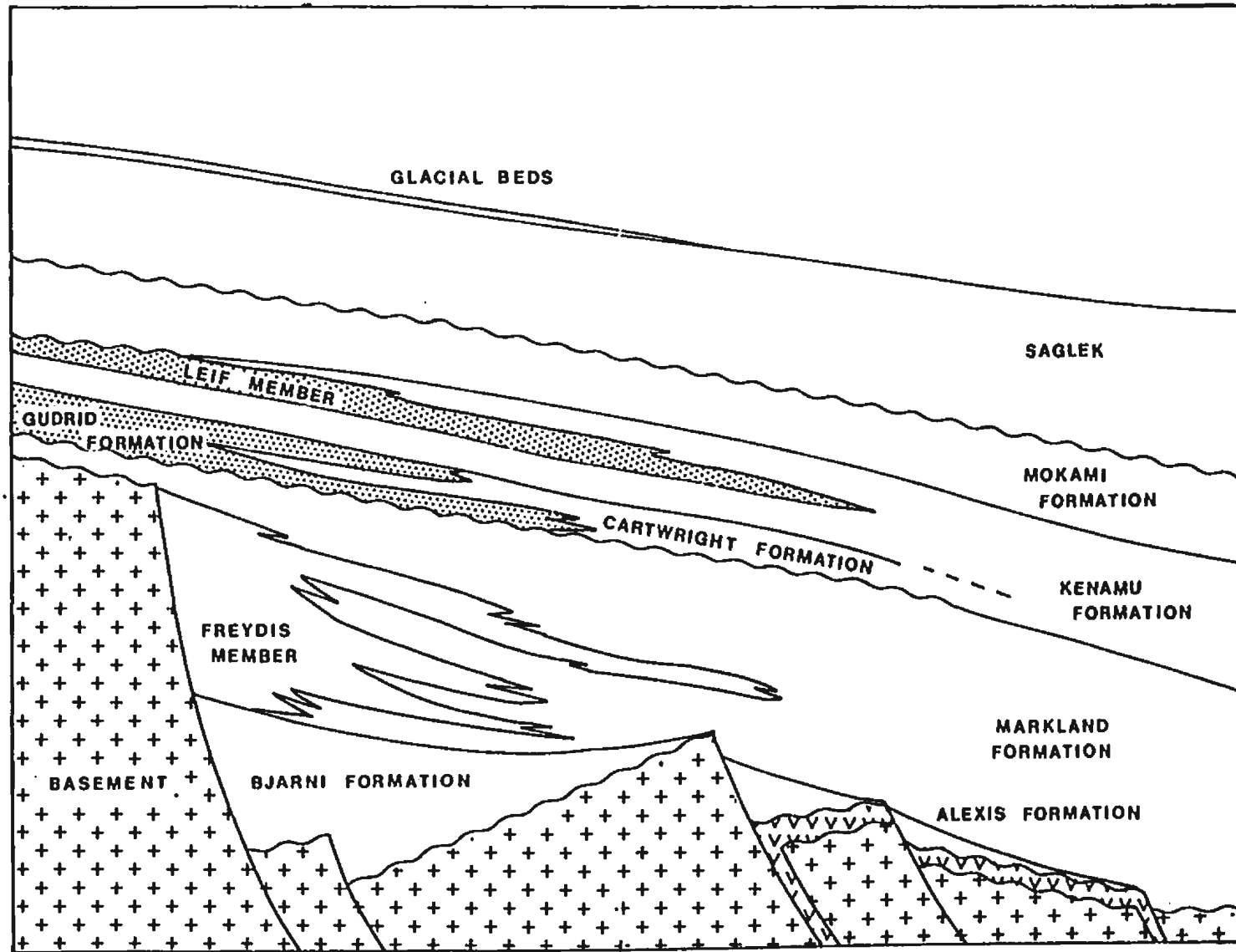
TABLE of FORMATIONS

TABLE 2.1 Table of Formations

| | | UMPLEBY, 1979 | McWHAE et al., 1980 | BALKWILL et al., 1987 | |
|-------------|------------|---------------|---------------------|---------------------------|----------------|
| TERTIARY | NEOGENE | PLEISTOCENE | UNNAMED | UNNAMED | |
| | | PLIOCENE | | SAGLEK FM. | |
| | | MIOCENE | SAGLEK FM. | MOKAMI FM. | MOKAMI FM. |
| | PALEOGENE | OLIGOCENE | | | |
| | | EOCENE | LEIF SAND MBR. | LEIF MBR. | LEIF |
| | | | BROWN MUDSTONE MBR. | KENAMU FM. | KENAMU FM. |
| | | PALEOCENE | GUDRID SAND MBR. | CARTWRIGHT FM. GUDRID FM. | CARTWRIGHT FM. |
| | CRETACEOUS | UPPER | MAASTRICHT | CARTWRIGHT FM. | |
| | | | CAMPANIAN | FREYDIS SAND MBR. | |
| | | | SANTONIAN | | FREYDIS MEMBER |
| CONIACIAN | | | | | FREYDIS MEMBER |
| TURONIAN | | | | | |
| LOWER | | CENOMANIAN | | | |
| | | ALBIAN | | | U. BJARNI SS |
| | | APTIAN | BJARNI FM. | BJARNI FM. | BJARNI FM. |
| | | BARREMAN | SNORRI MBR. | | L. BJARNI SS |
| | | HAUTERMAN | ALEXIS FM. | ALEXIS FM. | ALEXIS FM. |
| VALANIGNIAN | | | | | |
| BERRIASIAN | | | | | |

PRE-MESOZOIC
ROCKS

Figure 2.3 Diagrammatic cross-section of the Labrador Shelf



(Wade et al., 1977), delineated three sedimentary basins, separated by two arches, underlying the Labrador Shelf. Balkwill (1987) extended this structural definition to include tectonic elements on the southeast Baffin Shelf (Fig. 2.4).

Balkwill (1987) added the term "cratonic monocline" to the literature. Defined as "the rifted, extended, seaward-flexed cratonic basement surface that separates the low-standing oceanic basement floor from the high-standing cratonic basement rims", it does not coincide with the continental slope, which is a late Cenozoic, sediment-constructed surface (Balkwill, 1987). The cratonic monocline can be seen seismically, and is demarked by upper and lower hinge lines. The upper hinge line, lying at 1 to 2km below sea level, defines the landward limit of disrupted cratonic basement. The lower hinge line, between 7 to 8km below sea level, is where cratonic sialic basement gives way to oceanic basalts. The width of the monocline varies from about 25km where the basement is abruptly faulted or flexed, to about 125km where the surface dips gradually seaward by means of small syn-rift normal faults. The cratonic monocline is broken by Cretaceous rift-stage half grabens which have been infilled by disconnected wedges of Cretaceous basalts and younger post-rift sediments (Balkwill, 1987).

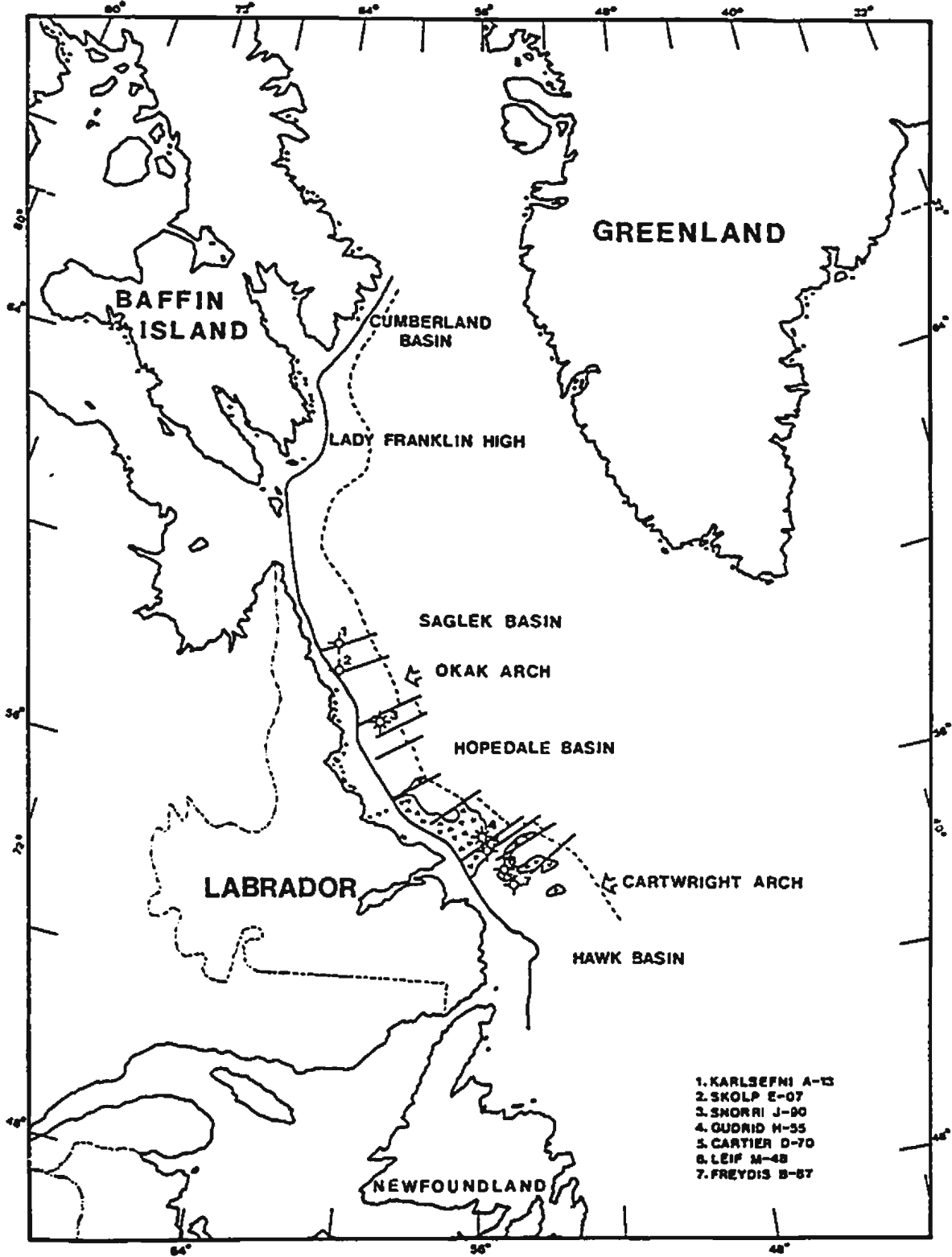


FIGURE 2.4 Tectonic elements of the Labrador and southeast Baffin Island shelves

Regional differences in strike and structural style have allowed the delineation of six tectonic elements along the Labrador-southern Baffin Island margins. From south to north these elements, which are subparallel to the present coastline, are the Cartwright Arch, Hopedale Basin, Okak Arch, Saglek Basin, Lady Franklin High and Cumberland Basin. The Geological Survey of Canada, Map 1400 (Wade et al., 1977) also defines the Hawke Basin to the south of the Cartwright Arch. The landward limits of the basins and arches are defined by the edge of the cratonic monocline; the seaward limits are where landward-sloping oceanic basalt flows form the outer flanks of the basins (Balkwill, 1987).

2.3.4 Stratigraphy and Lithology

The Labrador Shelf is underlain by an assemblage of Mesozoic-Cenozoic sedimentary and volcanic rocks which can be divided into three megasequences, deposited under three different sets of tectonic control: (1) intra-cratonic rifting; (2) separation and subsequent spreading of the Labrador Basin; and (3) post-spreading subsidence of the Labrador Sea crust (Balkwill, 1987; Balkwill et al., 1990). Pre-rift deposits include isolated Paleozoic relicts and Precambrian basement.

Northeast-southwest lateral extension of the

craton during the Early and early Late Cretaceous produced large rotated horsts and half grabens (Balkwill, 1987). Syntectonic terrigenous clastics infilled and partly covered these rift structures. The oldest known deposits of the intra-cratonic rift stage are non-marine Barremian sandstones which lie on Neocomian basalts, Paleozoic erosional remnants, and Precambrian gneissic basement rocks. The youngest rift deposits are Coniacian. With the deposition of the sediments confined to grabens and half-grabens on the landward part of the margin, the middle and outer parts of the extended margin were sediment starved.

Following cratonic separation, the sediment supply to the shelf increased dramatically during the Campanian. With cooling of the oceanic crust, there was an episode of ocean floor subsidence, allowing the cratonic monocline to acquire a seaward gradient. Campanian and Maastrichtian sediments prograded across the rift-phase grabens and horsts to the approximate position of the present day continental slope. For the duration of the ocean spreading period, successive sequences of seaward thickening, seaward inclined clastics were deposited. This depositional style continued until the late Eocene when there was a widespread phase of shelf shallowing, coastal erosion and seaward progradation of sand.

This period of shallowing coincides with the cessation of mid-Tertiary normal faulting in the Saglek and Hopedale Basins, large scale transcurrent faulting in the Cumberland Basin and intrusion of mafic plugs in the Cumberland Basin and northern Labrador Sea (Balkwill, 1987; Balkwill et al., 1990). It is also coeval with the postulated Late Eocene or early Oligocene cessation of Labrador Basin spreading, as inferred from the correlation of magnetic anomalies (Srivastava, 1978).

The post-spreading sequence covers the period from early Oligocene to Quaternary. Thermal subsidence of the ocean floor was dominant at this time, accompanied by uplift of the coastal margins. The cratonic monocline was tilted seaward and thick sequences of coarse clastic detritus were deposited, prograding across the shelf, constructing the present day outer continental shelf and slope (Balkwill, 1987). The fine-grained fractions bypassed the shelf and slope and were deposited as a thick blanket on the basin floor.

2.3.5 Syn-Rift Megasequence

The syn-rift megasequence comprises the Neocomian Alexis Formation, the ?Neocomian-Albian Bjarni Formation, and the Cenomanian-Campanian shales of the Markland Formation and its equivalent Freydis Member sandstones

(Balkwill, 1990).

2.3.5.1 Alexis Formation

The Alexis Formation, in its type section in Bjarni H-81, consists of repeated sequences of red and green weathered basalts alternating with fresh amygdaloidal basalt and intrabasaltic siltstones and sandstones (Umpleby, 1979). The basalts have been dated by K-Ar isotope decay methods, yielding ages ranging from $104 \pm 5\text{Ma}$ to $139 \pm 7\text{Ma}$ (McWhae et al., 1980). It appears, however, that the most reliable dates are 118 to 122Ma for the upper part (McWhae and Michel, 1975) placing the Alexis Formation in the Berriasian or Valanginian to Barremian (McWhae et al., 1980).

The character of the Alexis Formation varies from south to north. The basalts encountered in the Hopedale basin are lithologically similar to the type section Alexis Formation alkali basalts, contrasting with the tholeiitic nature of the basalts in the northern Saglek Basin and Cumberland Basin (Balkwill et al., 1990).

Onshore equivalents of the Alexis Formation may be the Ford's Bight volcanics (King and McMillan, 1975) which comprise breccia cut by lamprophyric-carbonatite dykes (McWhae et al., 1980). Ages were estimated to be $145 \pm 6\text{Ma}$ and $129 \pm 6\text{Ma}$, placing them in the Thithonian-Berriasian

and Valanginian-Hauterivian, respectively.

The Alexis Formation basalts rest unconformably on Paleozoic sediments or Precambrian basement and are overlain by various formations: the Bjarni Formation (McWhae et al., 1980), marine shales of the upper Cretaceous Markland Formation, or Paleocene Cartwright Formation in structurally high or more distal parts of the shelf (Balkwill, 1987).

2.3.5.2 Bjarni Formation

The Bjarni Formation was named by McWhae and Michel (1975) for gas-bearing Lower Cretaceous sandstones in the Bjarni H-81 well. Umpleby (1979) designated the type section of the Bjarni Formation in Herjolf M-92. The Bjarni sandstones have been the most pursued hydrocarbon target in the Labrador Shelf wells (Balkwill, 1990) and it is estimated that the North Bjarni F-06 gas field contains recoverable reserves of $13.6 \times 106\text{m}^3$ of condensate and $50.4 \times 109\text{m}^3$ of natural gas (Meneley, 1986). The Bjarni consists of predominantly non-marine (continental deltaic deposit) coarse grained arkosic sandstones of Barremian to early Cenomanian age (McWhae et al., 1980).

In the Hopedale Basin, the Bjarni Formation is discontinuous, occupying the structurally low parts of grabens and half grabens (Balkwill et al., 1990). The

Bjarni is also present in the southern part of the Saglek Basin. In both basins, it is overlain by Upper Cretaceous or younger rocks; viz., sandstones of the Freydis Member of the Markland Formation on the inner margin, and shales of the Markland Formation in the middle and outer shelf regions (Balkwill et al., 1990).

2.3.5.3 Freydis Member

Umpleby (1979) proposed the name Freydis Member for a 55m thick sand interval in the Cartwright Formation. McWhae et al. (1980) expanded Umpleby's type interval, retained the name, and included these sandstone dominated rocks in their newly named Markland Formation. Balkwill et al. (1990) recognized the Freydis Member of the Markland Formation and the lower part of the Markland Formation shales as being the last representative rocks of the syn-rift megasequence with the upper part of the Markland Formation shales as the earliest rocks of the drift-phase megasequence.

The Freydis Member consists of upward-coarsening cycles of shale, siltstone and argillaceous, arkosic sandstone (McWhae et al., 1980). This member is non-marine for the most part, however marine fossils also occur, being more prevalent towards the top of the unit (Umpleby, 1979). Downdip from the Freydis Member sands are thin

coeval successions of marine pelites of the lower part of the Markland Formation shales (Balkwill, 1987).

This member is limited in its aerial distribution, and is confined to inner part of the shelf. Two contrasting seismo-stratigraphic styles have been defined by Balkwill et al. (1990): (1) thick, narrow, half-graben confined wedges at or near the contact between the terrace wedge and the Precambrian basement; and (2) narrow, relatively thin, seaward facing prisms that locally overstep older rocks both landward and seaward.

2.3.6 Drift-phase Megasequence

The drift-phase megasequence comprises shale-dominated seaward-prograding successions and includes the Upper Cretaceous, Paleocene and Eocene Markland, Cartwright and Kenamu Formations (Balkwill et al., 1990). These formations overlie and are partly intercalated with Paleocene and Eocene basalts under the continental slope and on the basin plain. Sandstones, including the Lower Gudrid Member of the Markland Formation (Balkwill et al., 1990), the Upper Gudrid Member of the Cartwright Formation, and the Leif Member of the Kenamu Formation were deposited on the ancient continental shelf.

2.3.6.1 Markland Formation

The Markland Formation was defined by McWhae et al. (1980) and is one of the most widespread lithostratigraphic units on the Labrador Shelf. It occurs throughout the Hopedale Basin and in the Saglek Basin on the northern Labrador Shelf and Southeast Baffin Shelf (Balkwill et al., 1990). The type section of the Markland Formation is in Bjarni H-81. The formation consists mainly of marine shales, with rare siltstone and sandstone, and thin dolomitic limestone beds (McWhae et al., 1980). The Markland unconformably overlies the Bjarni Formation in grabens and oversteps the Freydis Member to lie directly on Precambrian basement, Paleozoic strata, or Cretaceous basalts (Balkwill et al., 1990). In the Saglek Basin, the Markland is intercalated and lies beneath late Cretaceous and Paleocene basalts.

The thickest occurrences of the Markland Formation are above the thick Bjarni Formation filled grabens along the inner part of the shelf (Balkwill, 1987), forming an elongate, shelf-parallel prism that thins seaward and landward from a regional maximum.

The Markland Formation is Albian-Cenomanian to Danian in age (McWhae et al., 1980). The shales form the seals for the Bjarni-gas bearing sandstones and the land-plant organic detritus may, in part, be source beds for the Bjarni gas.

2.3.6.2 Gudrid Members

The Lower and Upper Gudrid Members were originally described by Umpleby (1979) as a unit of arkosic sand with abundant clay matrix within the Cartwright Formation. McWhae et al. (1980) raised the status of the unit from a member to a formation, recognizing it to be a lateral equivalent of the Cartwright Formation. Balkwill et al. (1990) recognize three levels of coastal marine sandstone development in the Paleocene and Eocene which equate to McWhae et al.'s Gudrid Formation. Because each sandstone unit lies at the top of a coarsening upward cycle, these sands are referred to the lower, middle and upper Gudrid members (Balkwill et al., 1990), defined as:

- (1) the lower Gudrid member is Danian in age and is the coastal sand facies equivalent to the upper shales of the Markland Formation,
- (2) the middle Gudrid member is middle to late Paleocene in age and represents the coastal sand facies of the lower shales of the Cartwright Formation,
- (3) the upper Gudrid member is late Paleocene to early Eocene in age and represents the coastal sand facies of the upper shales of the Cartwright Formation.

2.3.6.3 Lower Gudrid Member

The lower Gudrid member forms a seaward-facing sediment wedge that tapers updip (or landward) as a result of truncation and downdip (basinward) because it grades abruptly into Markland shelf shales. The unit is light grey to light brown, fine-to-coarse-grained, poorly sorted, partly pebbly, slightly clayey, feldspathic, quartz sandstones (Balkwill et al., 1990). According to Balkwill et al., the lower Gudrid sandstones are coastal sand bodies, in part delta-mouth deposits and bar deposits, cleaned by wave and tide action and occupying paleotopographic lows along the Danian coastline.

2.3.6.4 Cartwright Formation

The Cartwright Formation was defined by Umpleby (1979) as the Upper Cretaceous, Paleocene, and Lower Eocene shales on the Labrador Shelf. He included two sand members, the Freydis Sand Member and the Gudrid Sand Member. McWhae et al. (1980) redefined the Cartwright Formation as being restricted to the Paleocene and Lower Eocene part of the shale unit, including the Freydis Member of the Markland Formation. Umpleby's (1979) type section for the Cartwright Formation was Gudrid H-55. McWhae et al. (1980) designated the interval 1820 to 1975m in the

Bjarni H-81 well as the type section.

The Cartwright Formation is a shelf parallel, elongate prism which thins landward, as a result of depositional overlap onto older rocks, and seaward by downlap onto, and intercalation with, Cretaceous and Paleocene volcanic rocks (Balkwill et al., 1990). The thickest succession of the Cartwright Formation is in the central Saglek Basin, off Hudson Strait. In the Hopedale Basin the Cartwright is much thinner as the lower member is absent or thinly developed. Generally, the formation thickens seaward.

The Cartwright Formation consists mainly of dark grey, partly silty, slightly calcareous shale and contains Paleocene and Lower Eocene marine fossils (Balkwill, 1987). The shales have been interpreted as pelites that accumulated as distal turbiditic muds, downdip from inner-shelf Gudrid sandstones which were deposited as small, low-relief Paleocene and Early Eocene deltas (Balkwill et al., 1990).

2.3.6.5 Middle Gudrid Member

The middle Gudrid member of the Cartwright Formation has been traced from the Hopedale Basin to the southeast Baffin Shelf, where it is referred to informally as the Hekja sand (Klose et al., 1982). The middle Gudrid

is thought to be present in the mid-central part of the Hopedale Basin, although it has not yet been drilled (Balkwill et al., 1990). The unit pinches out abruptly towards land and grades into shales in a seaward direction.

The middle Gudrid (Hekja sands) are Paleocene in age (Klose et al., 1982) and consist of light grey-brown, fine- to coarse-grained, subangular, poorly sorted quartz sandstones with calcareous and kaolinitic cement (Balkwill et al., 1990), with thin interbeds of black, brittle coal. Balkwill et al. have interpreted these sandstones as comprising a lower delta plain deposit. In the Hopedale Basin, delta plain and delta foreset seismic reflectors are discernible and merge downdips with a shallow marine fan (Balkwill et al., 1990).

2.3.6.6 Upper Gudrid Member

The upper Gudrid member refers to coastal sand deposits and associated downdip shelf fans that are the landward equivalents of the Upper Cartwright Formation (Balkwill et al., 1990). In the Gudrid H-55 well, the upper Gudrid sandstones are composed of fine- to coarse-grained, subangular to subrounded, clear to white quartz sand with abundant feldspar grains and some coarse pebbles and are Late Paleocene to Early Eocene in age (Balkwill et al., 1990).

Balkwill et al. (1990) have interpreted the upper Gudrid sandstones in the Hopedale Basin, on the basis of seismic and log information, as shallow marine, shoreface sands locally adjacent to a small system of deltas developed on a seaward-facing slope in the inner part of the shelf, fading into thin turbidite fans on the outer shelf.

Umpleby (1979) grouped all Tertiary rocks on the Labrador Shelf, Eocene age or younger, into the Saglek Formation. The Formation consists primarily of a thick monotonous sequence of sandy and silty mudstones.

Differentiated within the Saglek Formation are brown grey to dark grey mudstones of the Brown Mudstone Member, and the Leif Sand Member. McWhae et al. (1980) subdivided Umpleby's thick Saglek Formation to include Eocene age rocks as the Kenamu Formation, late Eocene to Middle Miocene age rocks as the Mokami Formation, and the uppermost part of the pre-Quaternary part of the sequence only as the Saglek Formation. The Leif Member is recognized as a part of the Kenamu Formation.

2.3.6.7 Kenamu Formation

McWhae et al. (1980) defined the Kenamu Formation as a thick, widespread, shale-dominated sequence of Eocene-age comprising three informal members:

- (1) the lower Kenamu member: upward fining, slightly silty grey marine shales of Lower Eocene age,
- (2) the middle Kenamu member: Lower and Middle Eocene marine shales which coarsen upwards to siltstone and, locally, fine-grained sandstone,
- (3) the upper Kenamu member: Middle and Upper Eocene mainly marine siltstones that coarsen upwards in some places to shoreface and coastal sandstones recognized as the Leif sandstone member (named by McWhae and Michel, 1975). The Leif Member is a fine-grained, quartzose, white to light grey-brown sandstone (McWhae et al., 1980).

The Kenamu Formation reaches maximum thickness (approx. 2200m) in the depocentre of the Saglek Basin. The formation thins rapidly to the south, onlapping the north flank of the Okak Arch, westward to the updip margin of the Tertiary wedge, and eastward to the north-central Labrador Sea (Balkwill et al., 1990). The Leif Sandstones are best developed in the Hopedale Basin east of Hamilton Inlet, in the same area where thick lower and upper Gudrid sandstones are developed (Balkwill et al., 1990).

The upper Kenamu surface is easily recognized in

seismic records and in well logs. It represents the top of a shelf-wide coarsening upwards sequence which is truncated in the inner and middle parts of the shelf by an unconformity (Balkwill et al., 1990). At this surface, siltstones and sandstones (Leif Member) of the upper Kenamu are overlain by basal marine shales of the Mokami Formation.

Fossil evidence from the shales of the lower and middle Kenamu Formation indicate deposition in outer neritic to bathyal water depths (McWhae et al., 1980). Fossil assemblages from the upper Kenamu indicate deep marine conditions (foraminifera) and shallow marine and coastal environments (palynomorphs). Balkwill et al. (1990) interpret a gradual subsidence and deepening of the shelf from the onset of deposition of the Kenamu Formation to the top when gradual shallowing resulted from depositional upbuilding during progradation of the middle and upper members. The Leif sands were deposited in widespread coastal settings resulting from further shallowing in the late Eocene.

The distribution of the upper Kenamu beds indicate contribution of clastics through river systems with outlets near Cumberland Sound, Hudson Strait, and Hamilton Inlet (Balkwill et al., 1990) Tides, waves and storms probably affected the deposition of the shallow sand facies.

The top of the Kenamu Formation is regionally tilted seaward from an Eocene hinge zone of the inner shelf, resulting from post-Eocene subsidence of the outer shelf (Balkwill et al., 1990) that is approximately coincident with the cessation of sea-floor spreading in the Labrador Sea (Srivastava, 1978). The surface of the Kenamu is considered by Balkwill (1987) to be the top of the drift-phase megasequence.

2.3.7 Post-Rift Megasequence

The post-rift megasequence rocks are Oligocene and younger and represented by the shale-dominated Mokami Formation and the sandstone-dominated Saglek Formation.

2.3.7.1 Mokami Formation

McWhae et al. (1980) introduced the Early Oligocene to mid-Miocene Mokami Formation to the literature. The formation consists of brown claystone and soft shale and rests disconformably on the older Kenamu Formation. The lower part of the Mokami is widespread over all of the Labrador and southern Baffin Island shelves, occupying structural depressions in the axial parts of the Hopedale and Saglek Basins in mid-Tertiary growth fault domains (Balkwill et al., 1990). The upper Mokami mudstones are present mainly on the Labrador Shelf,

becoming more sandy northward through the Saglek Basin to the southeast Baffin Shelf. Both the lower and upper members of the Mokami Formation are similar, exhibiting upward and landward coarsening tendencies (Balkwill et al., 1990).

According to Balkwill et al. (1990) fossil assemblages indicate a deep neritic environment for the Late Eocene lower Mokami member. There was a shallowing in the upper part of the lower member, with nonmarine or marginal marine conditions existing during the Oligocene at the boundary with the upper member. Seismic evidence indicates that the northern Labrador and southeast Baffin shelves were emergent during the mid-Late Oligocene allowing subaerial erosion and the accumulation of nonmarine (lacustrine?) muds and peats (Balkwill et al., 1990).

2.3.7.2 Saglek Formation

The Saglek Formation was originally named by Umpleby (1979) for the Middle Eocene to Upper Miocene silty and sandy mudstones. McWhae et al. (1980) restricted the Saglek Formation to be the uppermost pre-Quaternary part of the sequence, consisting of porous, unconsolidated, feldspathic, cherty, poorly sorted fine-to coarse-grained and conglomeratic sandstone.

Balkwill et al. (1990) recognize two parts within the Saglek Formation: lower Saglek conglomeratic sandstones of Late Oligocene to Late Miocene age; and upper Saglek conglomerates of Late Miocene to Pliocene age (Balkwill et al., 1990; Grant, 1980; McWhae et al., 1980). The Saglek Formation is widely distributed in the Saglek and Hopedale Basins and represents the proximal coarse grained facies of two thick sediment wedges that prograded seaward across the Labrador Shelf in the Late Oligocene to Middle Miocene (Balkwill et al., 1990). The geometry of the Saglek deposits indicates a broad system of small coalescing fan deltas, (Balkwill, 1987) with their source area likely the Torngat Mountains (Balkwill et al., 1990). On the Southeast Baffin Shelf, the lower Saglek is widely distributed and is the proximal facies equivalent to the upper Mokami beds on the Labrador Shelf. The upper Saglek fills structurally low areas and, as a result, its distribution is more restricted.

The boundary between the lower and upper Saglek members is, locally, an erosion surface with relief of a few hundred metres.

The Saglek Formation is unconformably overlain by relatively thick Pleistocene deposits.

2.3.8 Tectonic Evolution of the Labrador Sea

By the late 1960's sea-floor spreading was recognized as having occurred in the Labrador and Norwegian Seas and the North Atlantic (Vogt et al.; 1969). Since that time much work has been done refining the timing and evolution of tectonic events in the Labrador Sea and Baffin Bay area. Parallel magnetic anomalies 20 to 24 in the central portion of the Labrador Sea (Laughton, 1971; Kristofferson & Talwani, 1977) and 31 to 25 lying on either side of the central zone (Srivastava, 1978) have been identified, allowing the definition of the timing of events in the Labrador Sea.

The oldest anomaly recognized in the southern Labrador Sea is anomaly 32, defined as Campanian in age. It is in close proximity to the ocean-continent crust boundary (Srivastava, 1978), indicating that active sea-floor spreading and generation of oceanic crust had commenced by that time. Prior to this, there was broad regional updoming resulting from thermal expansion of the upper mantle. Considerable stretching and block-faulting of the crust produced graben and half-graben structures, forming the initial rift valley, and foredeeps marginal to the updomed area.

Schneider (1972) defined these tectonic events as the rift valley stage. Infill of these structures is, ideally, a sedimentary mix of normal terrigenous material,

basic and alkaline volcanic rocks, country-rock derived conglomerates, river and lake deposits, and non-marine evaporites (evaporites, to date, have not been recognized on the Labrador Shelf).

The known syn-rift rocks in the Labrador Sea are the Neocomian Alexis basalt, the Barremian-Albian Bjarni Formation, and the Cenomanian-Lower Campanian Freydis member sandstone and equivalent shale of the Markland Formation (Balkwill, 1987). Syn-rift terrigenous clastics, Bjarni Formation and Freydis member, and Alexis Formation basalts are recognized as unconnected, fault-bounded wedges infilling graben and half-graben structures on the cratonic monocline. The foot of the cratonic monocline, where cratonic basement gives way to deep basin floor basalts, is recognized seismically as landward-sloping, mounded reflections of oceanic basalt.

The sediments deposited in the shoreward parts of the grabens are texturally and mineralogically immature, quartz- and feldspar-rich lithic arenites derived from adjacent highlands including cratonic headlands and horst blocks (Balkwill, 1987). These sediments were likely transported by short, high-gradient streams (Higgs, 1977). Facies studies suggest these sediments may be, in part, lacustrine or estuarine shales, with thin sandstones, and possibly shallow marine shales (Balkwill et al., 1990).

By late Albian time, marine conditions were firmly established, and with the exception of the innermost parts of the shelf, sedimentation throughout the Late Cretaceous was marine. From the Cenomanian to Santonian small amounts of sediments were trapped in early Late Cretaceous grabens on the inner continental margin. The middle and outer parts of the extended margin were sediment starved. A surge of fine-grained sediments, part of the upper Markland Formation, occurred during the Campanian, following cratonic separation and the development of a seaward gradient on the cratonic monocline, resulting from the cooling and subsidence of ocean crust. These events make up Balkwill's (1987) and Balkwill et al.'s (1990) drift-phase megasequence, and are recognized as Schneider's (1972) Red Sea Stage and the later turbidite-fill stage.

The drift-phase megasequence is shale-dominated, seaward-prograding, stacked, coarsening-upwards sequences of the Markland, Cartwright, and Kenamu Formations (Balkwill et al., 1990) representing repetitive shallowings of marine to non-marine depositional settings. This succession continued from Upper Cretaceous through Paleocene to Eocene time. The upper surface of the Kenamu Formation (late Eocene) is easily recognized (in both seismic records and well logs) and represents the top of a shelf-wide coarsening upwards sequence. The top of the

Kenamu is truncated in the inner and middle parts of the shelf by an unconformity and is regionally tilted seaward from an Eocene hinge zone on the inner part of the shelf, resulting from post-Eocene subsidence of the outer shelf (Balkwill et al., 1990).

Oligocene and younger sediments comprise the post-drift megasequence (Balkwill, 1987; Balkwill et al., 1990) and include the shale-dominated Mokami Formation and the sand-dominated Saglek Formation. Crustal dynamics at this time were dominated by massive thermal subsidence of the Labrador Sea oceanic basin floor and rejuvenated uplift of the coastal margins during the Late Miocene, Pliocene and Quaternary (Balkwill, 1987). The volume of clastic deposition exceeded the rate of shelf subsidence allowing the clastics to prograde basinward, constructing the modern outer continental shelf and slope. The fine-grained fractions were deposited as a thick blanket on the basin floor. Four coarsening upwards sequences can be distinguished in these formations. Within the Mokami Formation two regional sequences with different areas of distribution and tectonic significance can be distinguished (Balkwill et al., 1990): the lower neritic, shale-dominated Mokami member extends over the Labrador and southern Baffin Island shelves, lying disconformably on the Kenamu Formation erosional surface which marks a phase of

regional emergence of the Labrador Shelf; and the upper Kenamu Formation, found mainly on the Labrador Shelf, is the distal, shaley facies of a regional stratigraphic sequence that includes proximal coarse grained sands currently assigned to the lower part of the Saglek Formation.

The Saglek Formation consists of two parts: a lower Saglek composed of conglomeratic sandstones; and an upper Saglek conglomeratic sequence that lies on a pronounced regional unconformity on the upper Mokami-lower Saglek sequence (Balkwill et al., 1990). The Saglek represents the coarse grained facies of two progradational wedges. The boundary between the lower and upper Saglek members is locally an erosion surface with relief (seen on seismic sections) of a few hundred metres (Balkwill et al., 1990).

According to Balkwill et al. (1990) a fundamental change in the stratigraphic regime took place in the Oligocene, marked by the mid-Mokami unconformity. The lower Mokami is shale dominated while the upper Mokami and lower Saglek contain fresh, coarse grained sandstones, interpreted as evidence of rejuvenated uplift of the cratonic rim of Labrador and southern Baffin Island, accompanied by a major shift in the regional directions of clastic progradation. This phase of tectonic rejuvenation

culminated in the accumulation of the thick outer-shelf wedge of coarse grained upper Saglek clastics (Balkwill et al., 1990).

Thick Pleistocene deposits locally unconformably overlie the Saglek Formation.

2.3.9 Development of Drainage

The development of the present-day drainage patterns in Eastern Canada began with Late Paleozoic and Mesozoic stripping of Lower Paleozoic cratonic cover rocks from a series of Precambrian peneplains (Ambrose, 1964; Greene, 1974). The present drainage patterns are adjusted to bedrock structure (Ambrose, 1964). Other than Pleistocene scouring, the topography and drainage patterns of Eastern Canada have been little modified since the Tertiary (Greene, 1974), when a complex drainage system was in existence (Bird, 1967).

During the Mesozoic and early Cenozoic, pre-rift intracontinental up-doming produced uplift in Labrador, Baffin Island, and parts of Greenland (Cooke, 1929; Christie, 1952; Greene, 1974; Martin, 1973). Its effects are still recognized in the area by the regional tilt of the land surfaces away from Labrador Sea and Baffin Bay. Drainage over the dome would have been outward, away from the future site of the Labrador Sea, with sedimentation in

peripheral basins (Cramez, 1977). Collapse of the dome, with associated down-faulting, allowed rivers to flow towards the incipient Labrador Sea.

Bird (1967, P. 82) shows rivers flowing westward from Labrador, indicating a height of land between Hudson Bay and the Labrador Sea (Fig. 2.5). A height of land also existed in the Canadian Arctic, during the Cretaceous, resulting in a westward and northwestward drainage pattern (Bird, 1967) with extensive delta development in the Sverdrup Basin (Kerr, 1981). This effectively set northwestern limits to the Cretaceous drainage basin.

The distribution and textural and mineralogical immaturity of the Cretaceous sediments in the Labrador Sea suggest they were derived by erosion from nearby highlands (horst blocks and the craton) and were transported into grabens by a poorly integrated network of short, high gradient coastal rivers (Higgs, 1977; Balkwill, 1987). The Tertiary section, however, contains vast quantities of fine-grained, pelitic, material, leading McMillan (1973) to conclude that major, continent-wide rivers were necessary to supply the massive quantity of detritus. The Tertiary sequence also contains mineralogically immature, feldspathic sands that indicate further erosion of coastal cratonic areas.

The Hudson Bay basin shows evidence of the

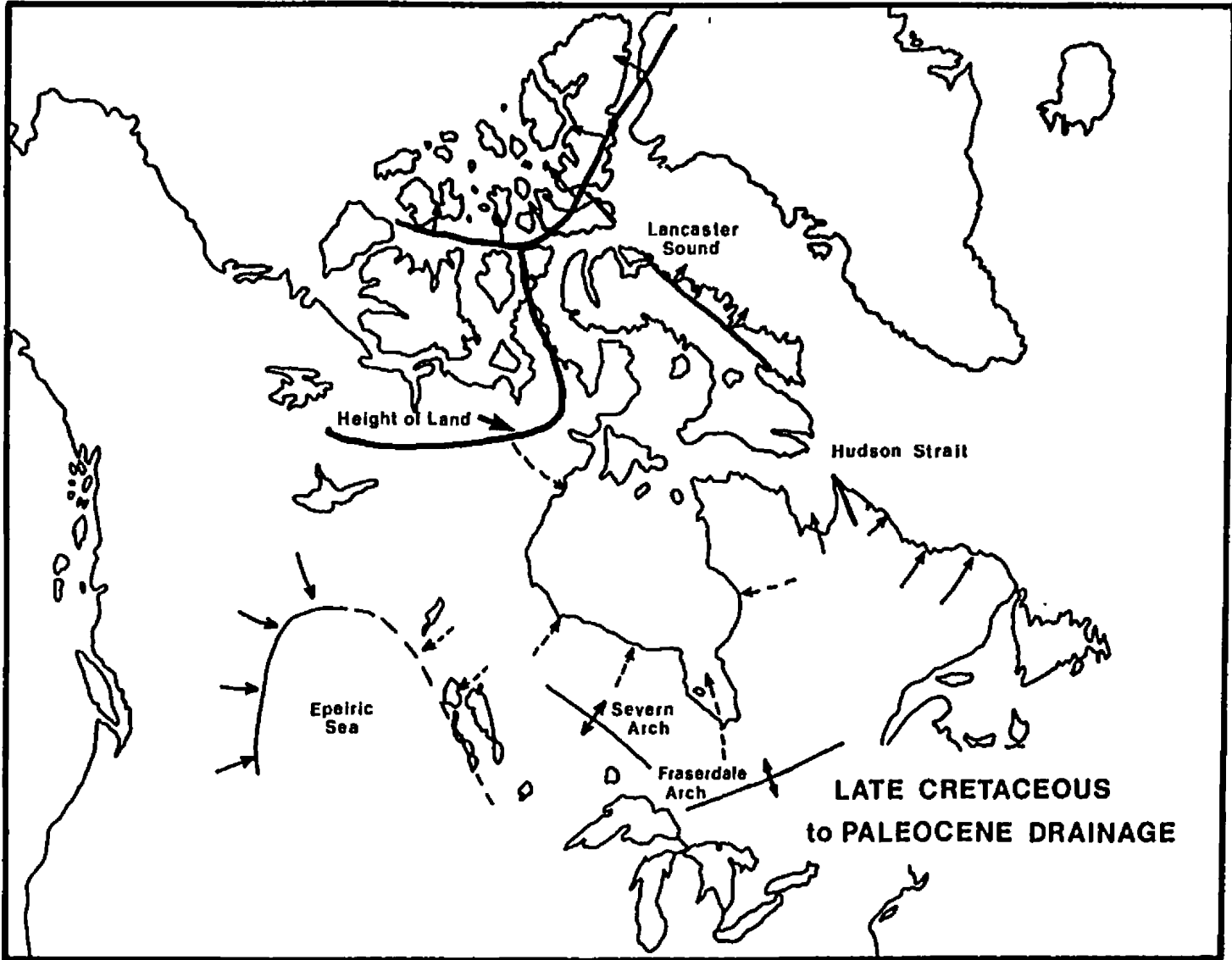


FIGURE 2.5 Cretaceous Drainage of North America

existence of a dendritic valley system prior to Pleistocene glaciation (Pelletier, 1968) indicating Hudson Bay was a collecting basin with outflow towards Hudson Strait. By Late Paleocene time rivers from western Canada and the midwestern United States flowed into the Hudson Bay basin. Bluemler (1972) documented pre-glacial rivers in North Dakota as flowing generally northeastward toward the Hudson Bay lowland. In western Canada, by the end of the Paleocene, the seas had completely withdrawn (Rahmani and Lerbekmo, 1975) allowing rivers to flow from the newly formed Rocky Mountains to Hudson Bay (Bird, 1967). This drainage pattern persisted through the Tertiary (Cumming, 1968) and still exists today.

The Tertiary, therefore, saw the development of a drainage system that effectively covered most of North America (Fig. 2.6). Bird (1967) estimated the Tertiary system drained about 6.5 million square kilometers, or an area roughly equal to the present-day Amazon system.

Miall et al. (1980) have correlated the Paleocene Eureka Sound Formation on Bylot Island in the Canadian Arctic as a time equivalent of the lower and middle Gudrid members and their equivalent Markland and Cartwright Formation shales. The Eureka Sound Formation is mainly non-marine sand and shale with locally abundant coal and thick marine intervals deposited in fluvial and deltaic

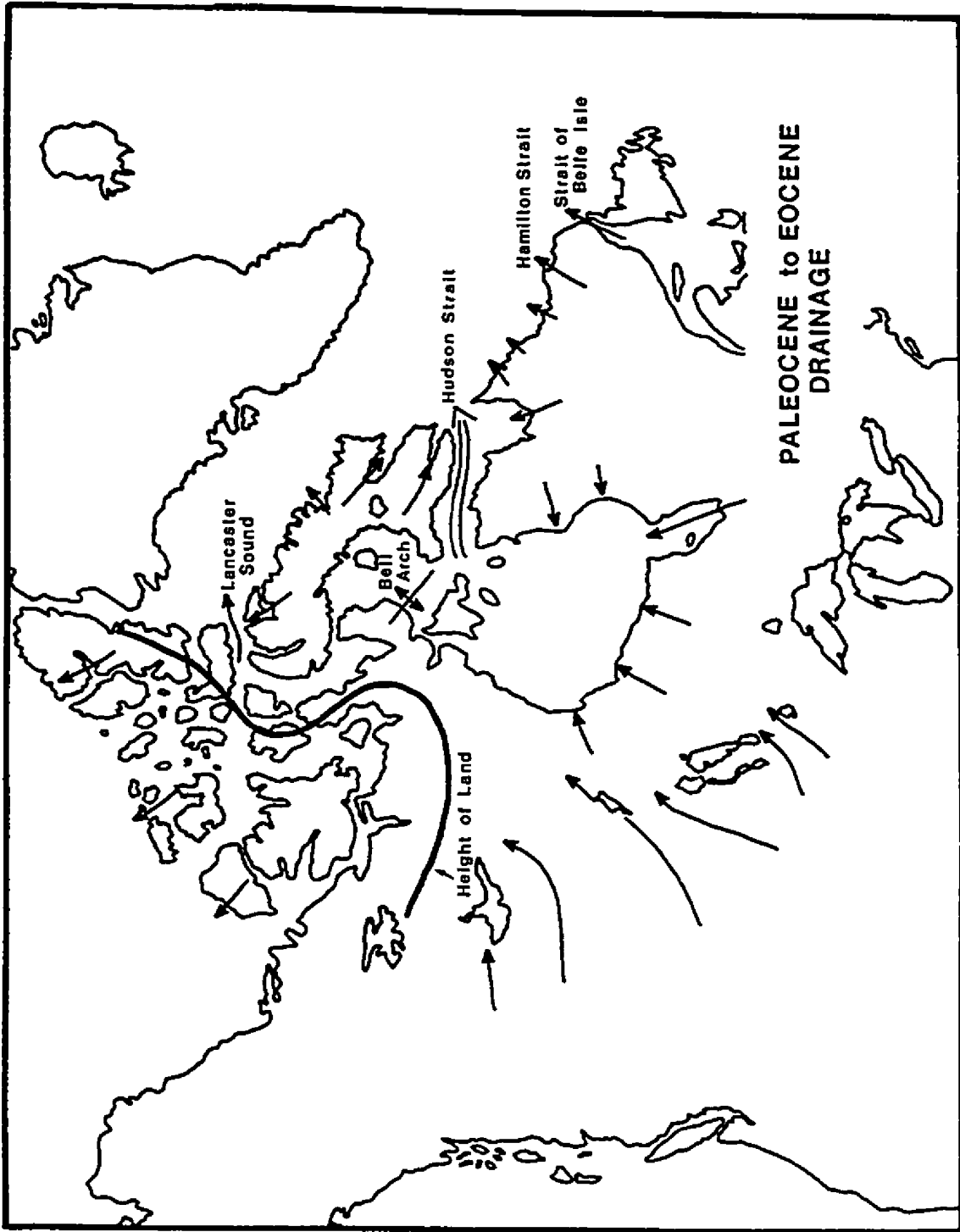


FIGURE 2.6 Eocene Drainage of North America

settings. The flow of the river system was north to northwest, away from the Labrador Basin, allowing some limits to be set on the Tertiary drainage basin.

McMillan (1973) described, in addition to the immediately adjacent mainland source, four sources of sediment for the Labrador Sea-Baffin Bay area: the present-day Strait of Belle Isle, Lake Melville-Hamilton Strait and the Churchill River drainage, Hudson Strait, and Lancaster Sound. The biggest source was likely through Hudson Strait with a watershed including the present-day Hudson Bay, part of the Northwest Territories, Alberta including parts of the Cordillera, Saskatchewan, Manitoba, and parts of Ontario and Quebec (Fig. 2.6).

Evidence for major rivers entering the early Labrador Sea and Baffin Bay comes from seismic reflection studies where prograding delta sequences (McMillan, 1973; McWhae et al., 1980) have been recognized. Onshore deltaic sequences of similar age have been recognized in western Greenland (Henderson et al., 1976).

By the Late Cretaceous, depocentres were established in the central parts of the Hopedale and Saglek Basins, persisting through the mid-Tertiary with the younger depocentres lying seaward of the older ones, the Pliocene-Pleistocene depocentre being the Labrador Sea Basin (Balkwill et al., 1990).

Estimates of the volume of Mesozoic-Cenozoic sediments in the Labrador Basin are approximately 4 million cubic kilometres, half of which comprises the terrace prisms along the Labrador and Greenland continental margins, with the remainder forming a thick blanket on the deep basin floor (Balkwill, 1987). The sedimentary sequence on the Labrador and Baffin Island continental margins is dominated by sandstone and shale, eroded from adjacent cratonic land masses. The Cretaceous units are generally thin (<1km) and restricted in distribution whereas the Tertiary sequence is up to at least 8km thick, widespread and of enormous volume (Hiscott, 1984).

Balkwill et al. (1990) agree with McMillan's (1973) interpretation that the Labrador Shelf was the principal Tertiary depocentre for eastward migrating fine-grained clastic detritus from the north-central parts of the North American craton. They (Balkwill et al., 1990) outline principal river systems contributing detritus to the Labrador and southern Baffin Island margins as occupying the present-day Hamilton Inlet, Hudson Strait, Frobisher Bay, and Cumberland Sound. McMillan's (1973) Lancaster Sound river system, interpreted as flowing into northern Baffin Bay, likely had little influence on the sediments of the study area.

CHAPTER 3

LIGHT FRACTION ANALYSIS

3.1 Introduction

The "light" minerals of a sand are those minerals with specific gravities less than 2.97gm/cm^3 , which is the specific gravity of the separation liquid tetrabromoethane. The minerals from this group that were studied are quartz and feldspar. Petrography and cathodoluminescence studies aided in understanding the characteristics of source area rock types.

3.2 Methodology

Thirty-seven grain mounts representing the Paleocene Gudrid and Eocene Leif sands were prepared for this study. The grain mounts were examined for mineralogical and general textural characteristics; a duplicate set was prepared for cathodoluminescence.

3.2.1 Laboratory Techniques

For the light fraction analysis, a grain size of 250 to 500 microns was chosen. The samples were prepared by the procedures detailed in Appendix 1. Separation of the heavy and light minerals was accomplished by the centrifuge-frozen tetrabromoethane method (Carver, 1971) using liquid nitrogen as the freezing agent. Each sample, weighing 2gm, was placed in a separation tube with 50ml of tetrabromoethane and centrifuged at 2500rpm for 20 minutes. The separation tube was then submerged in liquid nitrogen, freezing the sample. The light fraction was then quickly and easily removed, leaving the heavy mineral fraction in frozen tetrabromoethane in the bottom of the separation tube. This method substantially reduced contamination of either fraction by the other. Both the heavy and light mineral fractions were then soaked in a solution of stannous chloride and hydrochloric acid for 12 hours to remove iron oxide stains and carbonate cements.

The light and heavy mineral grains were mounted on glass slides in clear epoxy resin (refractive index = approx. 1.55 - 1.59). A second set of grain mounts was prepared using acrylic disks so that polished sections could be made for identification of problematic heavy minerals and cathodoluminescence.

3.2.2 Apparatus

Mineral identifications and grain counting were done on the glass slide mounts and carried out using a Zeiss petrographic microscope with a medium power ocular (10x magnification) with a 10x magnification eye piece.

Aids in mineral identification were standard mineralogy texts by Heinrich (1965), Deer et al. (1966), and Mason and Berry (1968).

3.2.3 Petrographic Procedures

Grain counting was done on both the light and heavy mineral fractions, however different methods were used. Heavy mineral counts were done by a modified ribbon method (see Chapter 4, p.). Because of the difficulty in distinguishing between orthoclase and quartz, the line method was chosen for counting the light fraction grains, enabling interference figures to be obtained for each grain, aiding in identification.

The line method of grain counting (Galehouse, 1971) involves counting those grains encountered by the intersection of the cross-hairs along linear traverses equidistantly spaced along the slide. The result of this method is a number frequency that simply shows how often a particular species was encountered during the count. Because the results of the light mineral fraction were not being treated statistically, number frequencies, rather

than number percentages, were acceptable. Both number frequencies and number percentages are commonly used for subsequent interpretations such as correlation, source area determination, and dispersal patterns (Galehouse, 1971).

For the light mineral fraction, an average of 212 grains per grain mount were counted.

Quartz and orthoclase were distinguished by optical and physical properties (Folk, 1974; p. 83). Microcline and plagioclase were readily identified by their distinctive twinning characteristics.

Four categories of quartz types were distinguished, as defined by Basu et al. (1975): monocrystalline, non-undulatory; monocrystalline, undulatory; polycrystalline, 2 to 3 crystal units per grain; and polycrystalline, more than 3 crystal units per grain. Undulosity refers to the angular separation between C-axes in different parts of a grain (Basu et al., 1975).

Cathodoluminescence of polished grain mounts is an effective method for identifying quartz types, such as luminescing and non-luminescing varieties, and the distinction between metamorphic and non-metamorphic quartz. Zinkernagel (1978) defined three quartz types, each characteristic of rocks with distinct temperature histories: violet luminescing quartz indicates igneous rocks, brown luminescing quartz indicates regional

metamorphic rocks, and non-luminescing diagenetic quartz.

The presence of muscovite was noted for the various grain mounts, and the number of occurrences noted. The micas were not included in the grain count data.

The textural features examined were grain roundness and sphericity; grain size variation and sorting were effectively eliminated because of sample sieving and the choice of one sample size range. Roundness and sphericity were recorded for the first 10 grains of each type encountered. Both were determined by comparison with Powers (1953) roundness scale.

3.3 Results

The results of the light mineral grain count analysis are presented in Table 3.1. The table gives the number frequencies of the various minerals, rock fragments, and quartz/feldspar ratios.

The quartz, feldspar, and rock fragments (including chert) counts were recalculated to 100% and the results for each samples were plotted on a ternary classification diagram (Fig. 3.1). This plot allows compositional names to be given to the sands; most of the Labrador Shelf sands are sub-arkoses and arkoses.

The results of the quartz-type analysis are shown on a diamond diagram (Fig. 3.2), modified after Basu et al.

TABLE 3.1 Results of Light Fraction Analysis

| | Quartz | Feldspar | Rock Fragments | Q/F |
|-----------------------|--------|----------|-------------------|-----|
| <u>Karlsefni A-13</u> | | | | |
| 2188 | 67 | 24 | 9 | 2.8 |
| 2235 | 81 | 12 | 7 | 6.8 |
| 2299 | 78 | 16 | 6 | 4.9 |
| 2374 | 80 | 14 | 6 | 5.7 |
| <u>Skolp E-07</u> | | | | |
| 550 | 64 | 29 | 7 | 2.2 |
| 900 | 58 | 39 | 3 | 1.5 |
| 1350 | 49 | 43 | 8 | 1.1 |
| 1600 | 64 | 34 | 2 | 1.9 |
| 1850 | 63 | 27 | 10 | 2.3 |
| 2200 | 57 | 39 | 4 | 1.5 |
| 2450 | 77 | 20 | 2 | 3.9 |
| 2700 | 78 | 18 | 4 | 4.3 |
| 2950 | 45 | 43 | 12 | 1.1 |
| <u>Snorri J-90</u> | | | | |
| 1800 | 73 | 18 | 9 | 4.1 |
| 1850 | 70 | 14 | 16 | 3.0 |
| 2522 | 63 | 34 | 4 | 1.9 |
| <u>Gudrid H-55</u> | | | | |
| 2178 | 74 | 19 | 7 | 3.9 |
| 2230 | 72 | 25 | 3 | 2.9 |
| 2250 | 64 | 36 | 0 | 1.8 |
| 2355 | 78 | 18 | 4 | 4.3 |
| 2393 | 71 | 23 | 6 | 3.1 |

TABLE 3.1 Results of Light Fraction Analysis - cont'd

| | Quartz | Feldspar | Rock Fragments | Q/F |
|---------------------|--------|----------|-------------------|-----|
| <u>Cartier D-70</u> | | | | |
| 1256 | 49 | 34 | 17 | 1.4 |
| 1274 | 71 | 18 | 11 | 3.9 |
| 1353 | 55 | 22 | 23 | 2.5 |
| 1731 | 57 | 33 | 10 | 1.7 |
| 1774 | 57 | 38 | 5 | 1.5 |
| 1847 | 52 | 43 | 5 | 1.2 |
| <u>Leif M-48</u> | | | | |
| 1259 | 63 | 32 | 5 | 2.0 |
| 1270 | 72 | 25 | 3 | 2.9 |
| 1673 | 52 | 46 | 2 | 1.1 |
| 1691 | 52 | 43 | 5 | 1.2 |
| <u>Freydis B-87</u> | | | | |
| 908 | 43 | 46 | 11 | 0.9 |
| 969 | 50 | 46 | 9 | 1.1 |
| 1411 | 56 | 43 | 1 | 1.3 |
| 1436 | 56 | 36 | 8 | 1.6 |
| 1443 | 50 | 48 | 2 | 1.0 |
| 1475 | 56 | 41 | 3 | 1.4 |
| Average | 57.9 | 28.5 | 6.2 | |

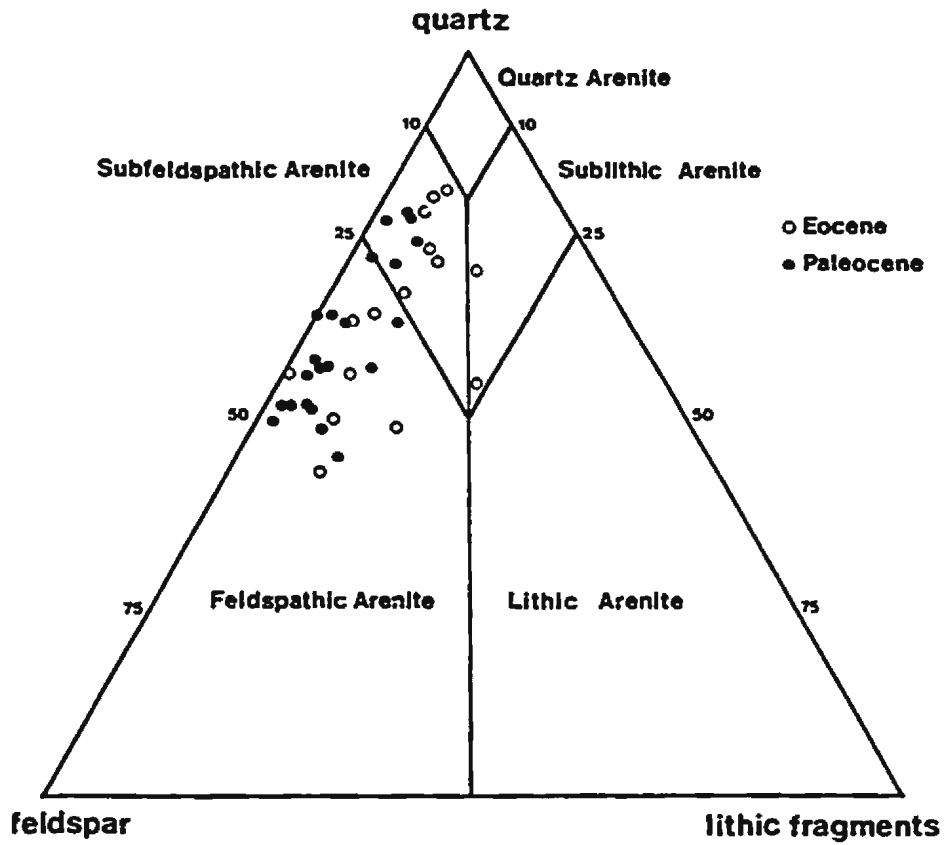


FIGURE 3.1 Classification of samples studied

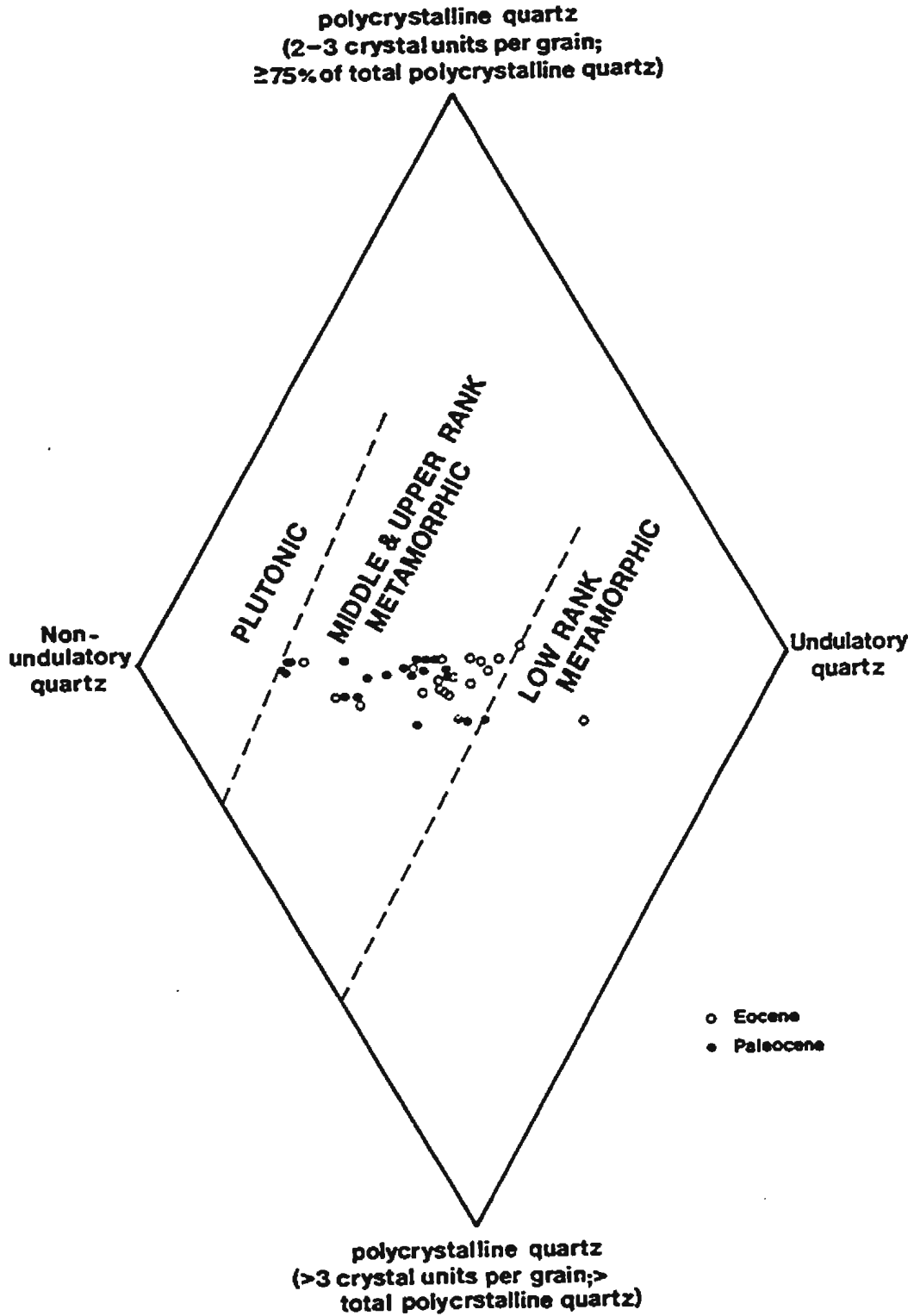


FIGURE 3.2 Four variable plot showing the nature of the quartz population in the samples studied

(1975). This diagram can be divided into two ternary plots: samples containing 75% or more of total polycrystalline quartz, with 2 to 3 crystal units per grain, plot in the upper triangle; in the lower triangle plot samples containing more than 25% of total polycrystalline quartz, with more than 3 crystal units per grain. The positioning of each sample depends also on the relative percentages of monocrystalline, undulatory and monocrystalline, non-undulatory quartz, which plot on the horizontal axis of the diamond plot.

Paleocene and Eocene samples from the Labrador Shelf plot within the middle- to upper-rank metamorphic fields.

Cathodoluminescence studies of the light minerals indicate each of the defined quartz types were present. The most common colours were dull brown and reddish-brown, indicating the predominance of metamorphic quartz (Zinkernagel, 1978).

3.4 Characteristics of the Light Fraction

3.4.1 Quartz

Quartz, of the various types outlined by Basu et al. (1975) ranges from 45 to 81%, with an average of 57.9%. Within the 1 to 2 phi size range examined, the grains are very angular with low sphericity to subangular

with high sphericity. Monocrystalline, non-undulatory quartz was the most abundant. Authigenic quartz is very weakly developed.

Inclusions, such as zircon, tourmaline, rutile, apatite, and opaques, are common in the quartz grains.

3.4.2 Feldspar

The total feldspar content varies from 2.4 to 43.3%, with an average of 28.5%. The feldspars are angular with a low sphericity. The feldspars were relatively fresh; kaolinite degradation was rarely seen.

The content of orthoclase ranges from 7 to 32%, averaging 16.5%. The grains are very angular to subangular with low to moderate sphericity. The orthoclase are untwinned.

Microcline ranged from 0 to 9%, with an average of 2.3%, and are very angular to subangular. Spindle shaped lamellae were common.

Plagioclase content ranged from 0 to 24%, averaging 9.7%. The grains were very angular to subangular with low to moderate sphericity, and showed albite twinning.

3.4.3 Rock Fragments

Plutonic and schistose metamorphic rock fragments

occur. Abundances range from 0 to 23% with an average of 6.2%. Plutonic rock fragments are the most common. The mineralogy of the plutonic rock fragments, predominantly quartz, alkali feldspars, plagioclase and mica, suggests an acidic source, probably adamellite to granite in composition.

The metamorphic rock fragments contain abundant polycrystalline quartz with traces of amphibole (hornblende), suggesting amphibolite facies metamorphic rocks in the source area.

CHAPTER 4

HEAVY MINERAL ANALYSIS

4.1 Introduction

Heavy minerals occur as minor, high density accessory grains of sandstones and have long been used as indicators of provenance (Pettijohn et al., 1972). It is well known that certain mineral species are characteristic of certain source rocks and that specific detrital mineral associations are indicative of major classes of source rocks; Table 4.1 summarizes these associations. Because certain mineral species occur in more than one of the major associations, recognition of the varietal characteristics of these minerals can be useful in distinguishing the occurrences from one another.

Inferences about provenance are dependent on the degree of modification affecting the minerals during transportation and deposition. Weathering under intense conditions can be appreciably recognized in sediments deposited at low sedimentation rates. In basins with

TABLE 4.1 The Provenance of Some Common Heavy Minerals

| <u>Rock Type</u> | <u>Indicative Heavy Minerals</u> |
|-----------------------|---|
| Reworked sediments | <u>Well-rounded grains of rutile, tourmaline, zircon.</u> |
| Low-rank metamorphic | <u>Biotite, chlorite, spessartite garnet, tourmaline</u> (especially small, euhedral, brown crystals with graphite inclusions). |
| High-rank metamorphic | <u>Actinolite, andalusite, apatite, almandine garnet, biotite, diopside, epidote, clinozoisite, glaucophane, hornblende</u> (including blue-green varieties, <u>ilmenite, kyanite, magnetite, sillimanite, sphene, staurolite, tourmaline, tremolite, zircon.</u> |
| Sialic igneous | <u>Apatite, biotite, hornblende, ilmenite, monazite, muscovite, rutile, sphene, tourmaline, zircon.</u> |
| Mafic igneous | <u>Augite, diopside, epidote, hornblende, hypersthene, ilmenite, magnetite, olivine, oxyhornblende, pyrope garnet, serpentine.</u> |
| Pegmatites | <u>Apatite, biotite, cassiterite, garnet, monazite, muscovite, rutile, tourmaline</u> (especially indicolite). |
| Ash falls | Euhedral crystals of apatite, augite, biotite, hornblende, and zircon. |
| Authigenic | Hematite, leucoxene, limonite, tourmaline, zircon; euhedral crystals of anatase, brookite, pyrite, rutile, and sphene. |

(Underlined minerals are present in the samples studied; after Hubert, 1971.)

moderate to rapid sedimentation rates, modification of heavy mineral compositions is negligible (van Andel, 1959). Grain elimination during transportation is unlikely, however, some loss due to abrasion and rounding is to be expected.

Hydraulic conditions during deposition can modify heavy mineral assemblages. Under given hydraulic conditions, the heavy minerals are deposited with light minerals of somewhat larger size (Rittenhouse, 1943). Heavy minerals also tend to be concentrated in the finer grained portions of sandstones (Rubey, 1933). This phenomenon of selective sorting can have profound effects on the resultant heavy mineral suites. Potter (1955) illustrates this relationship between grain size and heavy mineral frequencies.

In closely spaced samples of varying grain size the heavy mineral assemblages can differ markedly. To reduce the effects of selective sorting, comparisons between heavy mineral samples should be restricted to comparable portions of sandstones that have essentially the same grain size and degree of sorting (Rubey, 1933). The choice of grain size to be studied requires some consideration.

4.2 Choice of Grain Size

It is necessary to restrict heavy mineral studies to a size class narrow enough to produce uniform optical effects and reduce or eliminate variation in heavy mineral proportions caused by differences in grain sizes in the samples (Carver, 1971). With this in mind, the 0.250 to 0.063mm fraction was used for this study. This grain size enabled confident and reproducible mineral identification and grain counts, ensured sufficient yields of heavy minerals from the bulk samples, and allowed comparison with other information and data sources.

Muller (1967) recommends the study of 0.63 to 0.200mm grains; Carver (1971) considers 0.125 to 0.250mm to be ideal. The use of 0.63 to 0.250mm is in keeping with heavy mineral studies in the literature but contrasts with a similar study of the Cretaceous sands on the Labrador Shelf by Higgs (1977) who used the 0.045 to 0.075mm grain size which is much finer than the size range suggested by previous workers. Higgs had to deal with the persistent problem of sample shortage and found through preliminary work that the 0.045 to 0.075mm size range provided the greatest abundance of heavy minerals, even though identification of minerals becomes difficult for such fine grains.

4.3 Methodology

4.3.1 Laboratory Techniques

Sample treatment procedures are provided in detail in Appendix 1 and a brief discription outlined in Chapter 3 (p. 57).

Prior to mounting the heavy mineral grains, the magnetic minerals (magnetite and ilmenite) were removed. These portions were weighed and the weights recorded in Appendix 2.

4.3.2 Apparatus

Mineral identifications were carried out on the same apparatus used for the light mineral analysis (see Chapter 3, p. 57). Additional identification aids include: Milner (1962), Larsen and Berman's (1934) tables for determining non-opaque minerals, and Russel's (1941) tables of non-opaque heavy minerals.

4.3.3 Petrographic Procedures

A modification of the ribbon method, yielding number percentages (Galehouse, 1971), was used during grain counting. This method involves counting all the grains that lie completely within specified limits, in this case, the field of view. The grain mount was moved across the microscope stage using a Zeiss click stage. The width of the field of view was 1.7mm with 3mm spacing between

traverses to ensure that grains were not counted twice.

Because non-opaque, non-micaceous, non-diagenetic minerals are the most useful in making genetic interpretations, Hubert's (1971) procedure was adopted. Initially, 100 grains of all types were counted from which relative proportions of opaques, micas, diagenetic, and other minerals were determined. Counting continued until 200 non-opaque, non-micaceous, and non-diagenetic minerals were counted. This method allows expression of the opaque, micaceous, and diagenetic minerals as percentages of the whole sample and the heavy minerals as relative minerals percents.

The roundness of the first 10 grains of each non-opaque, non-micaceous, non-diagenetic mineral type was recorded.

4.4 Results

The heavy mineral compositions (excluding opaque, micaceous and authigenic minerals) determined during grain counting are given in Table 4.2. This table also includes Hubert's (1962) the Zircon-Tourmaline-Rutile (ZTR) index. Force (1980) questioned the validity of the ZTR index, because of the restricted provenance of rutile (high-grade metamorphic rocks rather than igneous rocks), believing the use of rutile in the ZTR index is only partially valid.

TABLE 4.2 Results of Heavy Mineral Grain Counting

| MAJOR HEAVY MINERALS | | | | | | | | | MINOR HEAVY MINERALS | | | | | | | | ZTR INDEX |
|-----------------------|------|------|------|------|------|------|------|-----|----------------------|-----|------|-----|------|-----|-----|------|--------------|
| DEPTH | GNT | EPD | RUT | THL | ZIR | PYX | AMP | STR | KYH | AND | APT | SIL | MONA | DUM | SPH | UKN | |
| <u>Karlsefni A-11</u> | | | | | | | | | | | | | | | | | |
| 2188 | 35.5 | 9.0 | - | 5.0 | 7.5 | 2.0 | 0.5 | 0.5 | 36.5 | - | 3.0 | - | - | - | 0.5 | - | 12.5 |
| 2211 | 41.5 | 7.5 | 4.5 | 18.0 | 13.0 | T | - | 4.5 | 11.0 | T | T | - | - | - | - | - | 25.5 |
| 2235 | 42.5 | 9.0 | 1.5 | 5.5 | 11.5 | - | - | 5.0 | 22.5 | - | 1.5 | - | - | - | 1.0 | - | 18.5 |
| 2299 | 40.5 | 5.0 | 4.0 | 22.5 | 12.5 | 2.0 | - | 4.0 | 9.5 | - | - | - | - | - | T | - | 39.0 |
| 2336 | 39.5 | 6.0 | 3.0 | 26.5 | 15.5 | 1.5 | - | 5.0 | 1.0 | - | - | - | - | - | 1.5 | - | 45.0 |
| 2374 | 56.5 | 3.0 | 2.5 | 12.5 | 17.0 | 1.0 | - | 5.0 | 2.5 | - | - | - | - | - | - | - | 32.0 |
| 2400 | 32.0 | 6.0 | 3.5 | 22.0 | 8.5 | 1.5 | - | 4.0 | 1.5 | 4.0 | - | - | - | - | 3.5 | - | 34.0 |
| 4128 | 10.5 | 37.0 | 1.0 | 2.0 | 2.0 | 1.0 | - | 0.5 | 45.5 | - | 1.0 | - | - | - | - | - | 5.0 |
| 4139 | 22.0 | 18.0 | - | 2.0 | - | 2.0 | - | 2.0 | 46.0 | - | 6.0 | - | - | - | 2.0 | - | 2.0 |
| <u>Skolp E-07</u> | | | | | | | | | | | | | | | | | |
| 600 | 41.0 | 16.5 | 2.0 | 3.0 | 14.0 | 4.0 | 5.0 | 4.0 | 2.5 | - | - | 1.0 | T | - | - | 7.0 | 19.0 |
| 750 | 34.0 | 16.0 | - | - | 10.0 | 2.0 | 2.0 | 4.0 | 6.0 | 2.0 | - | - | - | - | - | 24.0 | 10.0 |
| 900 | 19.0 | 16.5 | 1.5 | - | 6.0 | 10.0 | 46.0 | - | - | - | - | - | 0.5 | - | - | 0.5 | 7.5 |
| 950 | 9.0 | 16.5 | - | - | 0.5 | 8.5 | 65.0 | - | - | - | - | - | 0.5 | - | - | - | 0.5 |
| 1000 | 9.5 | 17.0 | 0.5 | - | 2.0 | 11.5 | 60.0 | - | - | - | - | - | 3.5 | - | - | - | 2.5 |
| 1300 | 17.5 | 21.0 | 0.5 | 2.0 | 5.0 | 1.5 | 38.5 | - | 8.0 | - | - | - | 5.5 | T | T | 0.5 | 7.5 |
| 1700 | 22.0 | 26.0 | - | - | 11.0 | 3.0 | 7.0 | - | 31.0 | - | - | - | - | - | - | - | 11.0 |
| 1850 | 11.5 | 20.0 | 1.5 | - | 4.0 | 3.0 | 1.5 | 1.5 | 54.5 | - | 2.5 | - | - | - | - | - | 5.5 |
| 2200 | 51.0 | 5.0 | 2.0 | 7.5 | 1.5 | 6.5 | 1.5 | 0.5 | 18.0 | - | 4.0 | - | 0.5 | 0.5 | - | - | 11.0 |
| 2750 | 14.0 | 4.0 | 2.0 | 4.0 | 48.0 | 6.0 | - | - | 10.0 | - | 2.0 | - | 2.0 | 2.0 | - | - | 54.0 |
| 2950 | 69.0 | 0.5 | 0.5 | 5.0 | 7.0 | 3.0 | - | 1.0 | 10.0 | - | 3.0 | - | 0.5 | 0.5 | - | T | 12.5 |
| <u>Snorri J-90</u> | | | | | | | | | | | | | | | | | |
| 1789 | 42.5 | 13.0 | 2.0 | 10.5 | 15.0 | 2.0 | - | 6.5 | 2.5 | - | - | - | 1.5 | - | T | 4.5 | 27.5 |
| 1832 | 42.5 | 14.0 | 4.0 | 14.0 | 9.0 | 1.0 | - | 2.0 | 4.0 | - | - | - | 1.0 | - | - | 4.0 | 27.0 |
| 1850 | 40.0 | 11.0 | 3.5 | 13.0 | 6.5 | 4.0 | - | 8.5 | 3.0 | 0.5 | 1.0 | - | 1.5 | - | - | 2.0 | 23.0 |
| 1868 | 51.5 | 13.0 | 2.5 | 10.5 | 3.5 | 3.0 | - | 2.0 | 3.5 | - | - | - | - | - | 1.0 | 4.5 | 16.5 |
| 1887 | 43.5 | 8.5 | 2.0 | 13.5 | 4.0 | 3.5 | - | 1.5 | 5.5 | - | - | - | 3.0 | - | 5.0 | 9.0 | 19.5 |
| <u>Gudrid H-55</u> | | | | | | | | | | | | | | | | | |
| 2178 | 13.5 | 13.0 | 14.5 | 3.0 | 17.5 | 3.0 | - | 1.5 | 18.0 | - | 8.0 | - | 3.0 | - | - | 5.0 | 35.0 |
| 2230 | 15.5 | 5.5 | 8.5 | 1.5 | 58.5 | 0.5 | 1.0 | 1.5 | 1.5 | - | 2.5 | - | 2.5 | - | 0.5 | 0.5 | 68.5 |
| 2318 | 12.5 | 10.5 | 2.5 | 2.0 | 24.5 | - | 3.5 | 1.0 | 26.5 | - | 4.0 | - | - | - | - | - | 29.0 |
| 2355 | 24.0 | 10.0 | 6.0 | 10.0 | 10.0 | - | - | - | 28.0 | - | 10.0 | - | - | - | - | 2.0 | 26.0 |

TABLE 4.2 Results of Heavy Mineral Grain Counting - cont'd

| MAJOR HEAVY MINERALS | | | | | | | | | | MINOR HEAVY MINERALS | | | | | | ZTR INDEX | |
|----------------------|------|------|-----|------|------|-----|-----|-----|------|----------------------|-----|-----|------|-----|-----|-----------|-----------|
| DEPTH | GHT | EPD | RUT | TML | ZIR | PYX | AMP | STR | KYN | AND | APT | SIL | HONA | DMH | SPH | VMH | ZTR INDEX |
| <u>Carrier D-70</u> | | | | | | | | | | | | | | | | | |
| 1256 | 54.0 | 23.0 | 1.0 | 1.0 | 5.0 | 2.0 | - | 0.5 | 13.0 | 0.5 | T | - | - | - | - | 1.0 | 7.0 |
| 1274 | 56.0 | 9.5 | 3.5 | 10.0 | 8.0 | 1.0 | 1.0 | 1.5 | 2.0 | - | 0.5 | - | 3.0 | - | - | 3.5 | 21.5 |
| 1286 | 72.5 | 11.5 | 1.5 | 2.0 | 4.5 | - | - | 1.5 | 3.0 | 1.0 | - | - | 0.5 | - | - | 0.5 | 8.0 |
| 1302 | 66.0 | 14.0 | - | 3.0 | 3.0 | - | - | - | 7.0 | - | - | - | 1.0 | - | - | 2.0 | 6.0 |
| 1323 | 65.0 | 6.0 | 2.0 | 4.5 | 6.0 | 0.5 | 0.5 | 7.0 | 1.0 | 0.5 | - | - | 3.5 | 0.5 | - | - | 12.5 |
| 1353 | 48.0 | 11.5 | 2.0 | 11.0 | 9.0 | 2.0 | 2.0 | 1.0 | 4.5 | - | - | - | 4.0 | - | - | 4.0 | 22.0 |
| 1710 | 27.5 | 7.0 | - | 2.0 | 5.5 | 0.5 | 0.5 | 2.5 | 18.0 | 0.5 | 0.5 | - | 1.0 | - | - | 7.0 | 7.5 |
| 1774 | 32.0 | 11.0 | 2.0 | 1.0 | 4.0 | - | - | 1.0 | 15.0 | 2.0 | - | - | 1.0 | - | - | 5.0 | 7.0 |
| 1817 | 32.0 | 10.0 | - | 2.0 | - | - | - | 3.0 | 2.0 | 4.0 | 1.0 | - | 6.0 | - | - | 5.0 | 2.0 |
| 1847 | 55.0 | 10.0 | - | - | 12.5 | - | - | - | 15.0 | 2.5 | 2.5 | - | 2.5 | - | - | - | 12.5 |
| 1859 | 68.0 | 4.0 | - | - | 20.0 | - | - | - | 2.0 | T | - | - | - | - | - | - | 20.0 |
| <u>Leif H-48</u> | | | | | | | | | | | | | | | | | |
| 1259 | 66.0 | 9.5 | 1.5 | 2.5 | 6.5 | - | - | 2.5 | 6.5 | - | 0.5 | - | 0.5 | 2.0 | - | 0.5 | 10.5 |
| 1270 | 61.5 | 4.5 | 6.5 | 2.0 | 5.0 | 2.0 | T | 3.0 | 11.0 | - | 1.0 | - | - | - | - | - | 13.5 |
| 1286 | 49.0 | 16.0 | 2.0 | 3.0 | 9.0 | - | - | - | 20.0 | 2.0 | - | - | - | - | - | - | 13.0 |
| 1673 | 19.5 | 21.0 | 5.0 | 0.5 | 30.0 | 0.5 | - | - | 6.5 | - | - | - | 6.0 | 0.5 | 0.5 | - | 35.5 |
| 1582 | 21.5 | 31.5 | 2.0 | 1.5 | 22.5 | 0.5 | - | - | 2.0 | 4.0 | 4.5 | 0.5 | 4.5 | 0.5 | - | 4.5 | 26.0 |
| 1691 | 41.0 | 15.0 | 4.0 | 0.1 | 17.5 | 0.5 | - | - | 5.0 | 1.5 | 3.5 | - | 3.5 | 0.5 | 1.0 | 1.5 | 21.6 |
| <u>Freddie B-87</u> | | | | | | | | | | | | | | | | | |
| 908 | 67.5 | 16.5 | 2.0 | 2.5 | 5.0 | 1.5 | - | 1.5 | 2.5 | - | 0.5 | - | - | - | - | - | 9.5 |
| 930 | 65.0 | 17.5 | 3.0 | 3.5 | 1.0 | 2.5 | - | 2.0 | 4.0 | 1.0 | - | - | 0.5 | - | - | - | 7.5 |
| 969 | 61.0 | 22.0 | 2.0 | 4.5 | 3.0 | - | - | 2.0 | 2.5 | - | - | - | 0.5 | - | - | - | 9.5 |
| 994 | 41.0 | 19.5 | 2.5 | 6.0 | 6.0 | 0.5 | - | - | 10.0 | - | 2.0 | - | 1.0 | - | 0.5 | 1.5 | 14.5 |
| 1411 | 17.0 | 26.0 | 3.0 | 1.0 | 31.0 | 1.0 | - | 3.0 | - | - | 1.0 | - | 8.0 | - | - | 9.0 | 35.0 |
| 1425 | 38.0 | 15.0 | 2.5 | - | 17.0 | 1.0 | - | - | 1.0 | - | - | - | 5.5 | - | - | T | 19.5 |
| 1436 | 48.0 | 46.0 | 0.5 | 1.0 | 3.0 | - | - | 1.0 | 0.5 | - | - | - | - | - | - | - | 4.5 |
| 1445 | 32.0 | 56.0 | - | 0.5 | 4.5 | - | - | 5.0 | - | - | - | - | 1.5 | - | - | 4.5 | 5.0 |
| 1463 | 26.5 | 52.0 | 3.0 | 1.0 | 5.0 | - | - | 1.0 | 0.5 | - | 1.0 | 1.0 | 2.5 | - | 0.5 | 2.0 | 9.0 |
| 1475 | 26.5 | 52.0 | - | 0.5 | 15.5 | 1.5 | - | 1.0 | 1.0 | - | - | - | 2.5 | 1.0 | - | 1.0 | 16.6 |
| 1500 | 7.0 | 6.0 | 1.0 | - | 16.0 | - | - | - | 1.5 | - | - | - | 2.0 | - | - | 2.5 | 17.0 |

4.5 Mineralogical Characteristics of the Major Heavy Minerals

The following mineral descriptions are concerned primarily with the specific physical appearance, varietal features, and general optical characteristics of the major heavy minerals found in the sands on the Labrador Shelf. Detailed optical and physical characteristics are easily obtained from standard mineralogy texts and will not be reviewed here.

4.5.1 Non-Opaque, Non-Micaceous, Non-Diagenetic Heavy Minerals

4.5.1.1 Amphibole Group

The amphibole group is represented by green and brown hornblende, basaltic hornblende, and tremolite/actinolite. Glaucophanes was noted. Hornblende (Plates 4.1 and 4.2) is the most abundant and widespread mineral of this group. It occurs as angular to very angular elongate grains with "ragged" terminations. Striations are aligned parallel to the major axis and may display inclined cleavage (Plate 4.3). Most commonly, pleochroism is green to dark green and dark green-brown. Brown to brown-green and green-blue (basaltic hornblende) frequently occurs.

Tremolite/actinolite occurs as colourless to green, elongate, prismatic grains with the same "ragged" terminations as hornblende.

4.5.1.2 Barite

Barite is present in many, but not all samples, and is a result of contamination by drilling mud. Some problems arose during grain identification and counting because of the similarity between rounded kyanite and barite (see p. 79 for discussion of distinguishing between barite and kyanite).

Barite commonly occurs as sub-equant, rounded, white grains (Plate 4.4) often with a bluish colouration. Opaque carbonaceous (?) inclusions occur.

4.5.1.3 Epidote Group

The epidote group is represented by epidote (pistachite), zoisite, and clinozoisite. Allenite rarely occurred. Epidote and clinozoisite are almost equally widespread; zoisite is more restricted.

Epidote (pistachite) is easily recognized by its yellow-green, green-yellow, and colourless appearance (Plates 4.5, 4.6, 4.7, and 4.8) and moderate to strong pleochroism. The "broken bottle-glass", or hackly, appearance (Plates 4.6 and 4.9) are distinctive, as are the

bright rings of green-purple-red interference colours. Epidote occurs commonly as sub-angular grains (Plate 4.5) and occasionally as sub-rounded grains. Prismatic grains were rarely seen (Plates 4.6, 4.7, and 4.8). Striations aligned parallel to the C-axis (Plate 4.10) were encountered. Etched surfaces (Plate 4.9) were rarely seen.

Zoisite occurs as colourless to yellow-grey and yellow-brown, angular to sub-angular, sub-prismatic grains (Plate 4.11). Anomalous blue (Plate 4.12) and distinctive grey-blue interference colours were common, indicating the presence of non-ferroan zoisite. Some zoisite occurs without these anomalous interference colours, suggesting the presence of ferroan, or beta, zoisite. One grain of thulite (pink or Mg-zoisite) was noted.

Clinozoisite was seen as colourless, angular to very angular, prismatic to sub-prismatic grains (Plate 4.13).

4.5.1.4 Garnet Group

Garnet occurs almost exclusively as angular to very angular grains with conchoidally-fractured surfaces (Plates 4.14, 4.15 and 4.16). Colourless garnet (Plate 4.14 and 4.15) is dominant. Abundant pale pink, salmon-pink or pink-brown varieties (Plates 4.16 and 4.17), red-brown grains (Plate 4.18) and rare pale purple and

green grains occurred. Occasional anisotropic grains with weak pleochroism and maximum interference colours reaching first order pink were seen. The anisotropic garnet (Heinrich, 1965) commonly gave a biaxial negative interference figure with a moderate 2V angle.

Based on optical and physical properties, many of the garnet grains are of the almandine variety; spessartine garnet was recognized by its salmon-pink colour, and grossularite by its green and/or colourless nature combined with "typical" garnet features (grain morphology, cleavage, isotropic nature).

Etched surfaces, although not common, were recognized and exhibit a "toothed" or "hacksaw" texture (Plates 4.19 and 4.20). Rare garnet grains with embayed surface boundaries were seen (Plate 4.21).

Inclusions of rutile needles and possibly zircon were occasionally seen.

4.5.1.5 Kyanite

Kyanite generally occurs as colourless (with or without a pale blue tint), sub-angular to sub-rounded, elongate, prismatic grains flattened parallel to the (100) plane and displaying a prominent parting (Plates 4.22 to 4.26). Dusty inclusions (carbonaceous material; Plates 4.25 and 4.26) give the grains a greyish colour. More

commonly, however, the grains are clear and limpid (Plates 4.22 and 4.23). Alteration or decomposition was not seen. Interference colours are usually first order grey to yellow, although some first order red was seen in thicker grains.

Problems arose during grain counting in distinguishing between kyanite and barite. Although the former is biaxial negative with inclined extinction and the latter biaxial positive with straight extinction, the rounding of each mineral reduced the prominence of a long axis, making the extinction characteristic difficult to evaluate. Also, similarities in colour, inclusions, and interference colours made positive identification of each grain difficult unless an interference figure was obtained.

This problem was resolved by counting only those grains with distinctive kyanite features, such as a prominent elongate axis, good crystal shape, presence of cleavage and parting at right angles to each other, and clear first order interference colours. Admittedly, this procedure is unsatisfactory because many kyanite grains were probably ignored, but the author felt that a low kyanite count was more representative of that mineral's occurrence than an inflated one, particularly as kyanite-bearing source rocks are not widespread in the source area.

4.5.1.6 Pyroxene Group

The pyroxene group is represented by both clinopyroxene and orthopyroxene. Clinopyroxene usually occurs as colourless or pale green to yellow-green, sub-angular to angular, prismatic to irregular grains. Generally, identification of individual members of the clinopyroxene group was not possible; however, greenish-brown augite (Plate 4.27) and colourless to pale green diopside were distinguished.

Orthopyroxene grains are generally colourless to pale-yellow and green, angular, and prismatic. Pleochroic colour schemes are shades of pink to green (Plate 4.28). The orthopyroxenes were counted as a group, not as individual mineral species. The optical methods employed did not allow this fine level of mineral identification, and only enstatite and hypersthene could be identified with any degree of certainty.

4.5.1.7 Rutile

Rutile commonly occurs as yellow-brown and red-brown, angular, euhedral grains with bipyramidal terminations (Plates 4.29 and 4.30). Striations parallel to the principal axis are common. Genuiculate twins (Plate 4.31) were rarely seen.

4.5.1.8 Staurolite

Staurolite is usually found as sub-angular to angular irregular grains with distinctive pale yellow-brown to golden-amber pleochroism (Plates 4.32 to 4.35). Small, colourless inclusions commonly occur giving the staurolite grains a "swiss cheese-like" appearance (Russell, 1941; Plates 4.32 and 4.33). Staurolite grains without this distinctive texture were defined on the basis of pleochroism and the ragged, platy nature detrital staurolite exhibits (Heinrich, 1965).

4.5.1.9 Tourmaline

Tourmaline grains show three principal pleochroic schemes: colourless or pink to medium and dark blue (Plate 4.36) or colourless to green and blue (Plate 4.37); colourless or very pale pink to pale green-brown or dark green-brown (Plate 4.38) and colourless to pale yellow and yellow-brown (Plate 4.39). The colours indicate that three divisions can be made: (1) shorlite, which is very dark blue to black, is the most abundant and widespread, (2) elbaite, which is pink, red, green, or blue and (3) dravite, which is yellow to brown.

The grains are commonly angular to very angular (Plates 4.36 to 4.39) although rounded grains (Plates 4.40,

4.41, and 4.42) do occur. Rounded to well-rounded cross-sectional grains also occur (Plates 4.41 and 4.42). Prismatic grains with striations parallel to the principal axis are present (Plate 4.39). Zoning is rarely seen (Plates 4.37 and 4.40); basal, or cross-sectional grains, often show concentric colour zones. Elongate grains exhibiting a style of zoning which is green and blue on opposing ends were uncommon.

Authigenic tourmaline recognized as grain overgrowths are rare (Plate 4.43). Tourmaline grains did not display corrosion features.

Dumortierite was recognized and distinguished from tourmaline by its maximum absorption being at right angles to that of tourmaline. Dumortierite's colour scheme is similar to shorlite (ie. shades of blue).

4.5.1.10 Zircon

Zircon is usually colourless (Plates 4.44, 4.45, 4.46, and 4.53), although pink, lavender, and yellow grains occur. The grains are most commonly angular to very angular and euhedral, although sub-rounded to well-rounded grains frequently occur. Broken prismatic grains are common (Plates 4.45, 4.46, 4.47, 4.51, and 4.52).

Zoning is a common feature of dark-coloured grains, with the darker bands being opaque, suggesting

metamict alteration (Plates 4.45, 4.46, 4.47, 4.48, 4.49, 4.50, 4.51, and 4.52). Zoning in clear, colourless grains (Plate 4.44) was also recognized.

4.5.2 Opaque, Micaceous, Authigenic Minerals

4.5.2.1 Opaque Minerals

Opaque minerals encountered during grain counting include black opaques (magnetite and ilmenite) and pyrite. Magnetic opaques (magnetite and ilmenite) were removed from the heavy mineral fraction prior to grain mounting. Distinctions between magnetite and ilmenite were rarely made with confidence and, therefore, were not counted separately.

Pyrite is abundant in the sands examined in this study. Pyritized foraminifera are common, occurring with a pinwheel-like morphology. Pyritized, hollow rods (spines?) also frequently occur. Aggregates of cubic crystals of brassy-yellow pyrite were present.

4.5.2.2 Micaceous Minerals

Micaceous minerals are generally excluded from the heavy mineral splits. The densities of the micas straddle the heavy mineral/light mineral boundary (specific gravity of 2.9). Their platy morphology causes them to float, and surface tension keeps them accumulated at the top of the

separation liquid; micas also have slow settling velocities due to their large cross-sectional area.

Rare muscovite and biotite grains are present in the heavy mineral splits. Muscovite generally occurs as colourless, occasionally very pale yellow, irregular, platy grains, commonly with undulatory extinction. Inclusions may be present. Biotite is morphologically similar to muscovite and is usually brown to greenish brown.

4.5.2.3 Authigenic Minerals

Non-opaque diagenetic minerals, include the various carbonate minerals and glauconite. Diagenetic carbonate was removed as a result of the hydrochloric acid and stannous chloride treatment.

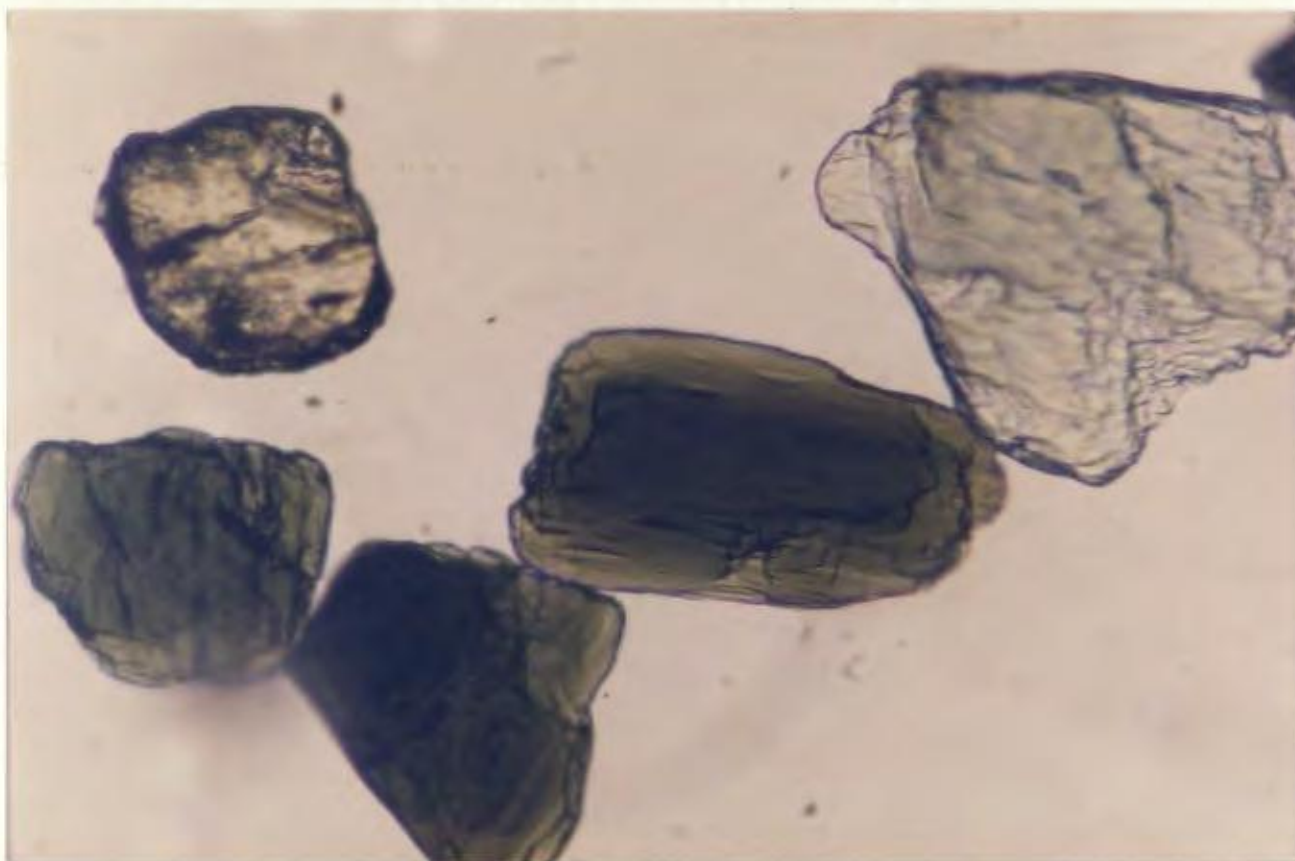
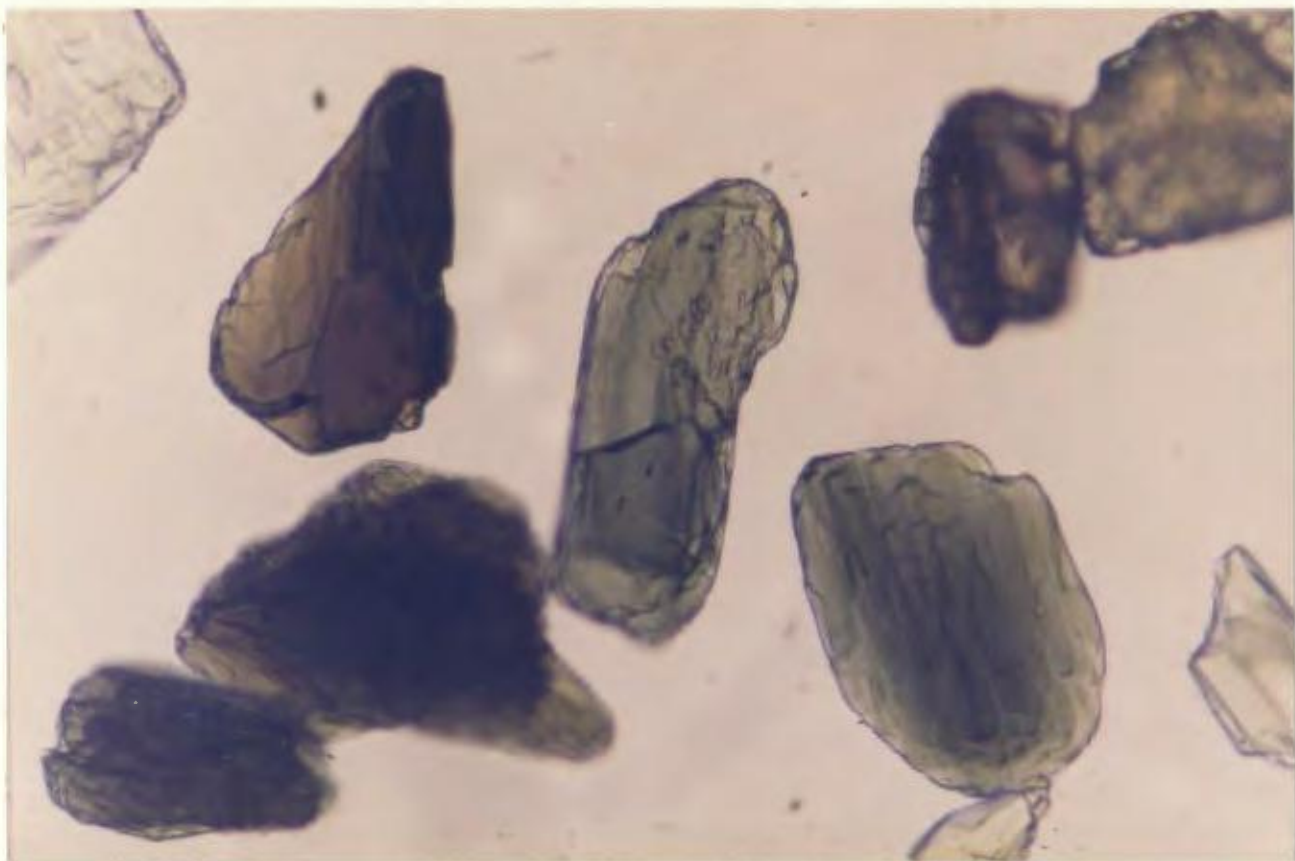
Glauconite occurs as dark green and dark brown (altered) pelletoidal grains. Its specific gravity is between 2.2 and 2.8, and concentrates in the light fraction.

100 microns

Plate 4.1: Green to brown pleochroic hornblende with "ragged" terminations on central elongate grain. Large colourless grain in lower left quadrant is tremolite/actinolite.

100 microns

Plate 4.2: Typical hornblende. Two central grains exhibit green pleochroic scheme; two adjacent grains show brown to brown-green pleochroism.

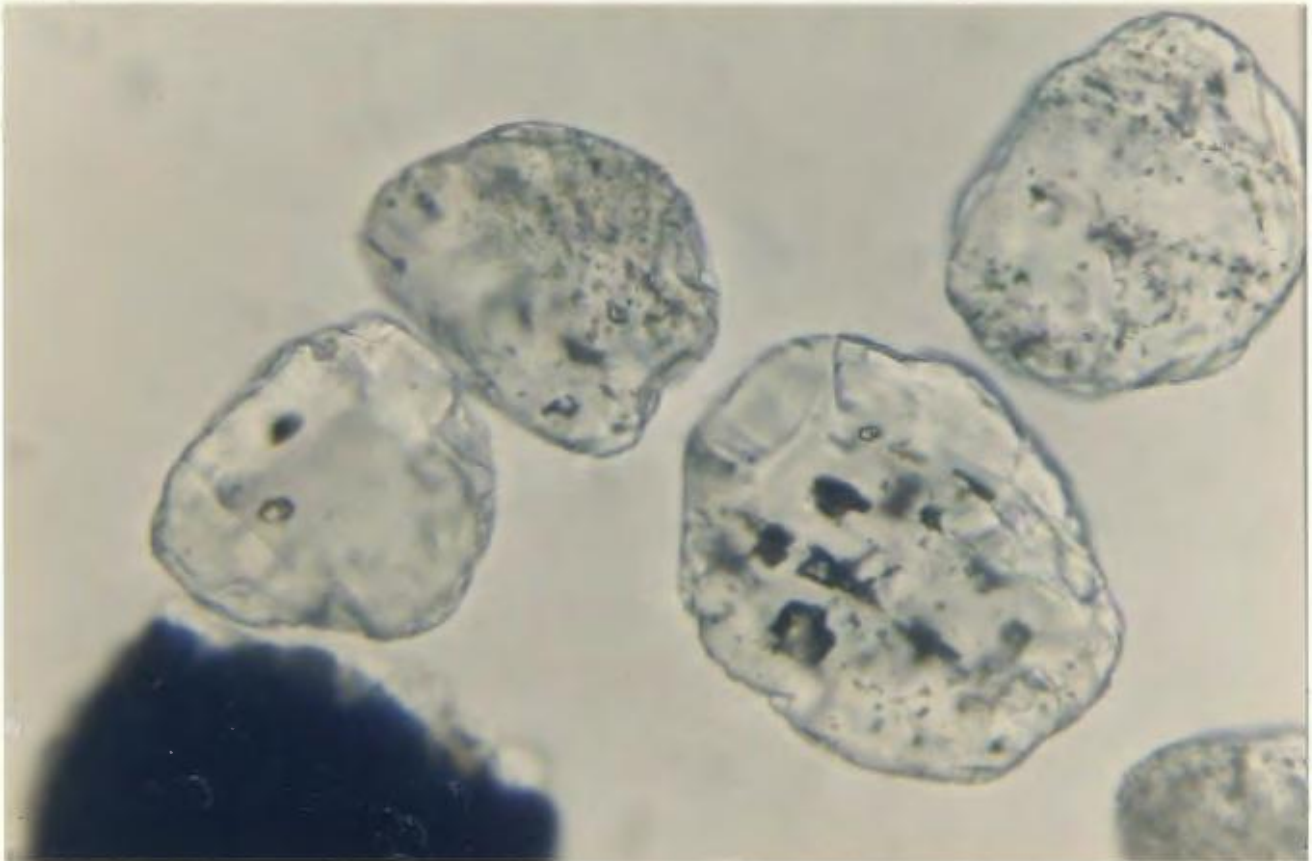


50 microns

Plate 4.3: Green to green-brown pleochroic hornblende with striations aligned parallel to the major axis and inclined cleavage.

100 microns

Plate 4.4: Well-rounded barite with carbonaceous inclusions. Note inclined cleavage.

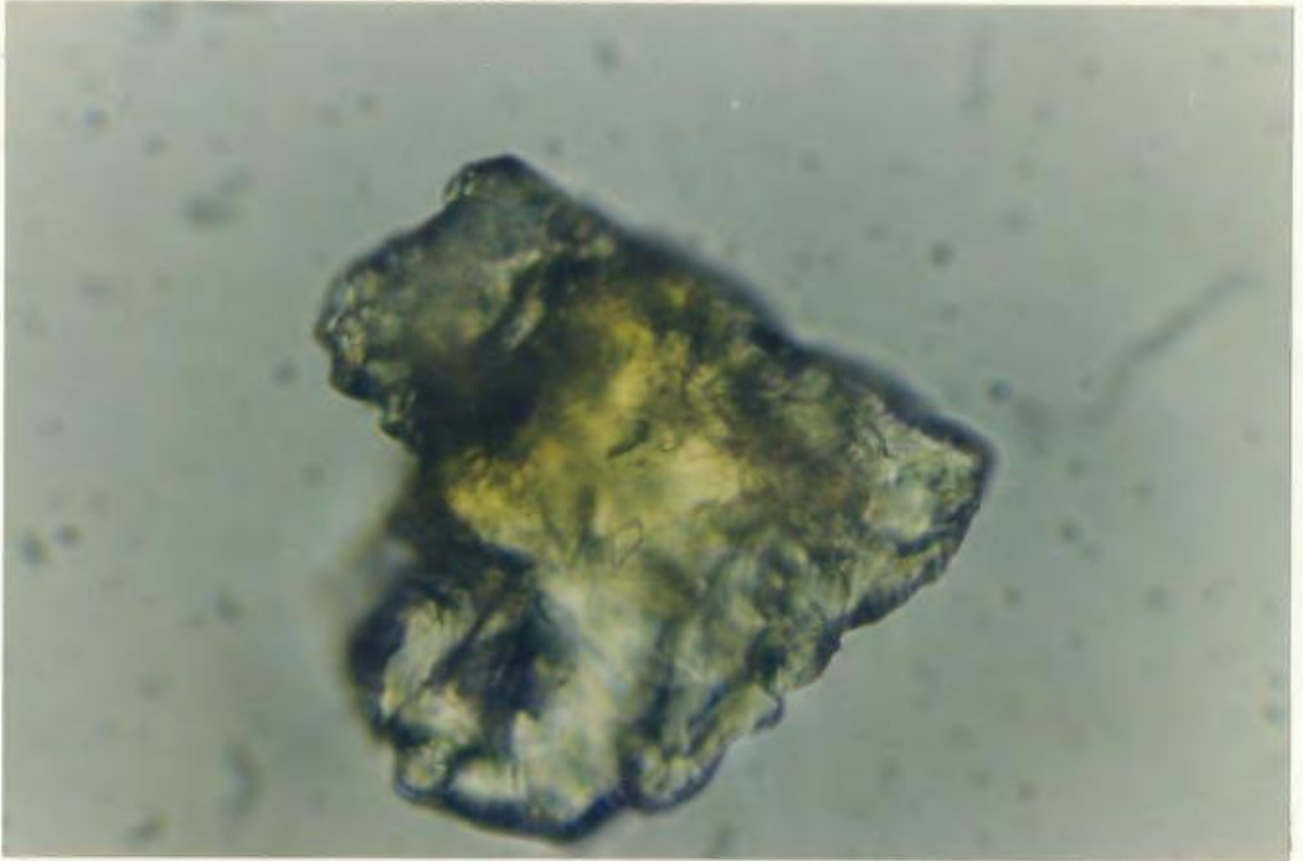


50 microns

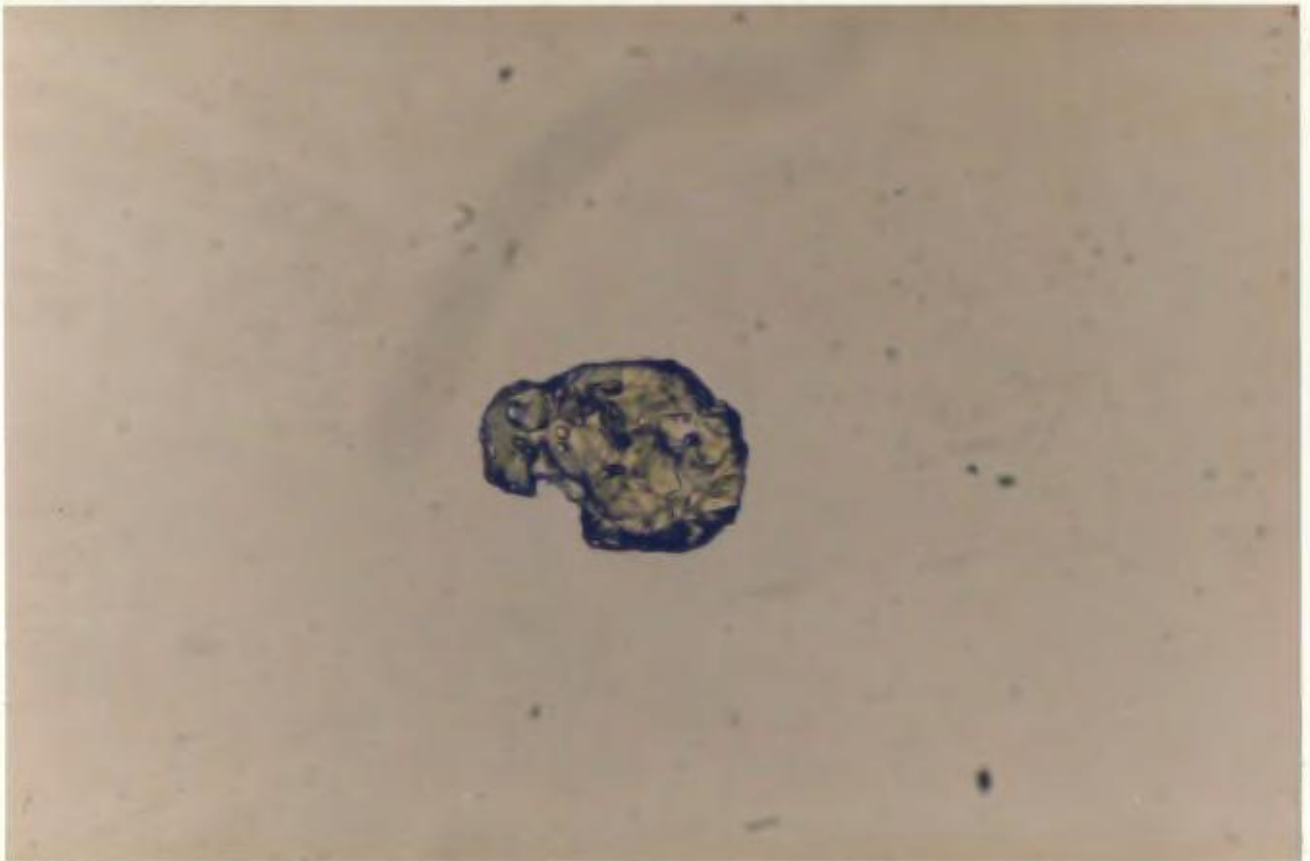
Plate 4.5: Epidote (var. pistachite). Irregular, angular grain with yellow-brown colour.

50 microns

Plate 4.6: Epidote (var. pistachite). Sub-equant, prismatic grain with "hackly" appearance and green-yellow colour.



Plate



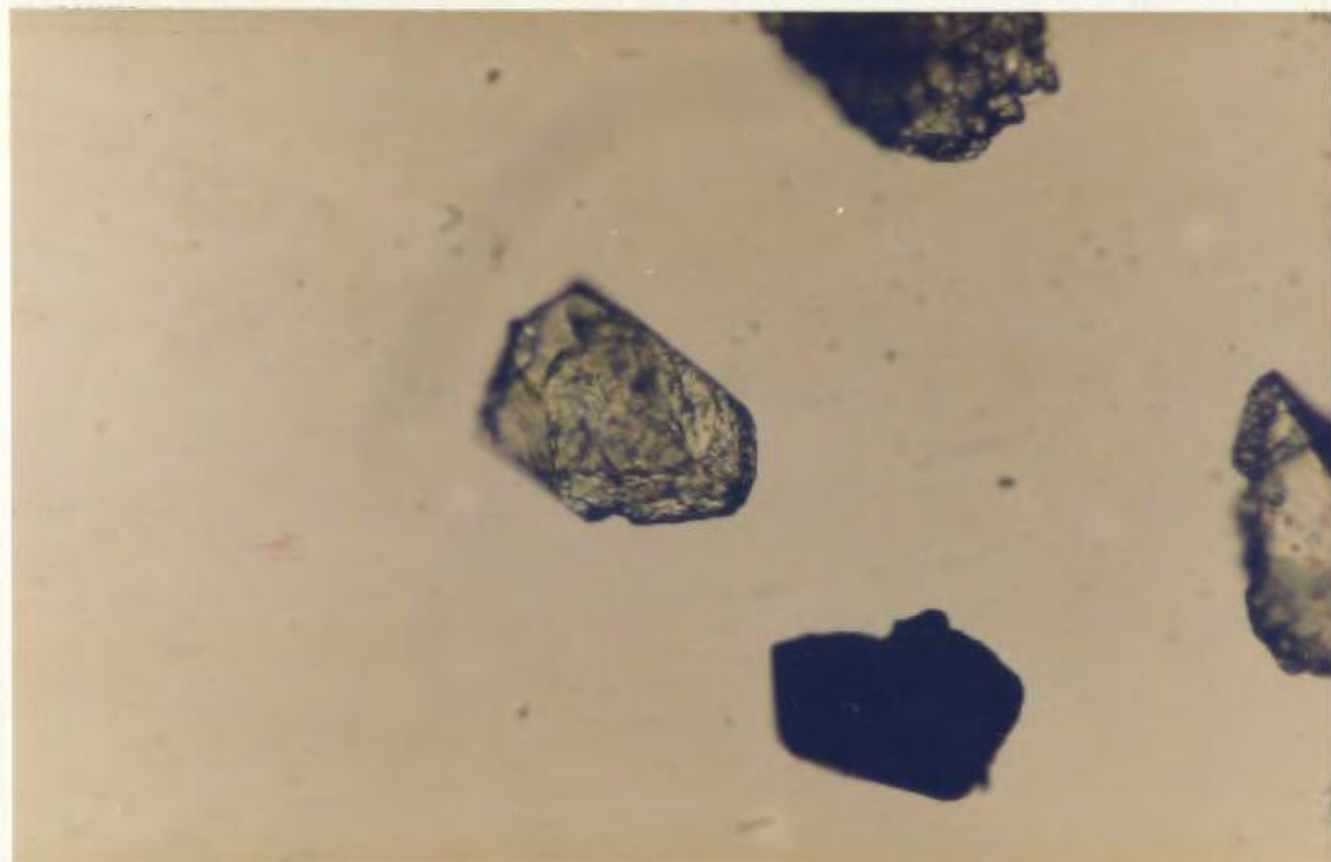
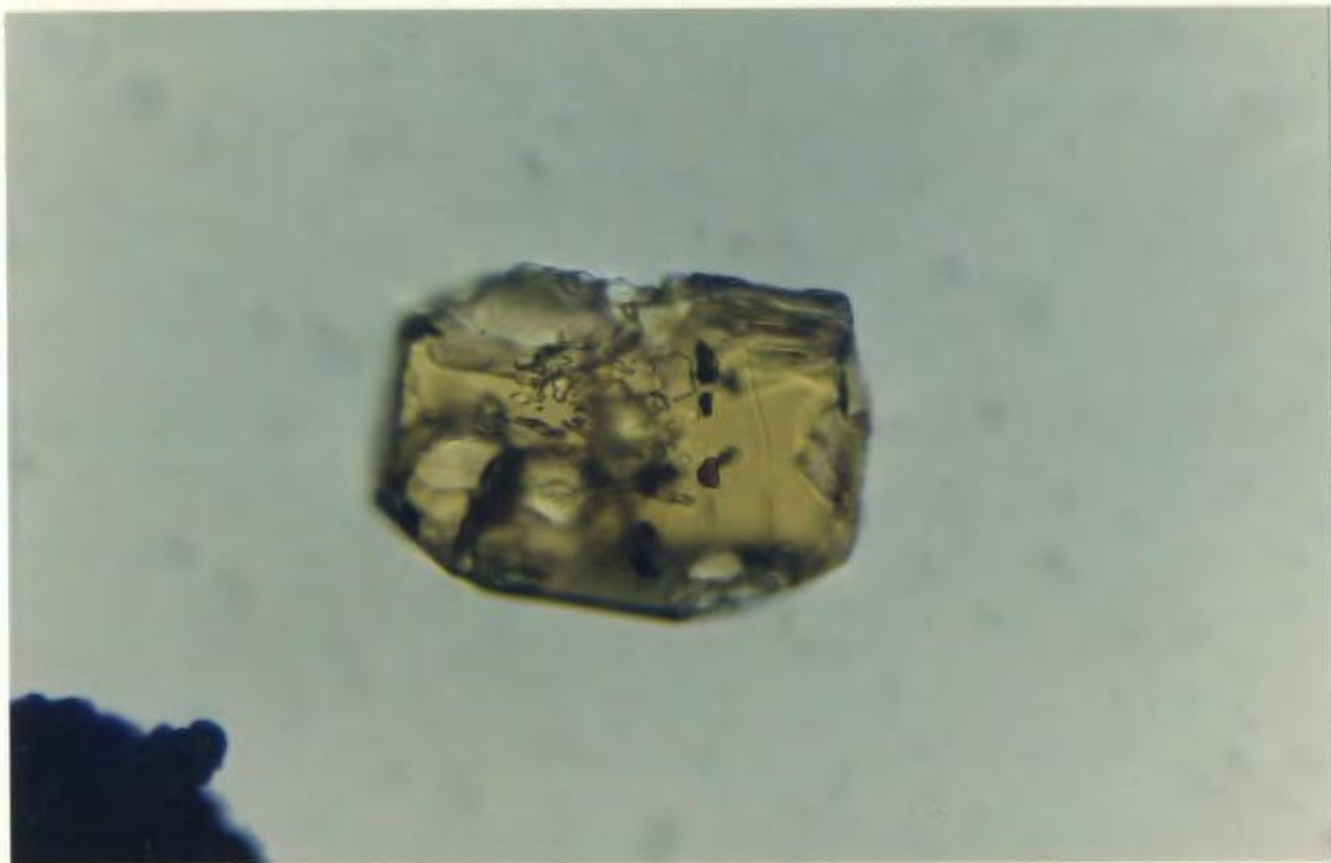
Plate

50 microns

Plate 4.7: Epidote (var. pistachite). Typical barrel-shaped prismatic grain with yellow to green pleochroic scheme.

100 microns

Plate 4.8: Epidote bipyramidal prismatic grain.

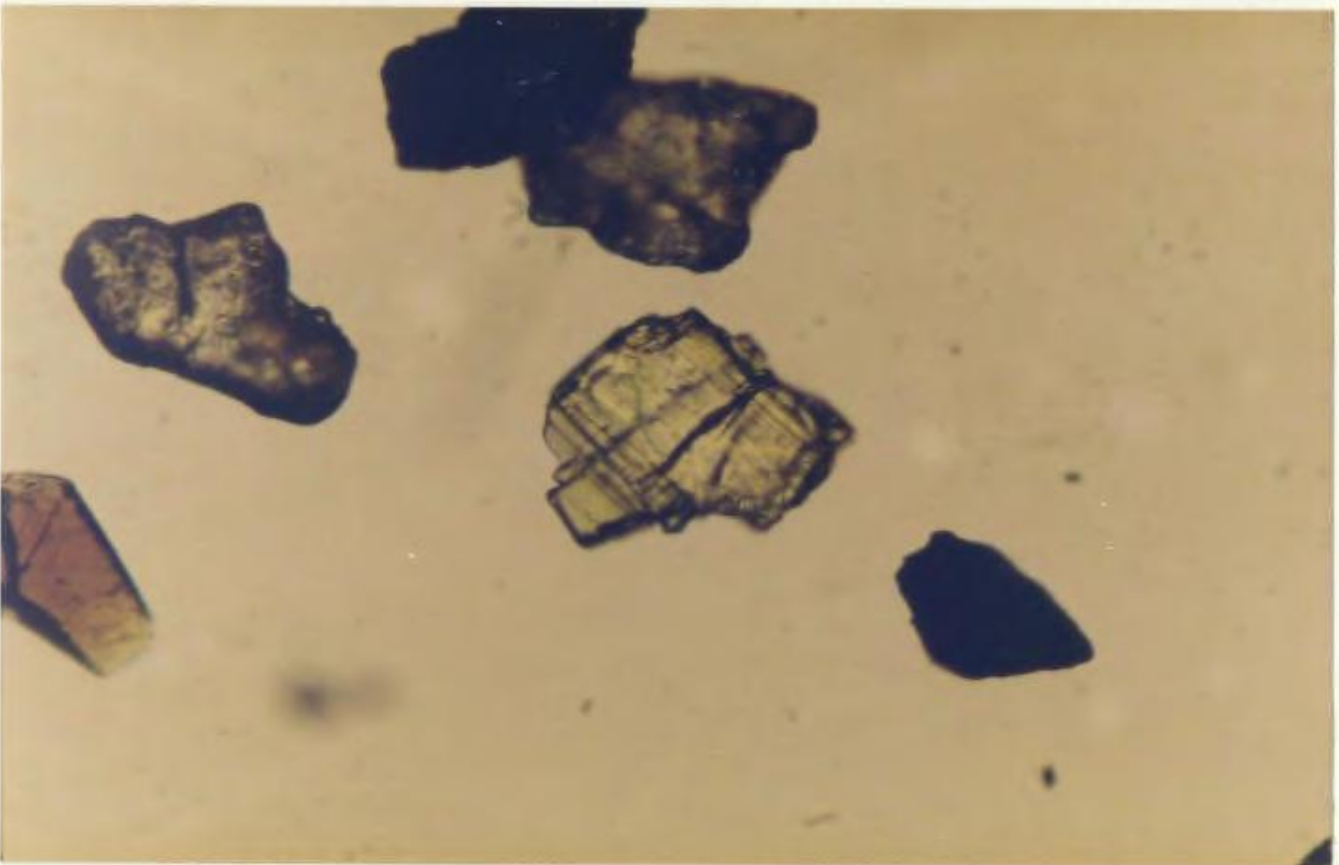
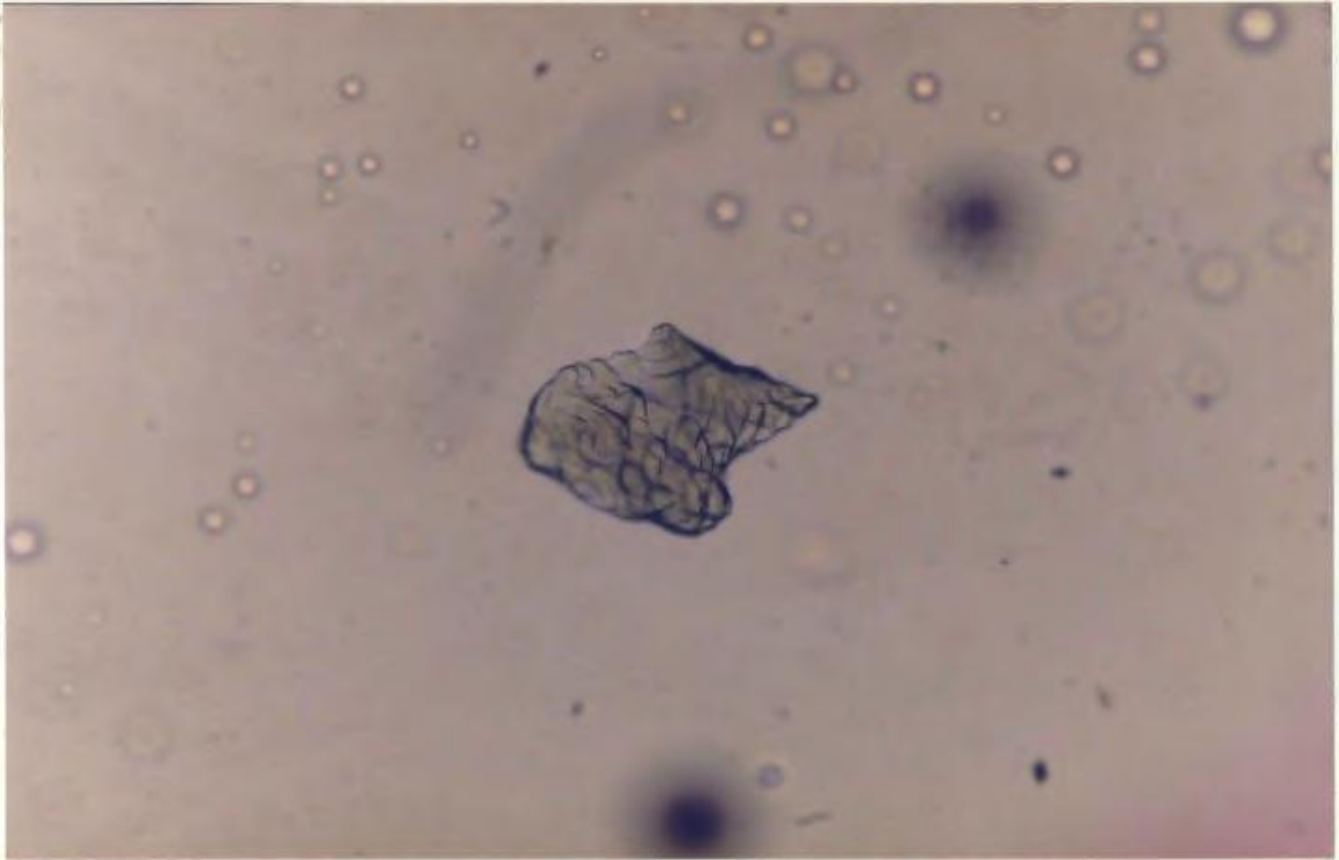


100 microns

Plate 4.9: Epidote grain showing surface etching.

100 microns

Plate 4.10: Epidote. Sub-prismatic grain with prominent striations.

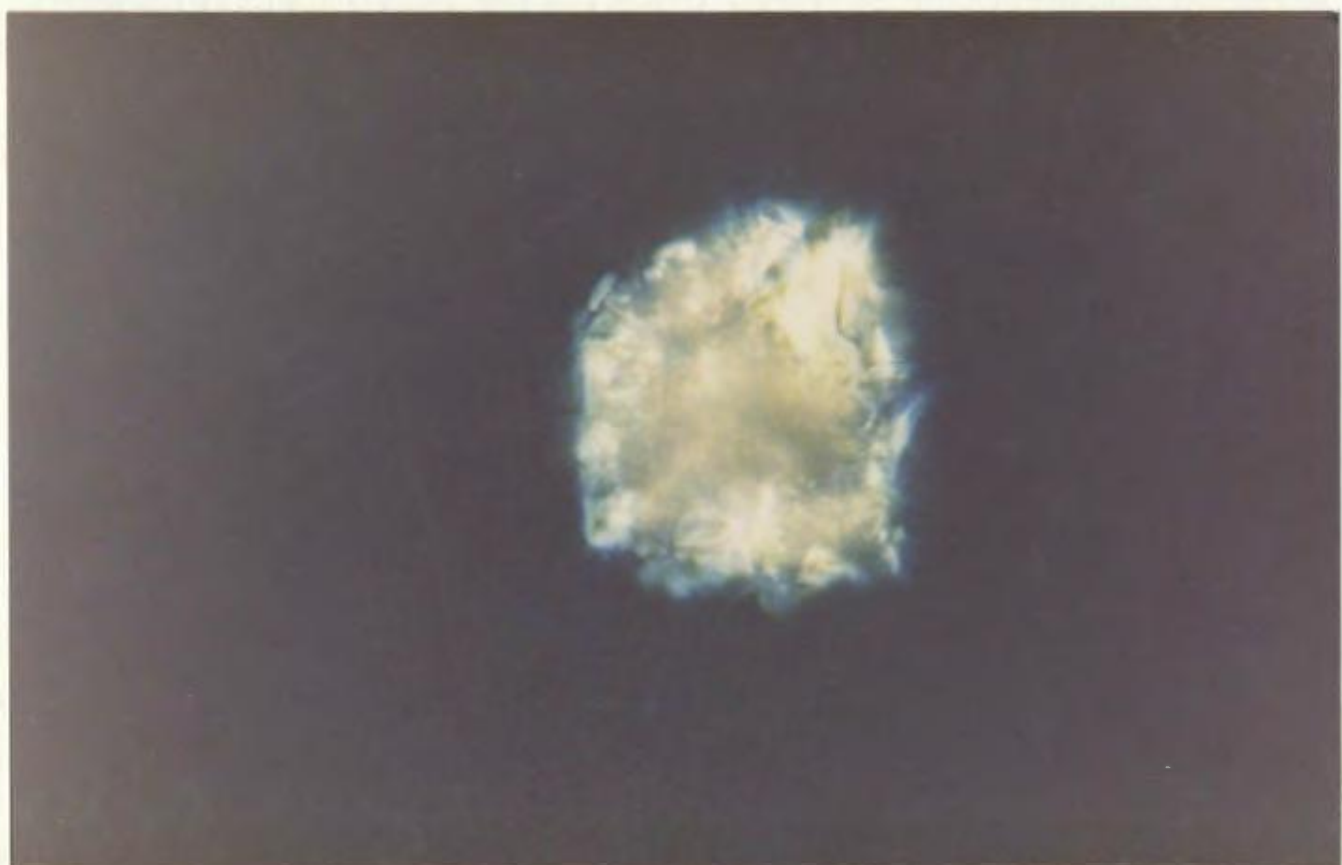
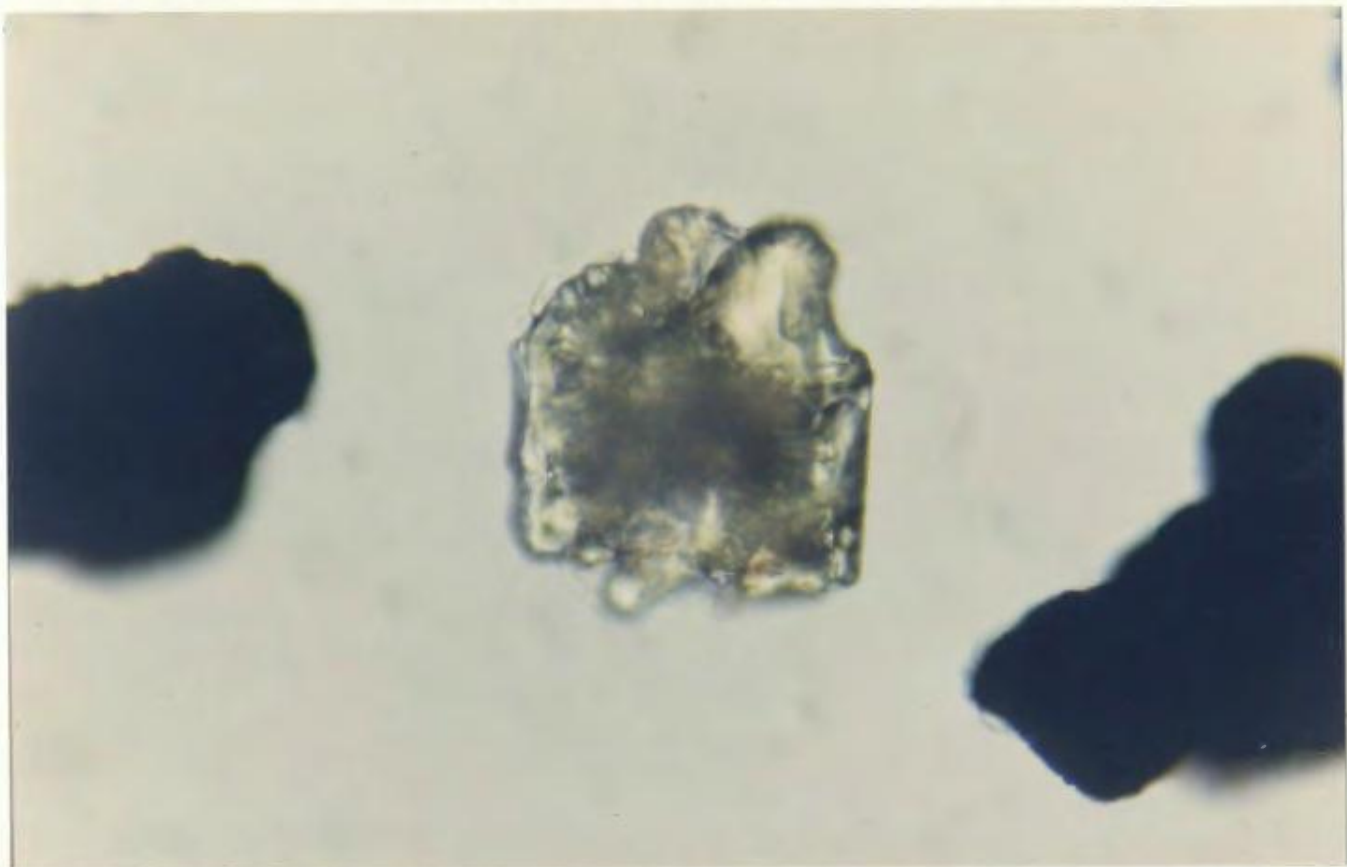


100 microns

Plate 4.11: Epidote (var. Zoisite). Common yellow-grey to yellow-brown, sub-angular, sub-prismatic grain.

100 microns

Plate 4.12: Ultrablue interference colours of non-ferroan zoisite (above grain, Plate 4.11, under crossed nicols).



100 microns

Plate 4.13: Clinozoisite.

100 microns

Plate 4.14: Garnet. Colourless grain with conchoidal fracture.



Plate



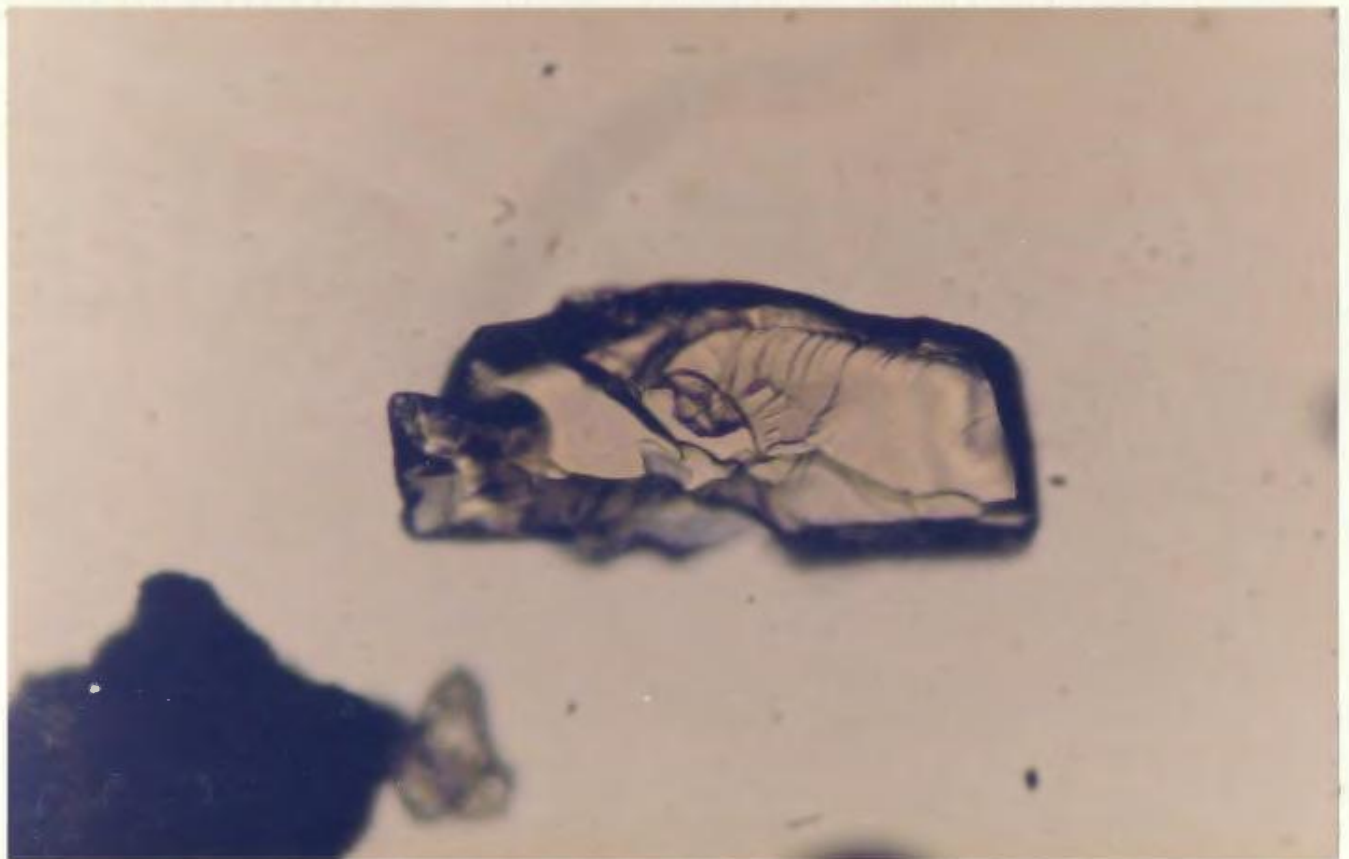
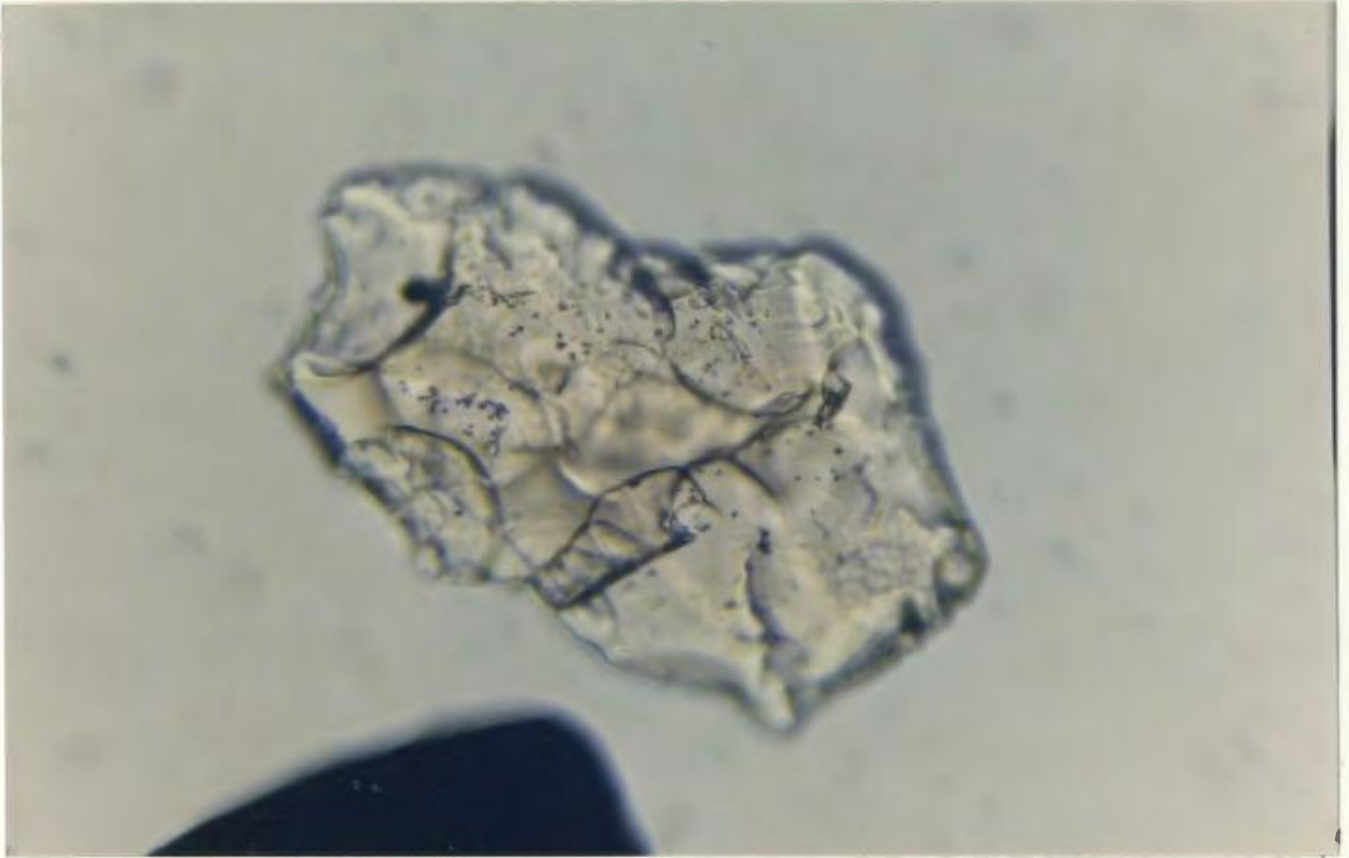
Plate

100 microns

Plate 4.15: Garnet. Colourless grain with conchoidal fracture and "hackly" appearance.

100 microns

Plate 4.16: Garnet. Salmon-pink (pink-brown) elongate grain with prominent conchoidal fracture.

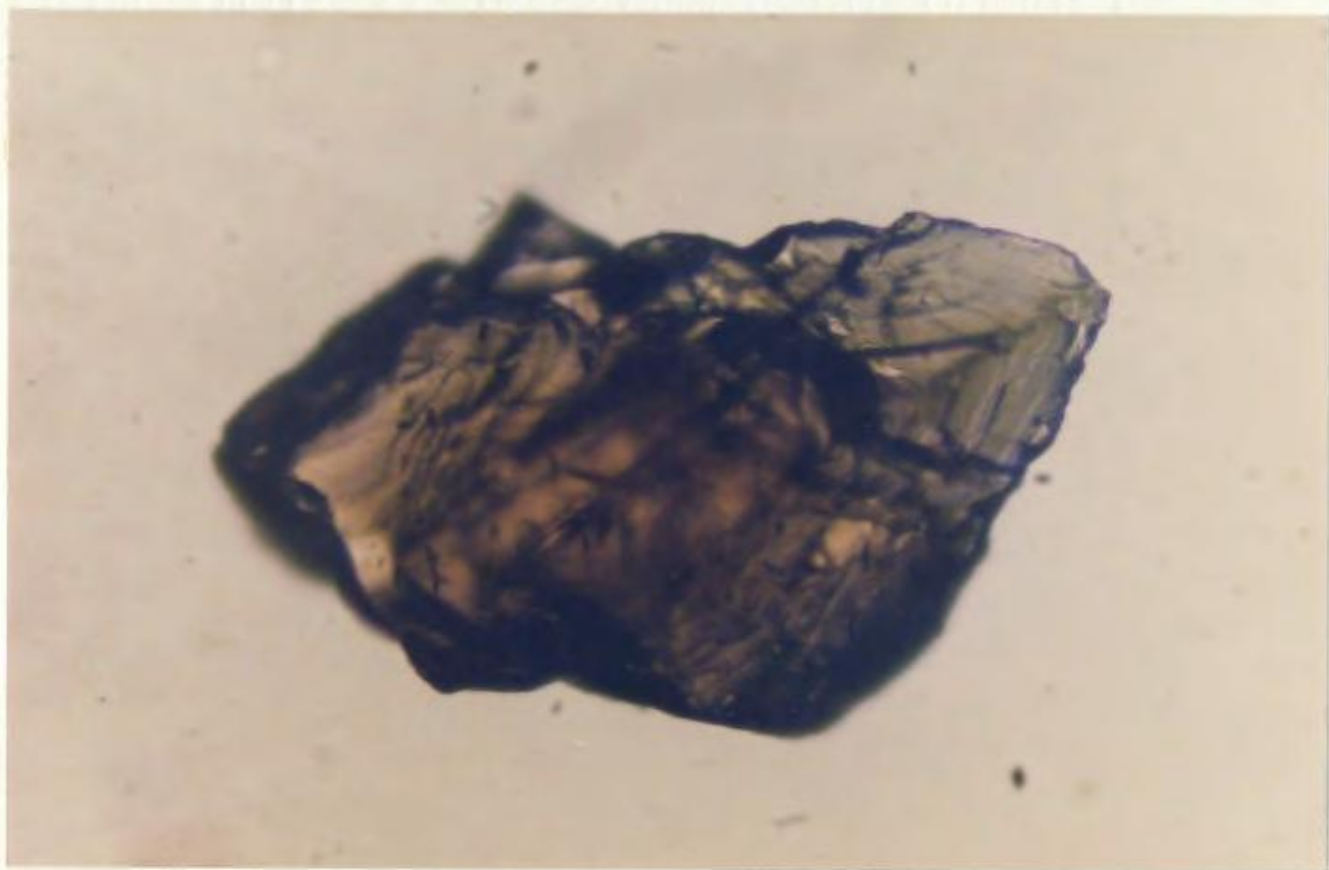
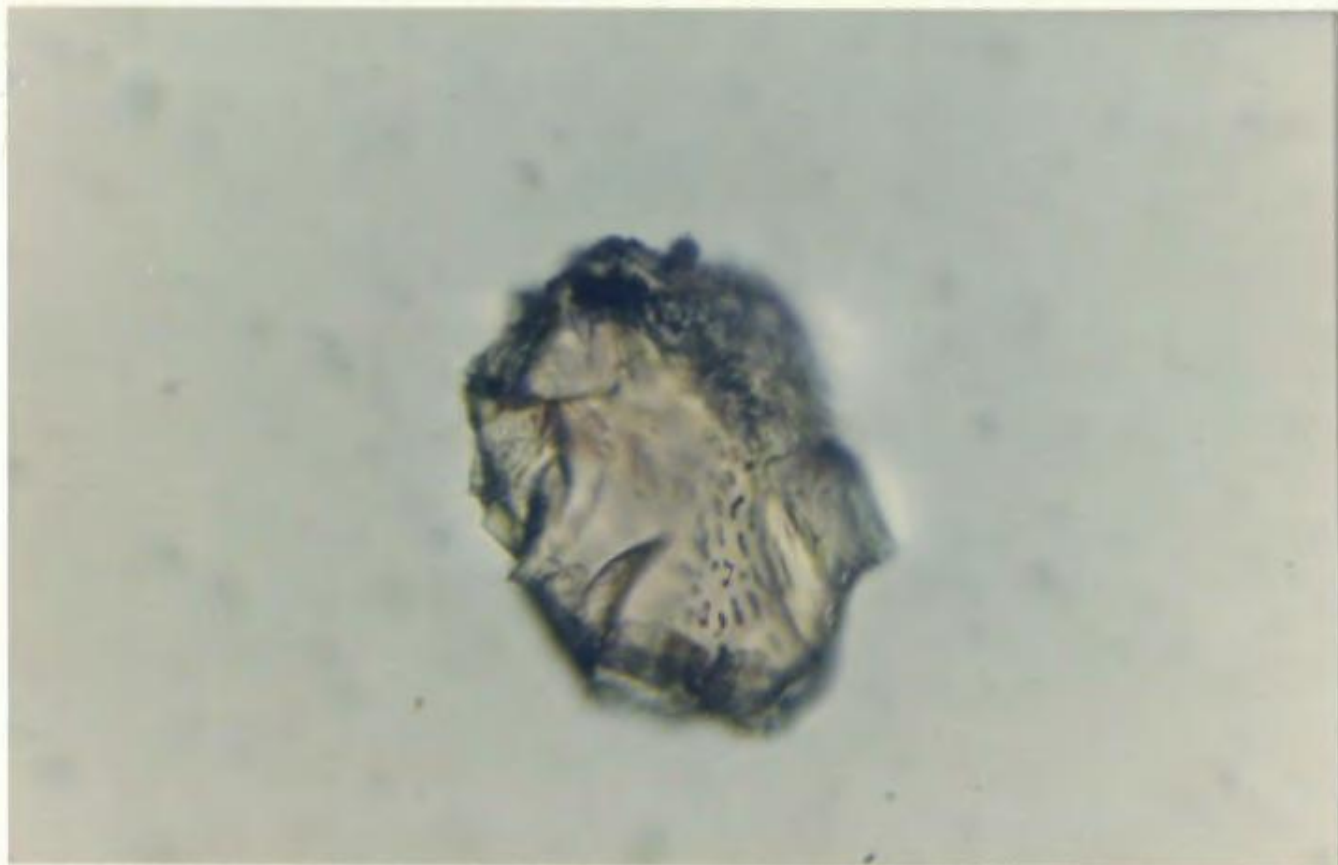


100 microns

Plate 4.17: Garnet. Salmon-pink (pink-brown), sub-angular, sub-equant grain. Note inclusions.

50 microns

Plate 4.18: Garnet. Red-brown, sub-angular grain with well developed conchoidal fracture.

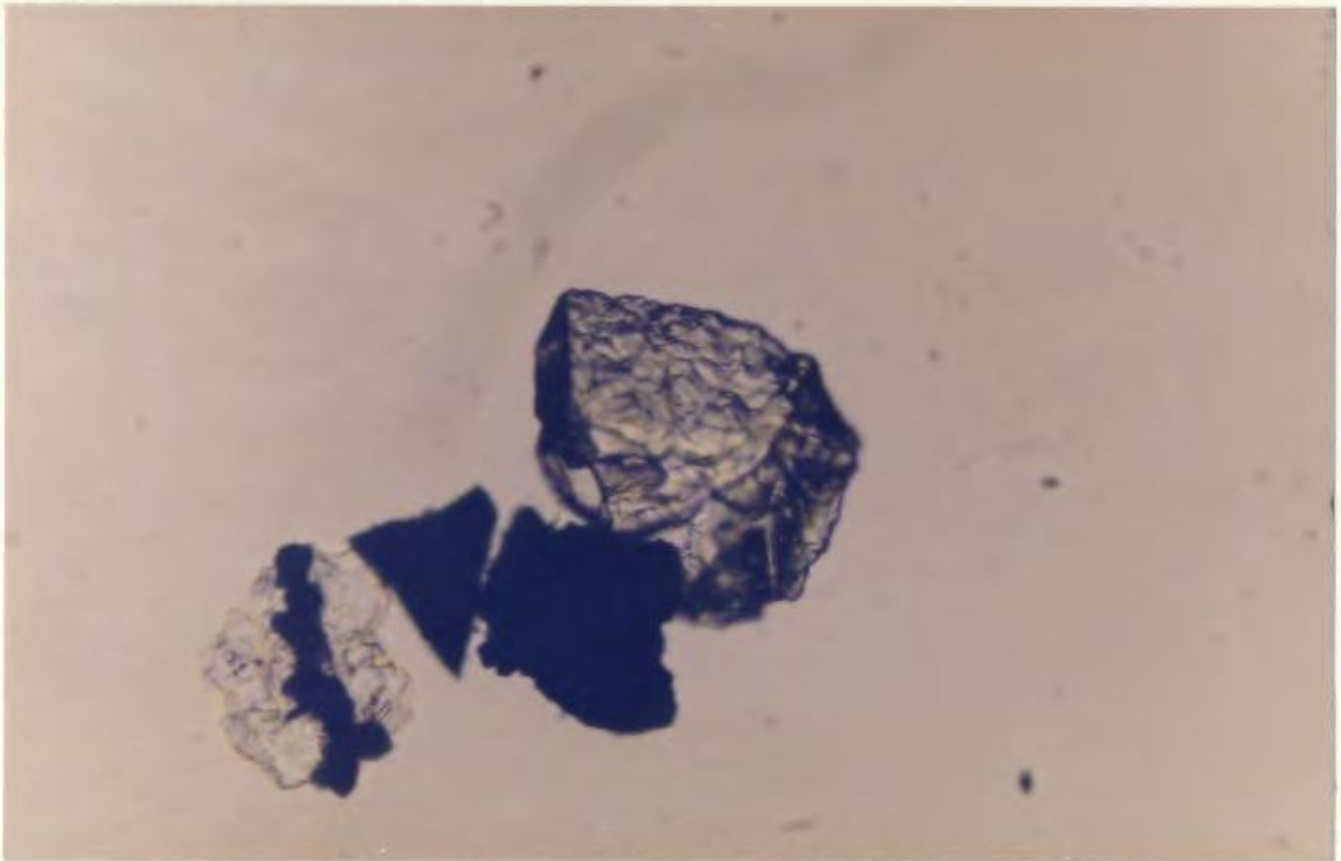
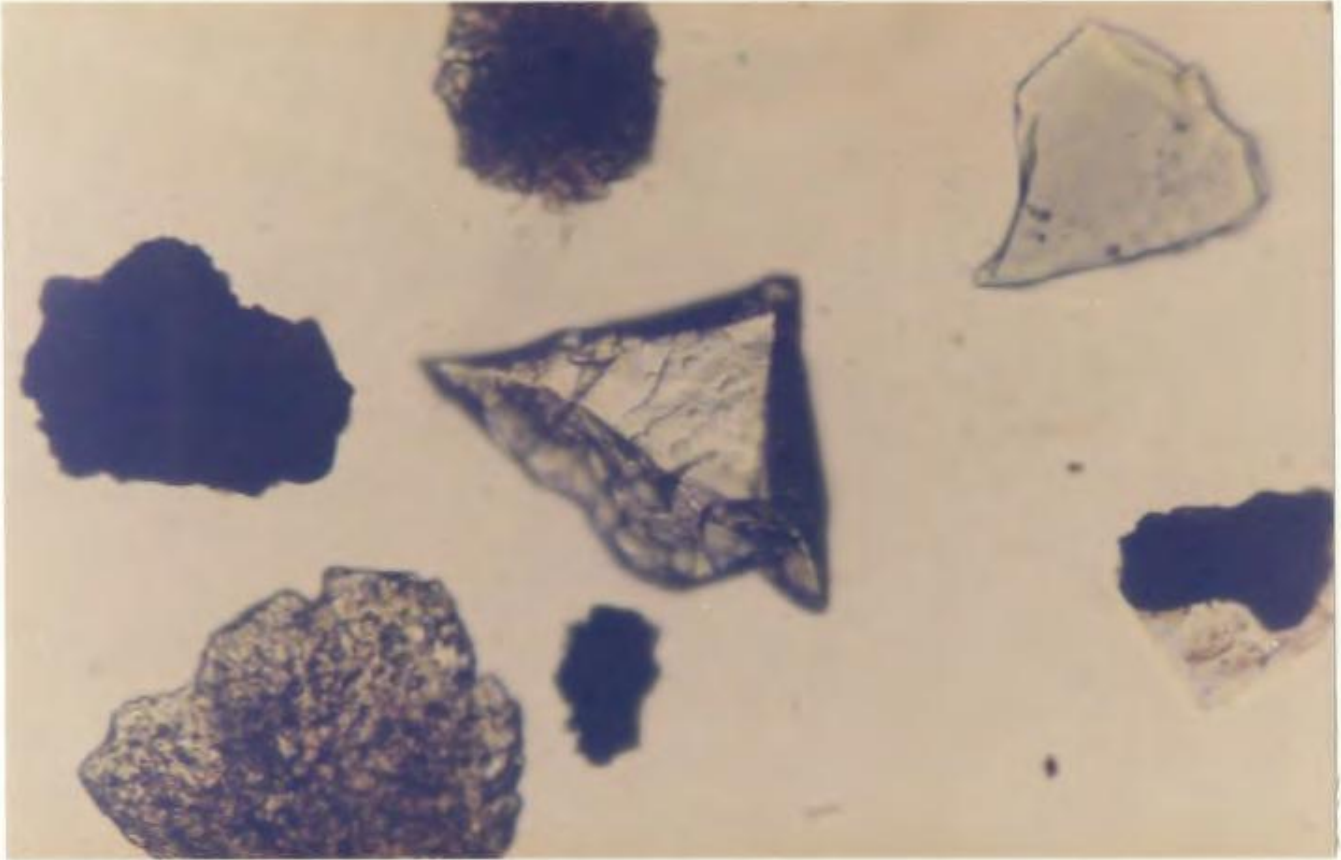


100 microns

Plate 4.19: Garnet. "Hackly" surface texture.

100 microns

Plate 4.20: Garnet. "Hackly" to "toothed" surface texture.

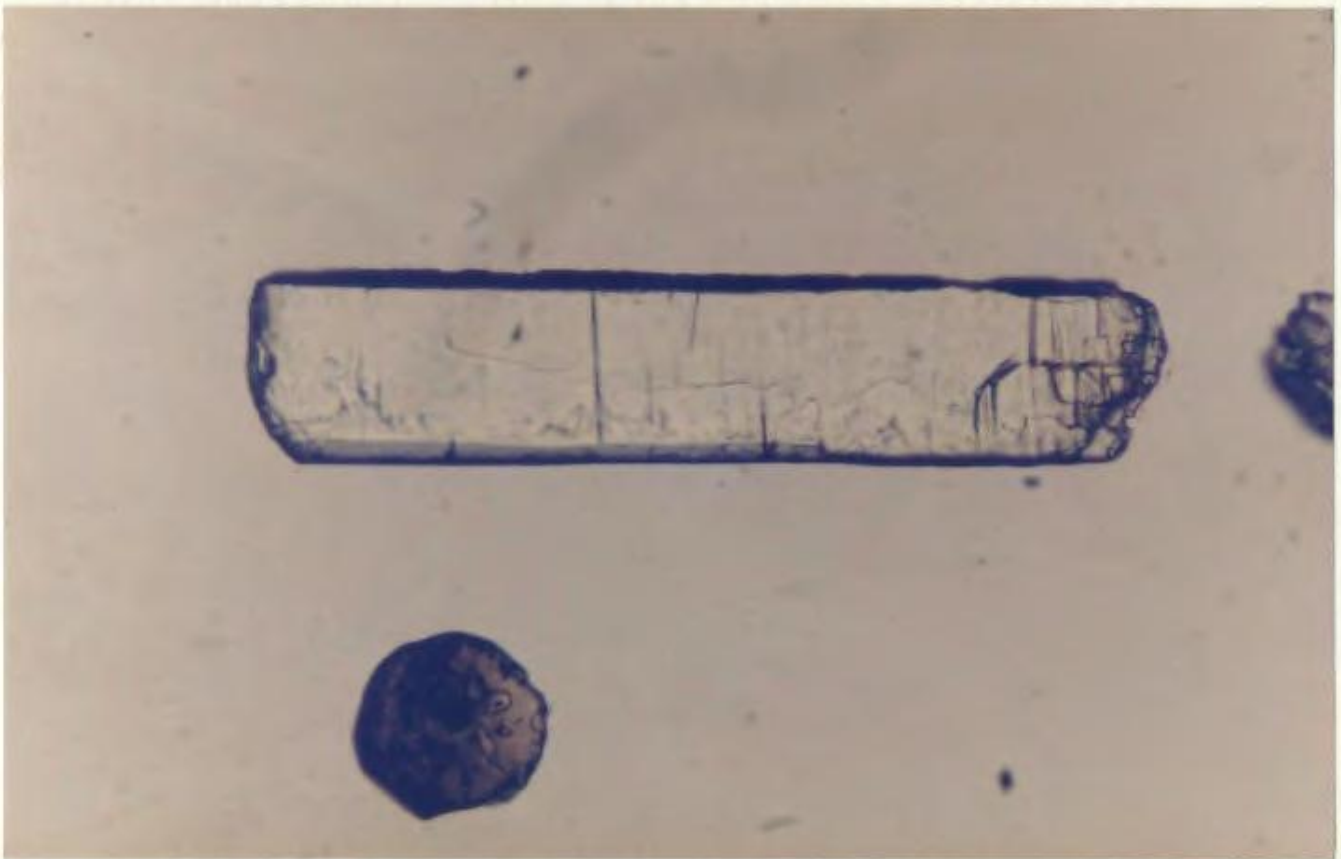
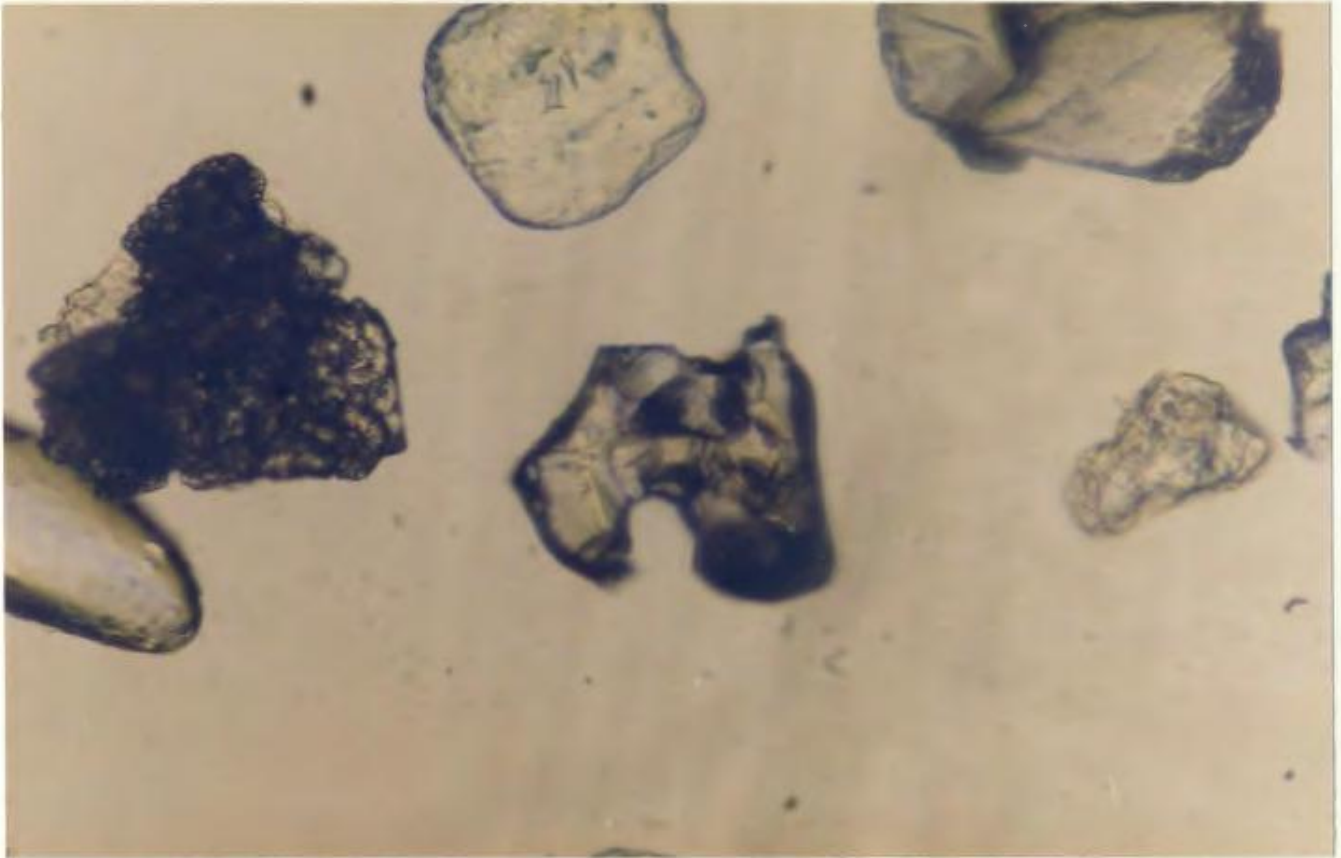


100 microns

Plate 4.21: Garnet. Embayed, colourless grain.

100 microns

Plate 4.22: Kyanite. Elongate, prismatic, colourless grain with right-angle parting. Note rounded cross-sectional (basal) tourmaline in lower left quadrant.

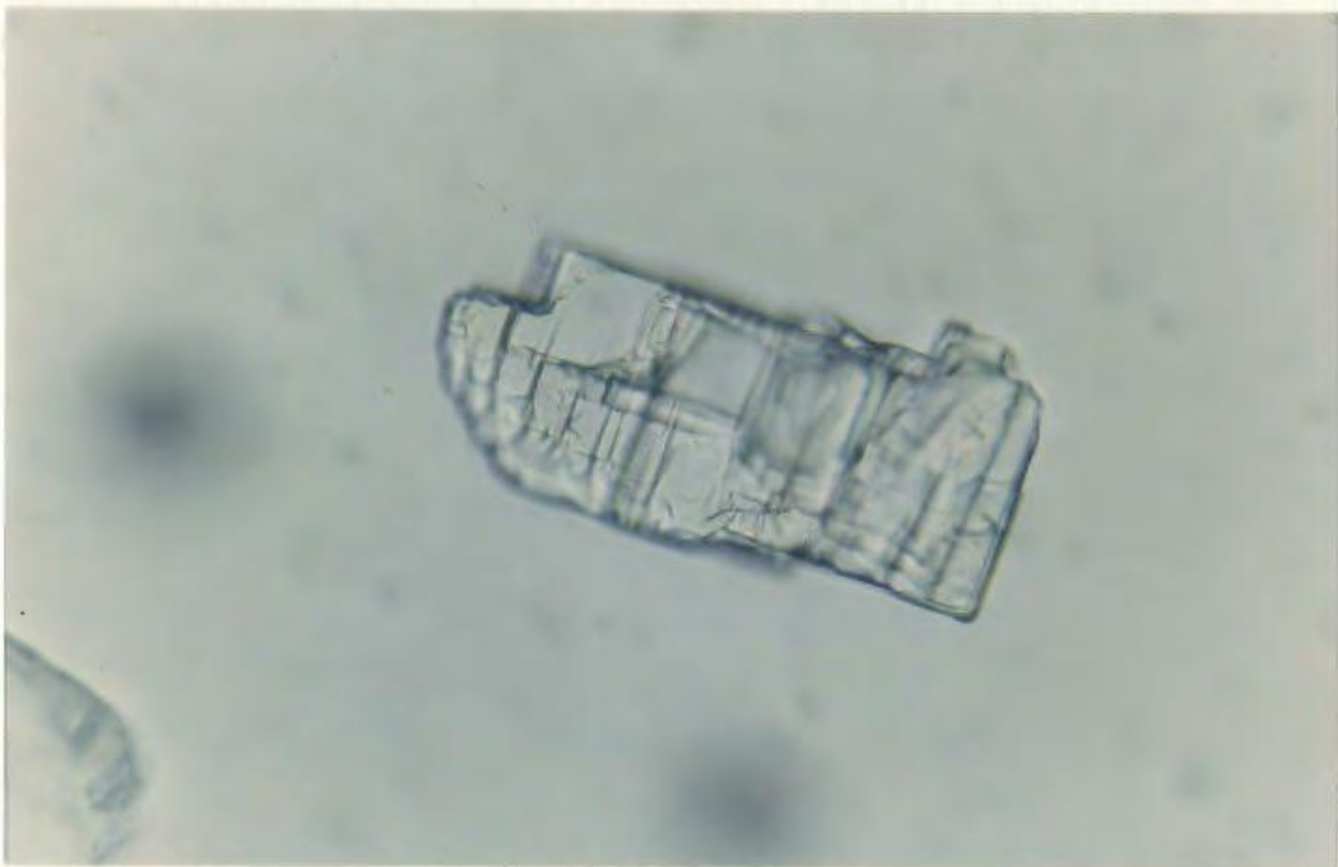
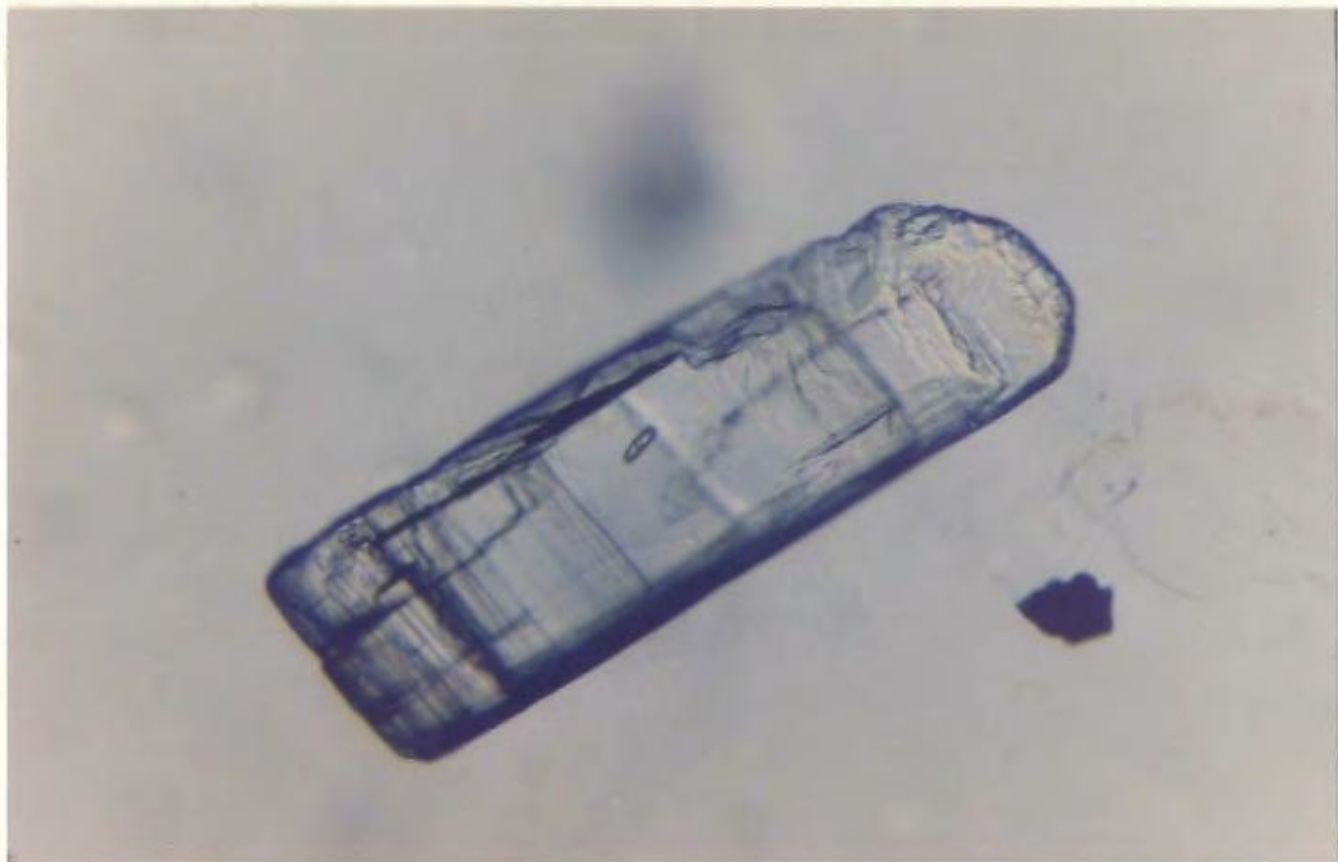


50 microns

Plate 4.23: Kyanite. As above (Plate 4.22) but exhibiting more prominent parting. Note inclusion.

50 microns

Plate 4.24: Kyanite. Elongate, sub-prismatic, colourless grain with prominent parting.

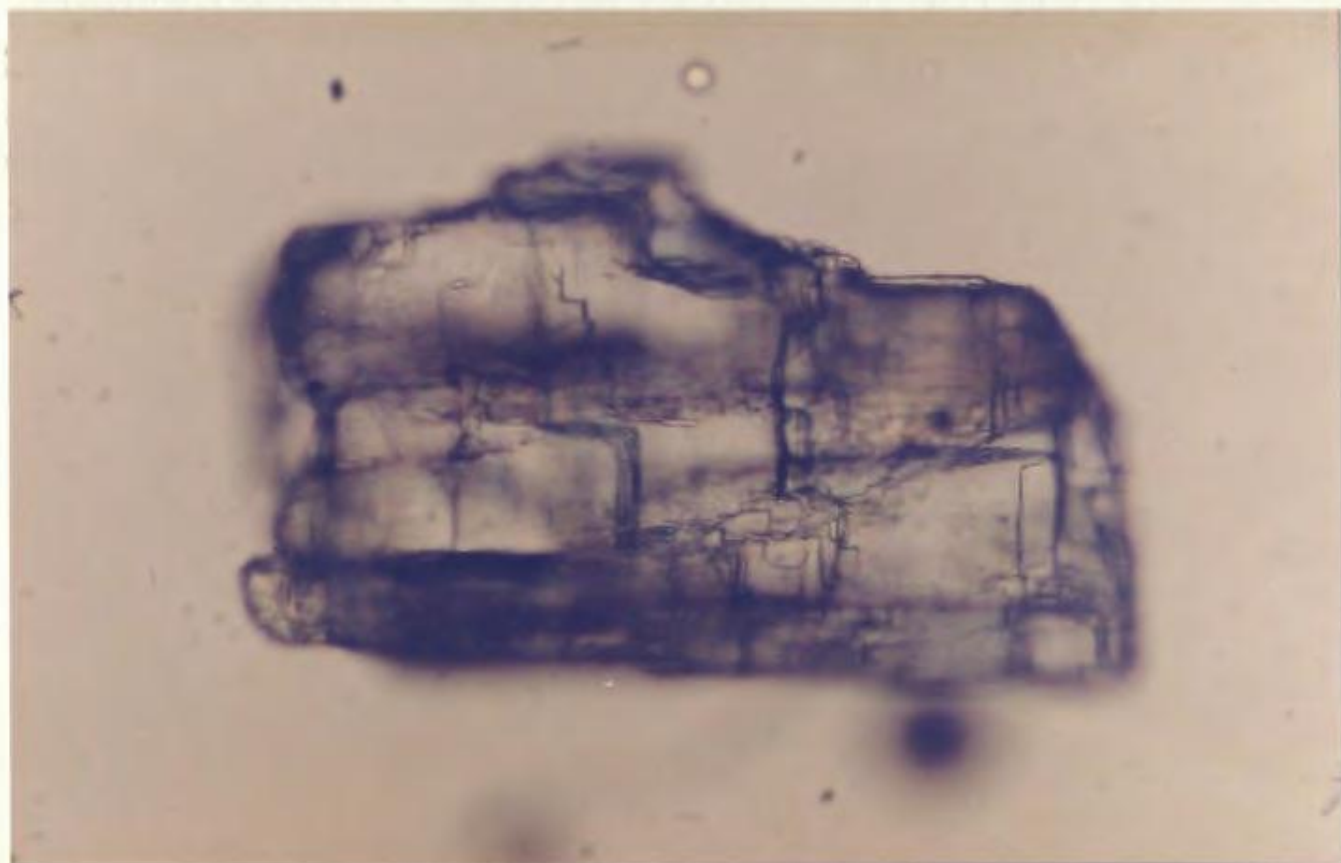
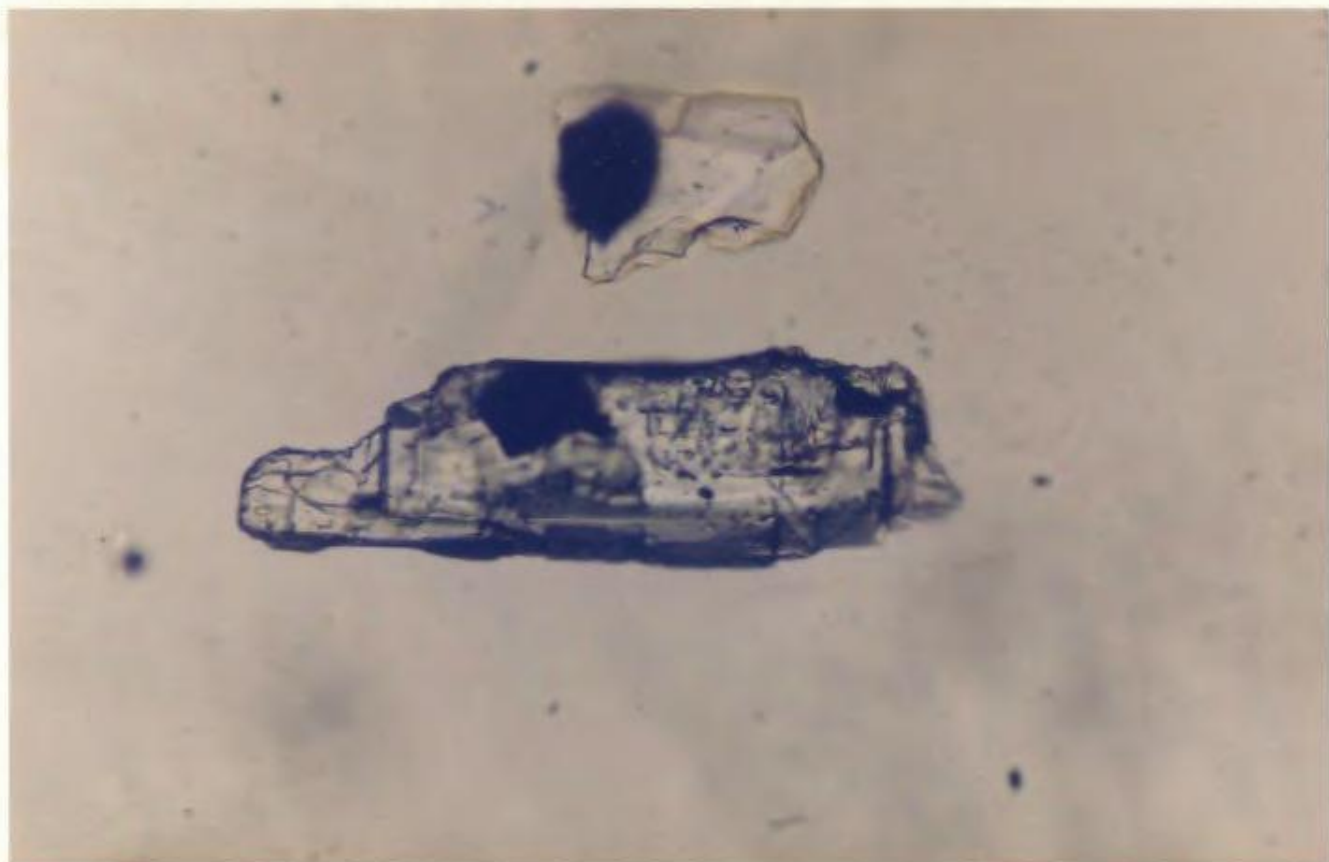


100 microns

Plate 4.25: Kyanite. Elongate, sub-prismatic grain with abundant carbonaceous inclusions.

50 microns

Plate 4.26: Kyanite. Abundant carbonaceous material gives dusty appearance to the grain.

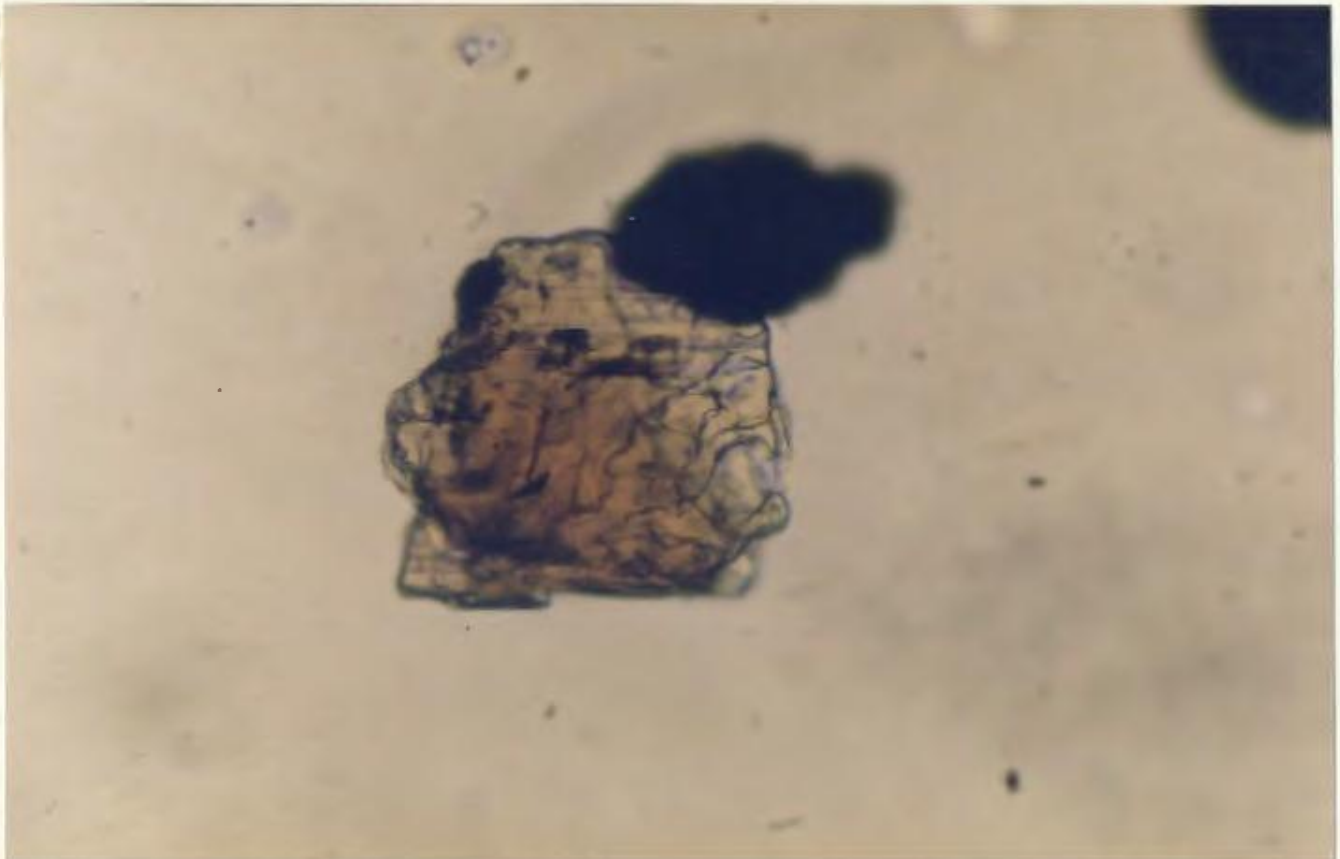
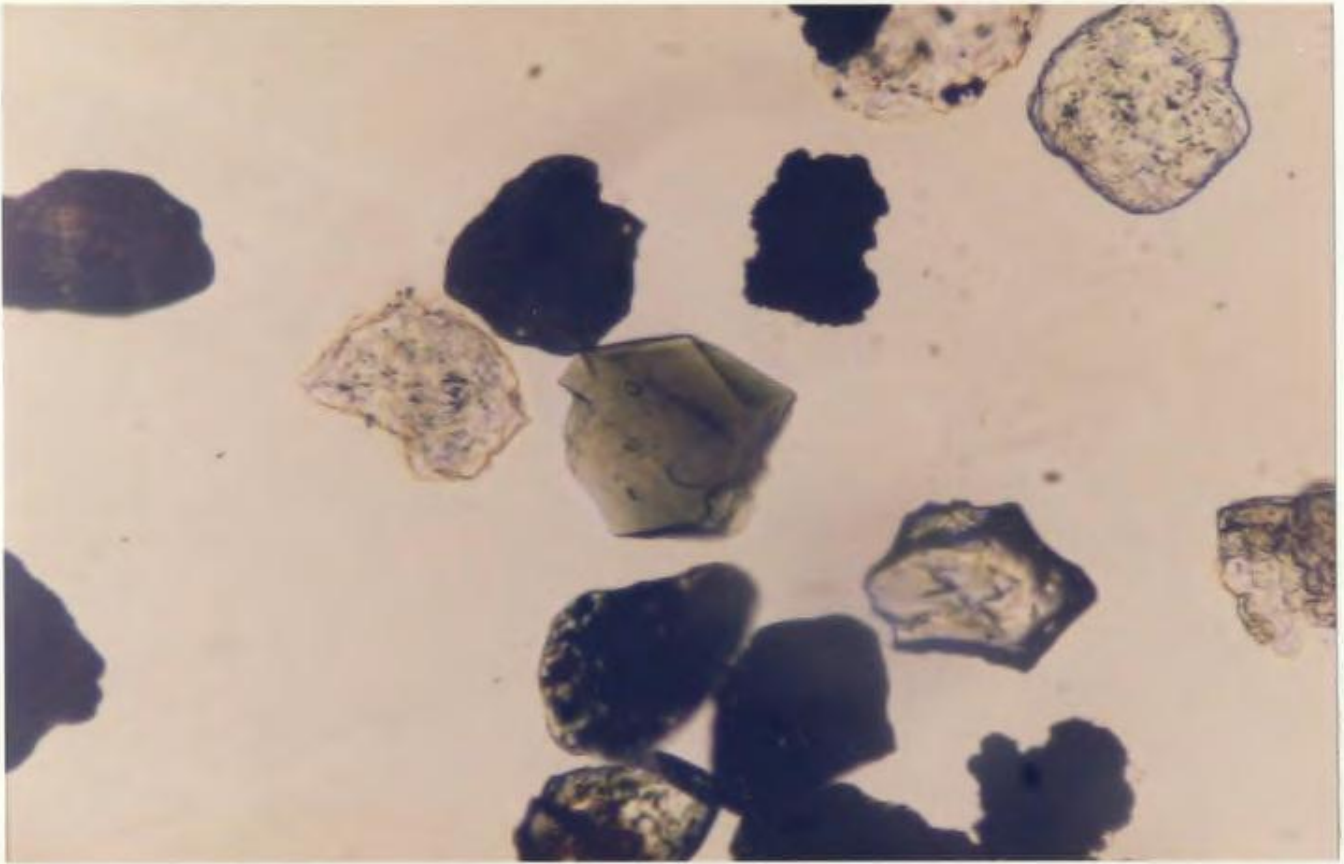


100 microns

Plate 4.27: Pyroxene (var. augite).

100 microns

Plate 4.28: Pyroxene (var. orthopyroxene). Sub-equant, sub-angular grain showing the pink of a pink to green pleochroic colour scheme.

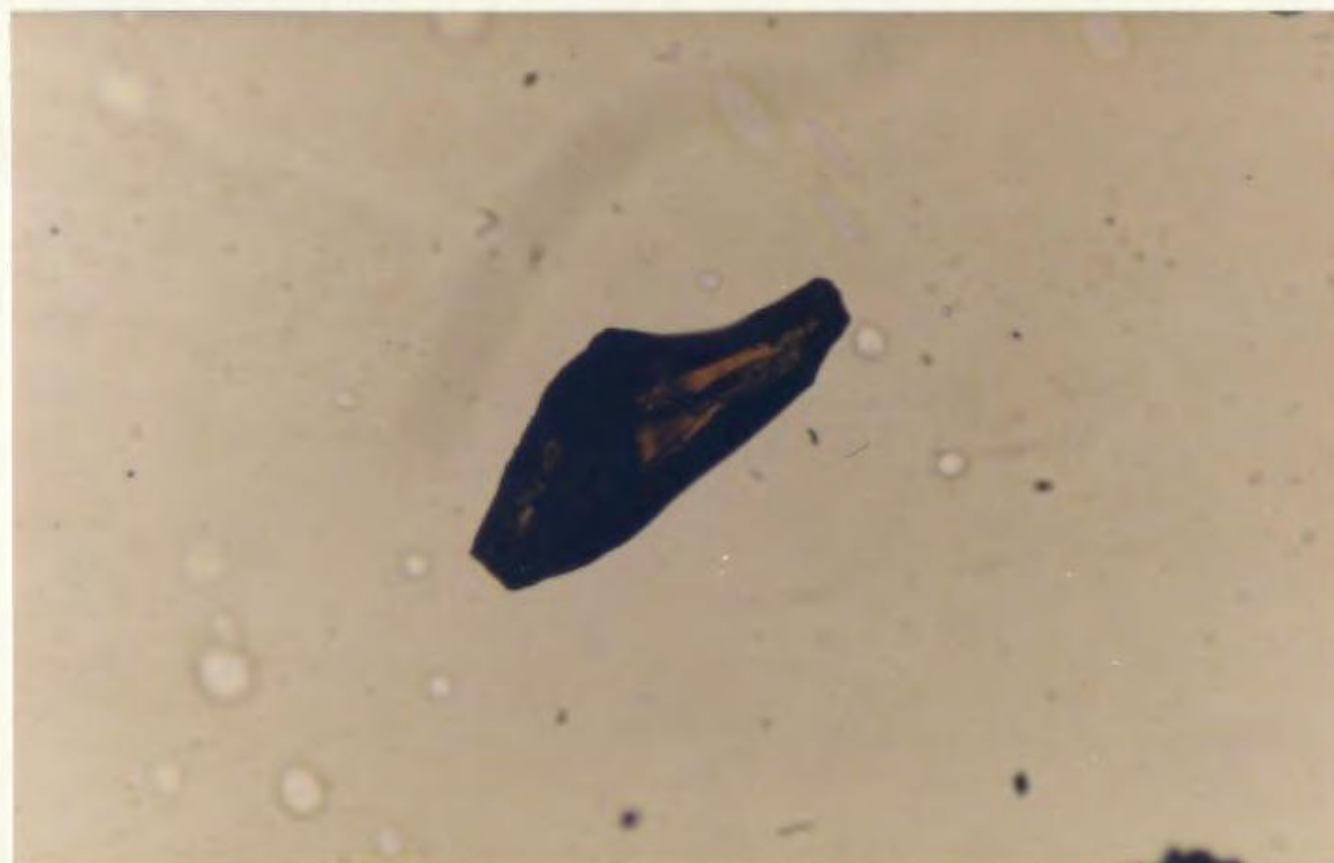


50 microns

Plate 4.29: Rutile. Dark yellow-brown, prismatic grain showing zoning.

100 microns

Plate 4.30: Rutile. Dark red-brown, elongate, angular, fragmented grain.

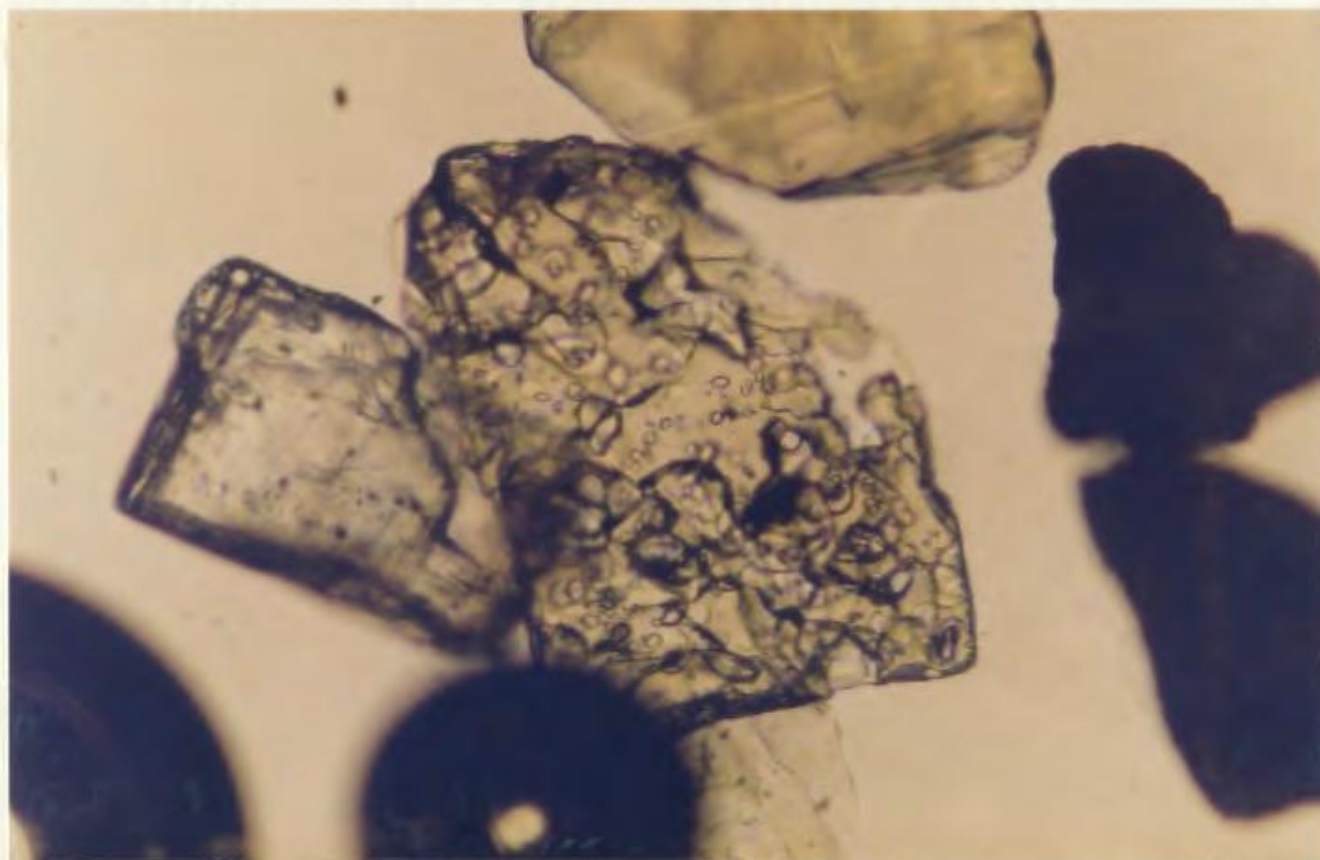
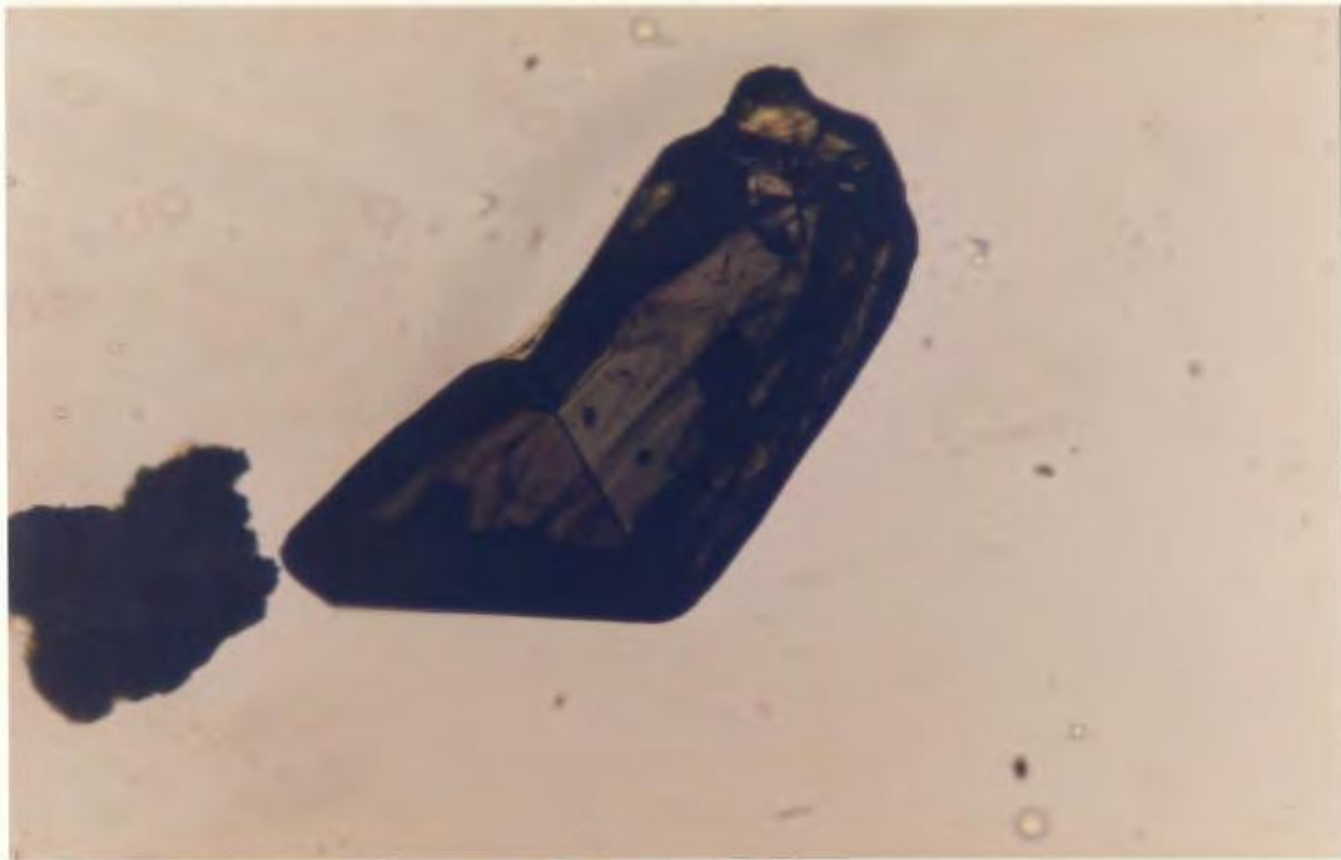


50 microns

Plate 4.31: Rutile. Genuiculate twins.

50 microns

Plate 4.32: Staurolite. Prismatic grain with "swiss
cheese-like" texture.

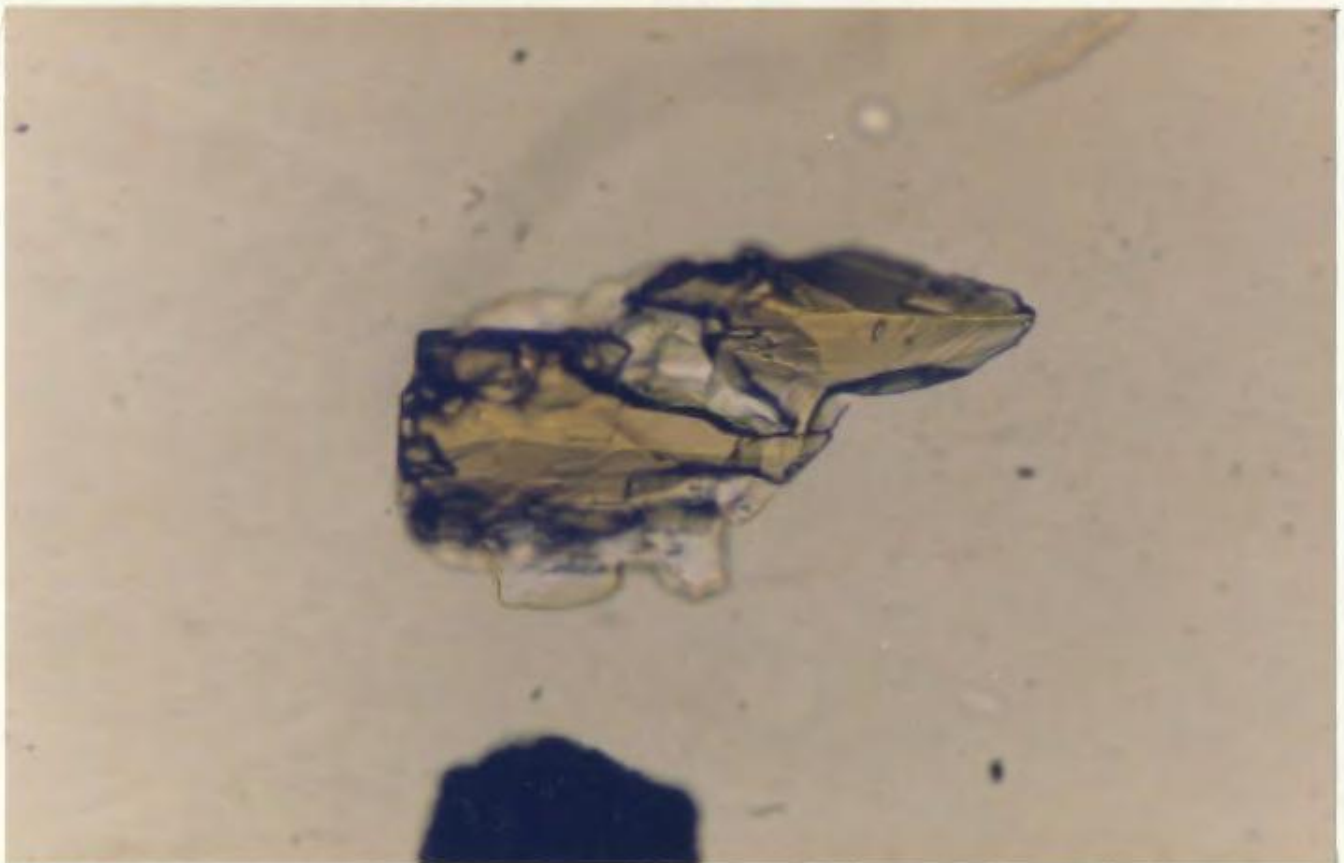
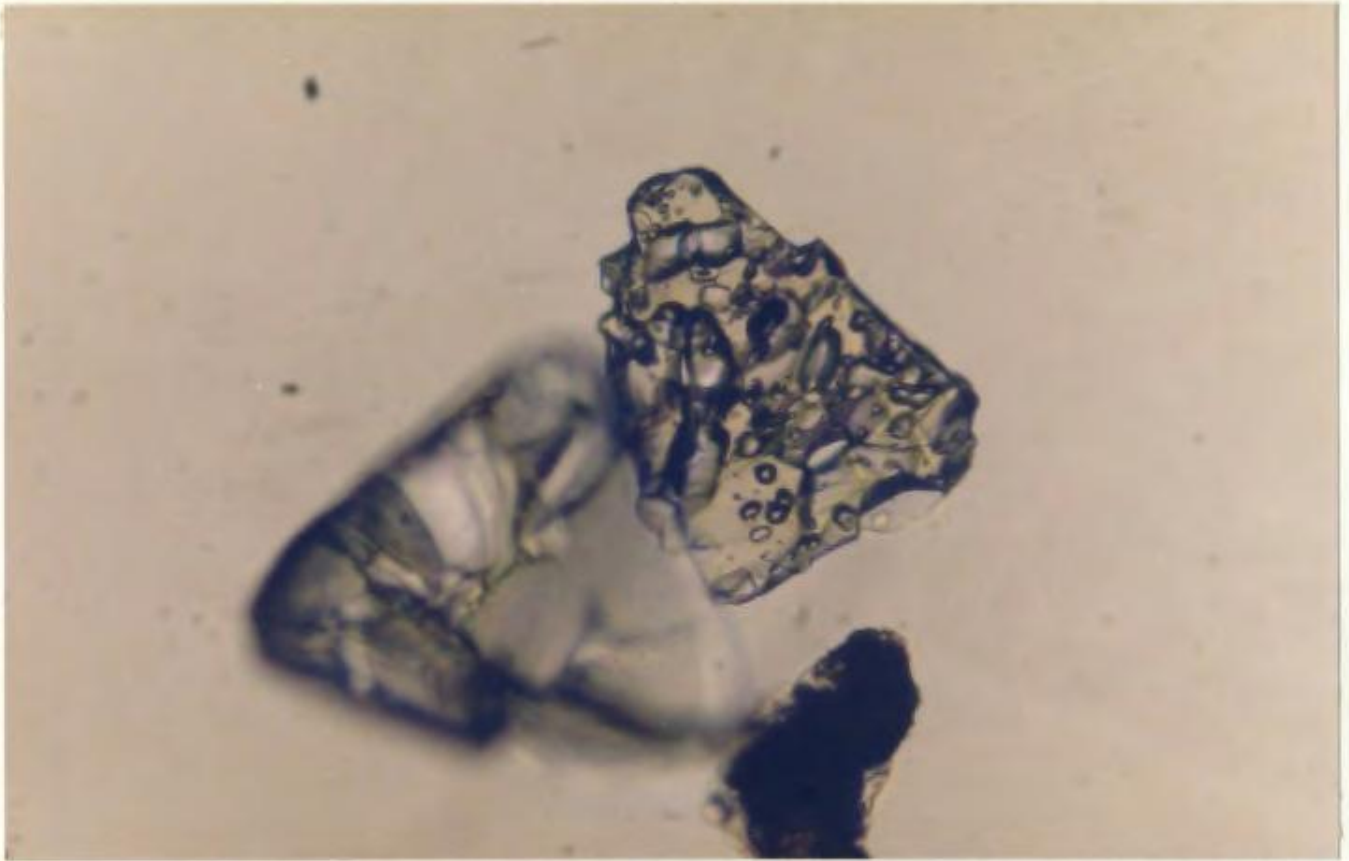


100 microns

Plate 4.33: Staurolite. Typical, irregular staurolite grain. Note common inclusion texture. The other large, colourless grain is garnet.

100 microns

Plate 4.34: Staurolite. Grains without inclusions rarely occur.

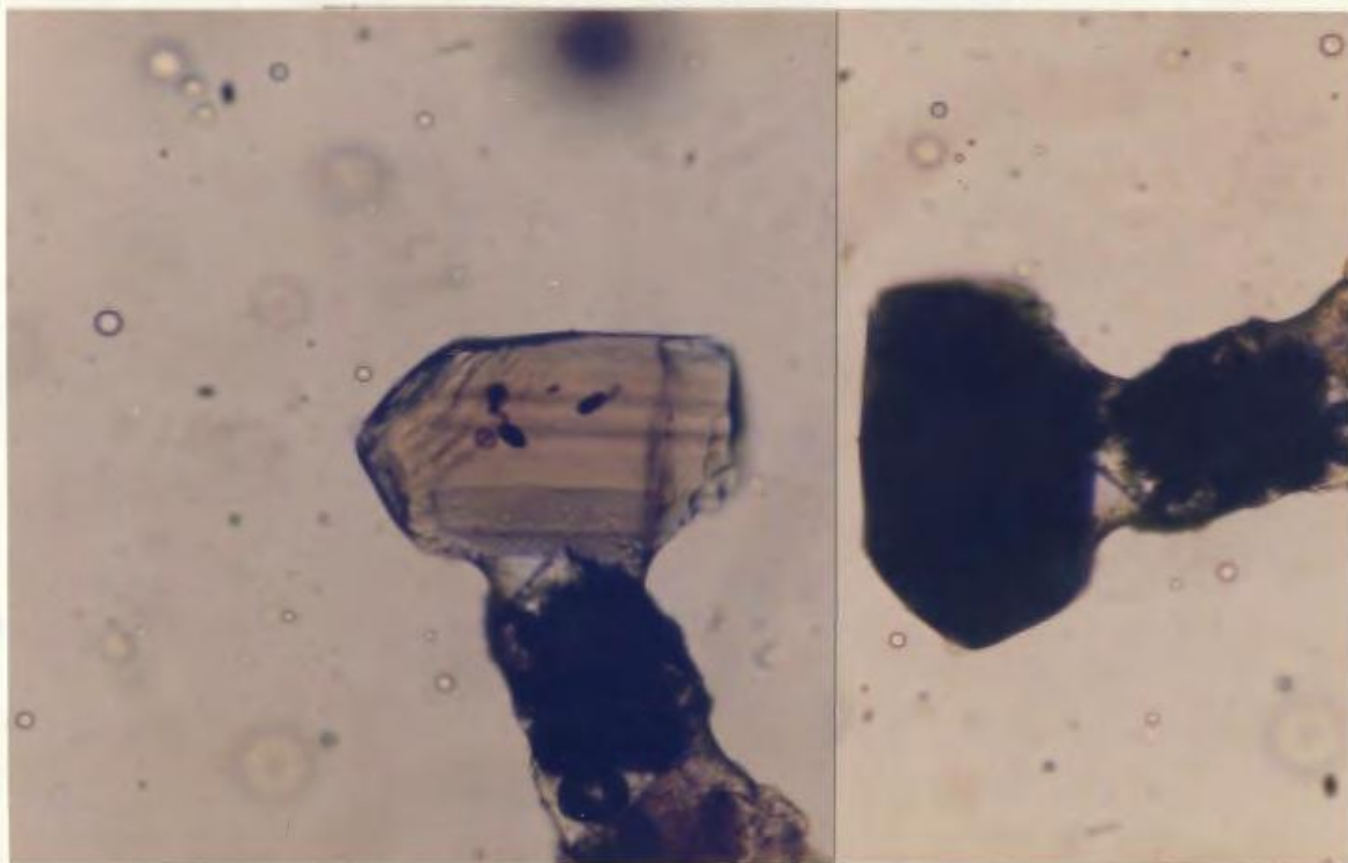
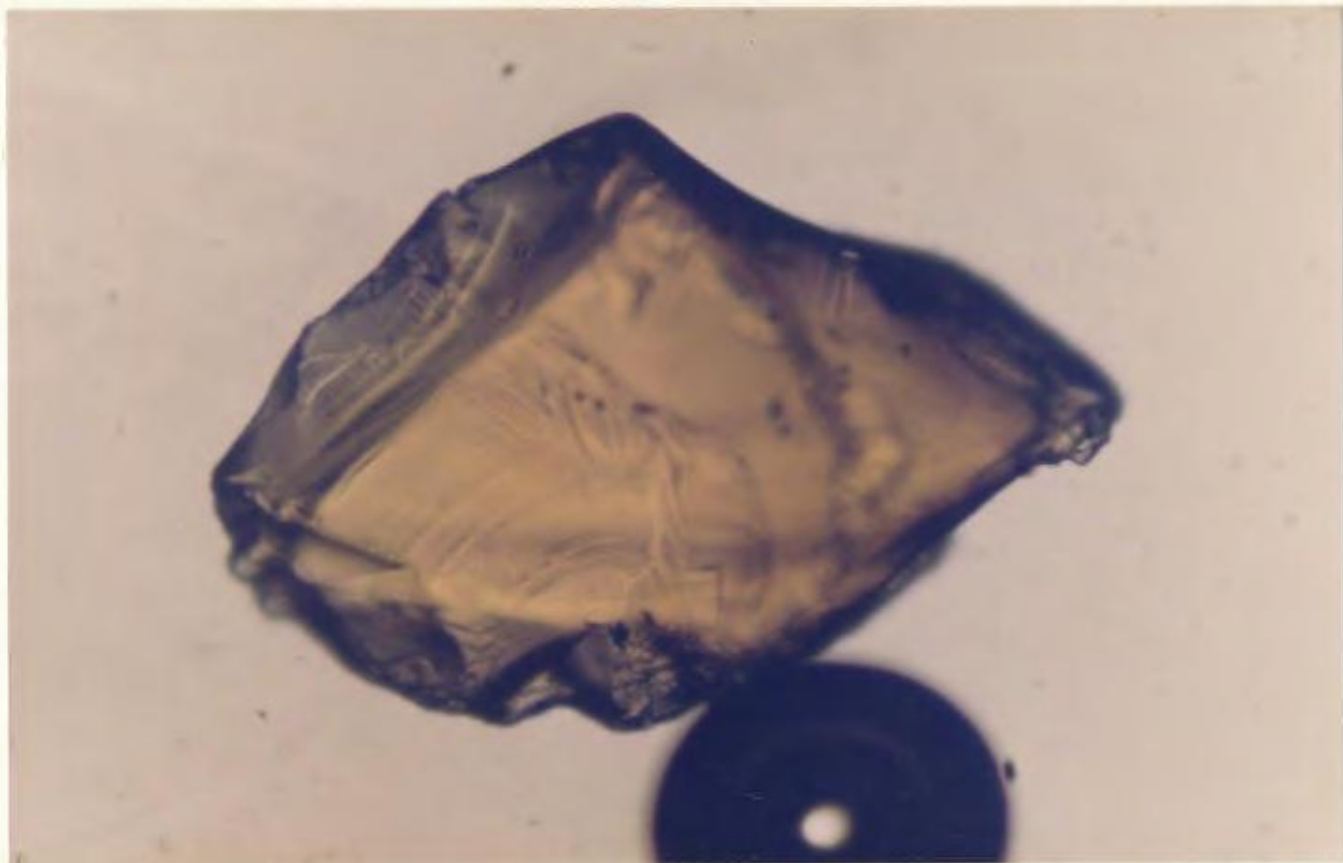


50 microns

Plate 4.35: Staurolite. Showing typical yellow-brown colour.

100 microns

Plate 4.36: Tourmaline. Elongate, prismatic grain with one set of terminations present. Pleochroic scheme is pink to dark blue.

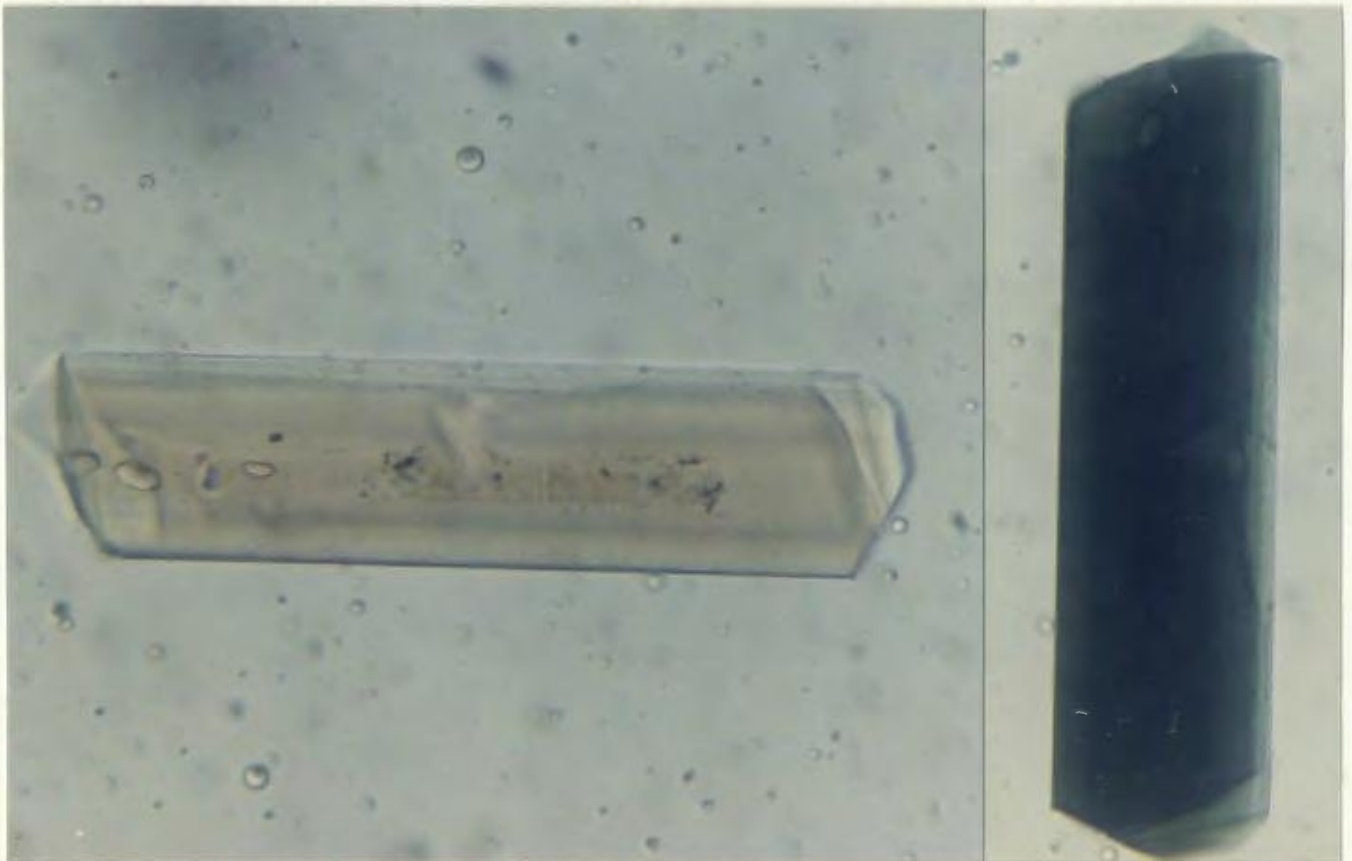
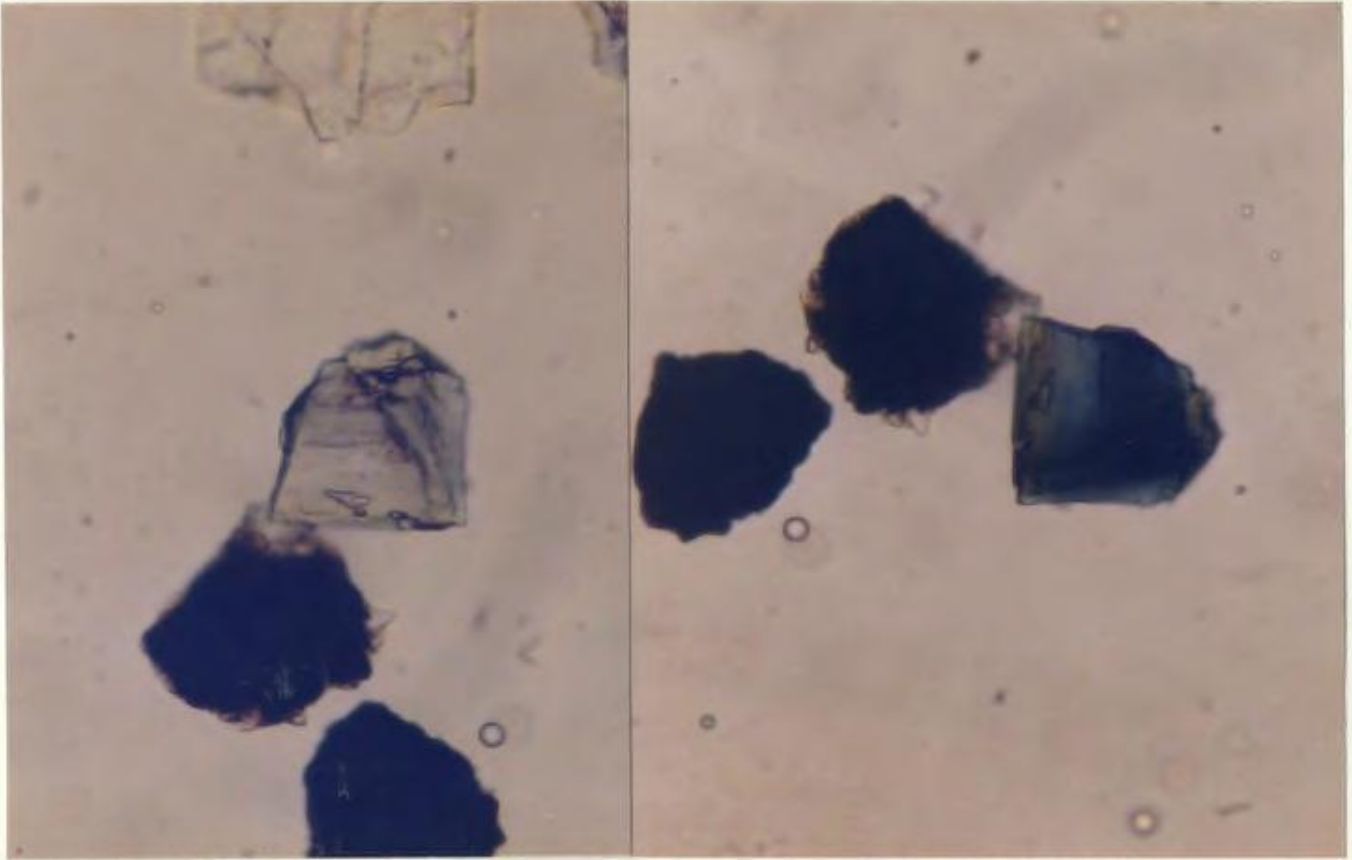


100 microns

Plate 4.37: Tourmaline. Exhibiting a colourless to green and blue colour scheme. Note colour zoning in Plate 4.37b.

100 microns

Plate 4.38: Tourmaline. Elongate, prismatic grain with pale pink to green-brown pleochroic scheme.

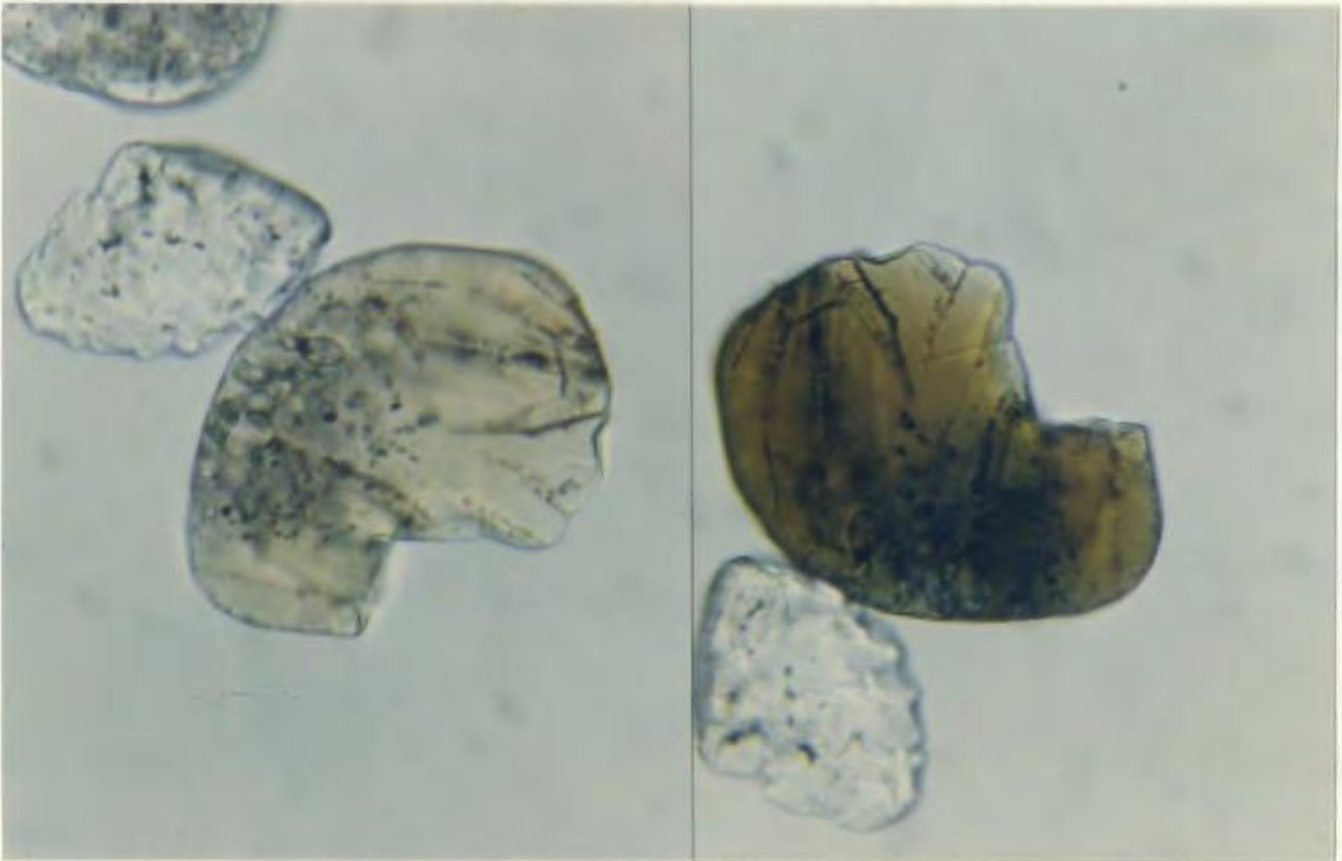
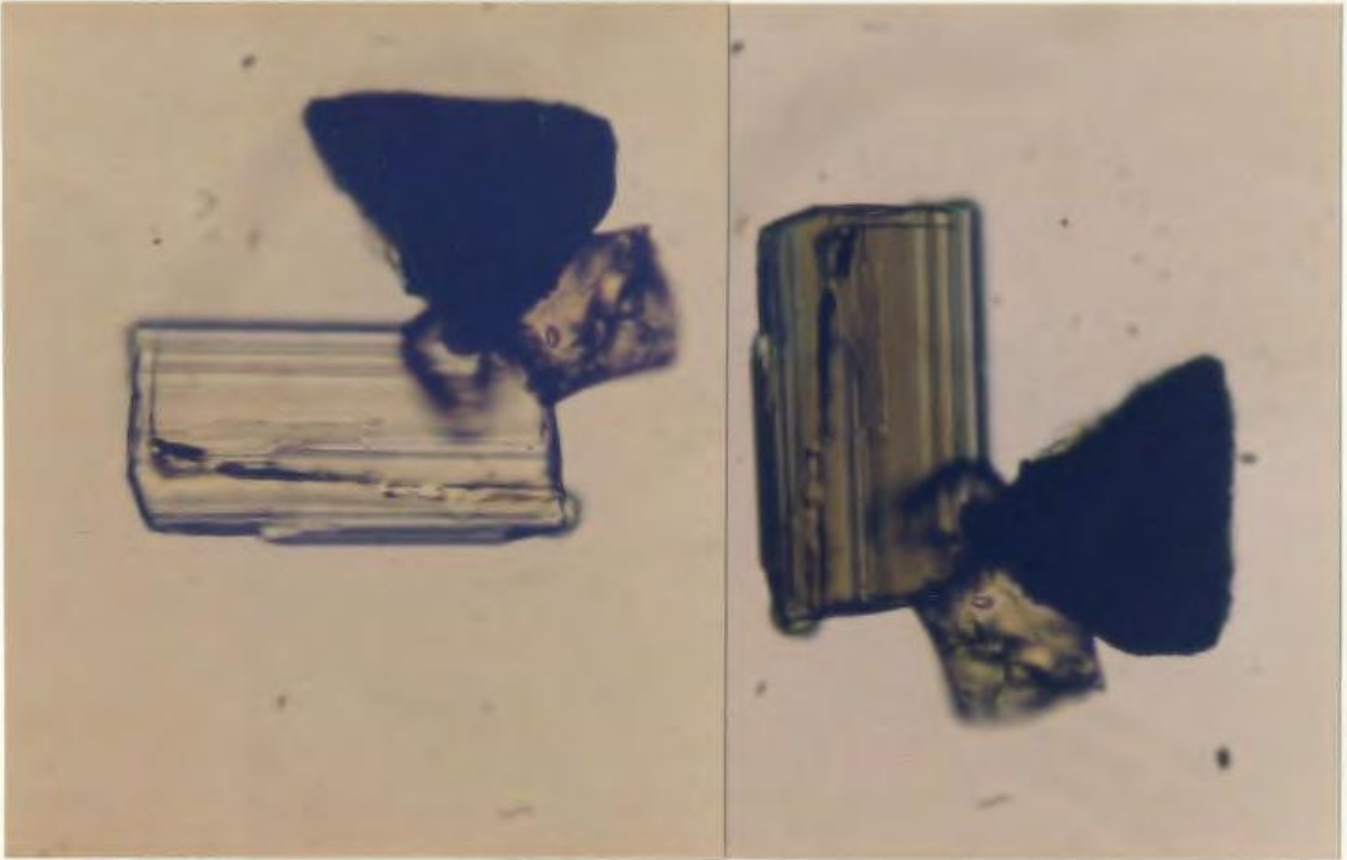


100 microns

Plate 4.39: Tourmaline. Elongate, prismatic grain with pale yellow to yellow-brown pleochroic scheme. Note striations parallel to the C-axis.

100 microns

Plate 4.40: Tourmaline. Well rounded grain with pale yellow to yellow-brown and green-brown pleochroic scheme. Note colour zoning at maximum extinction.

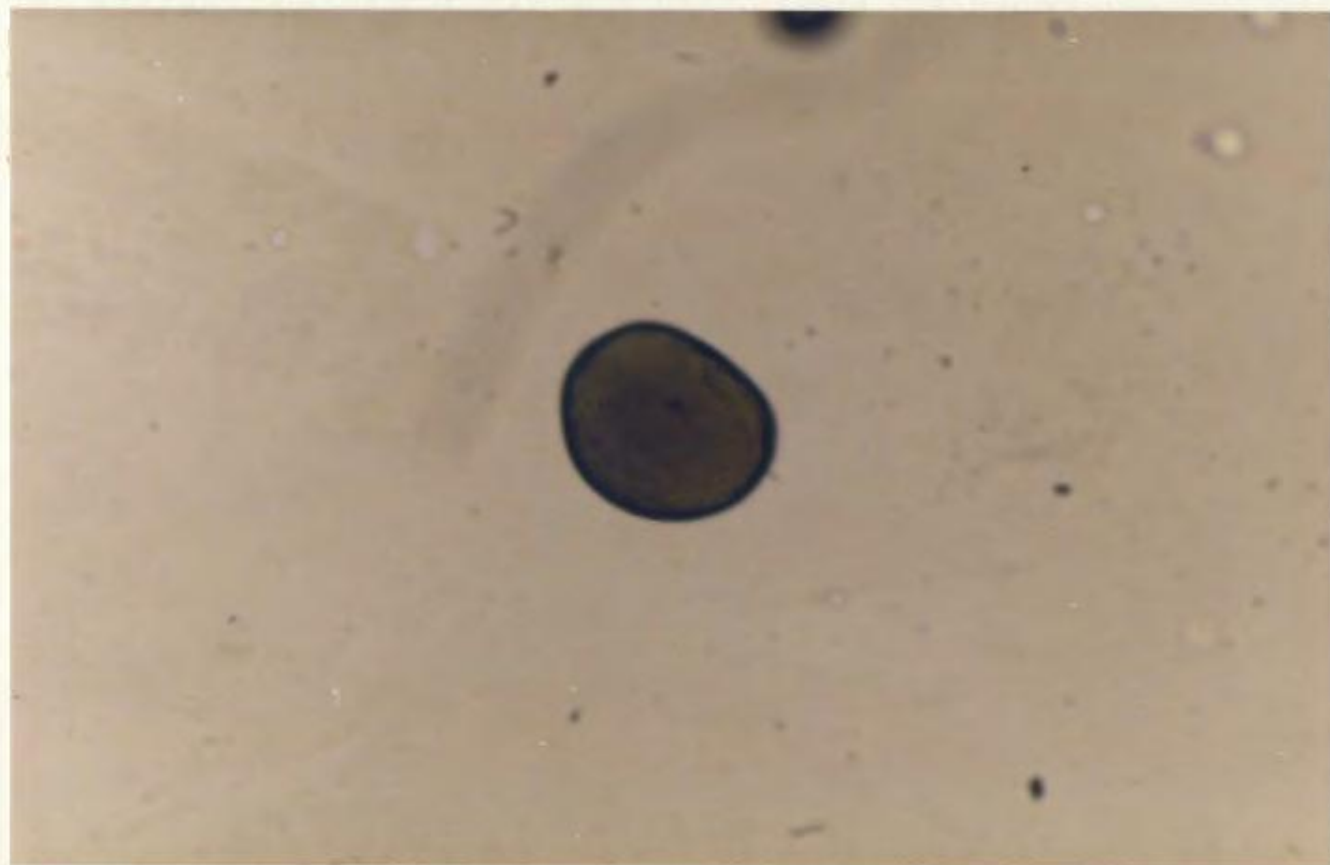
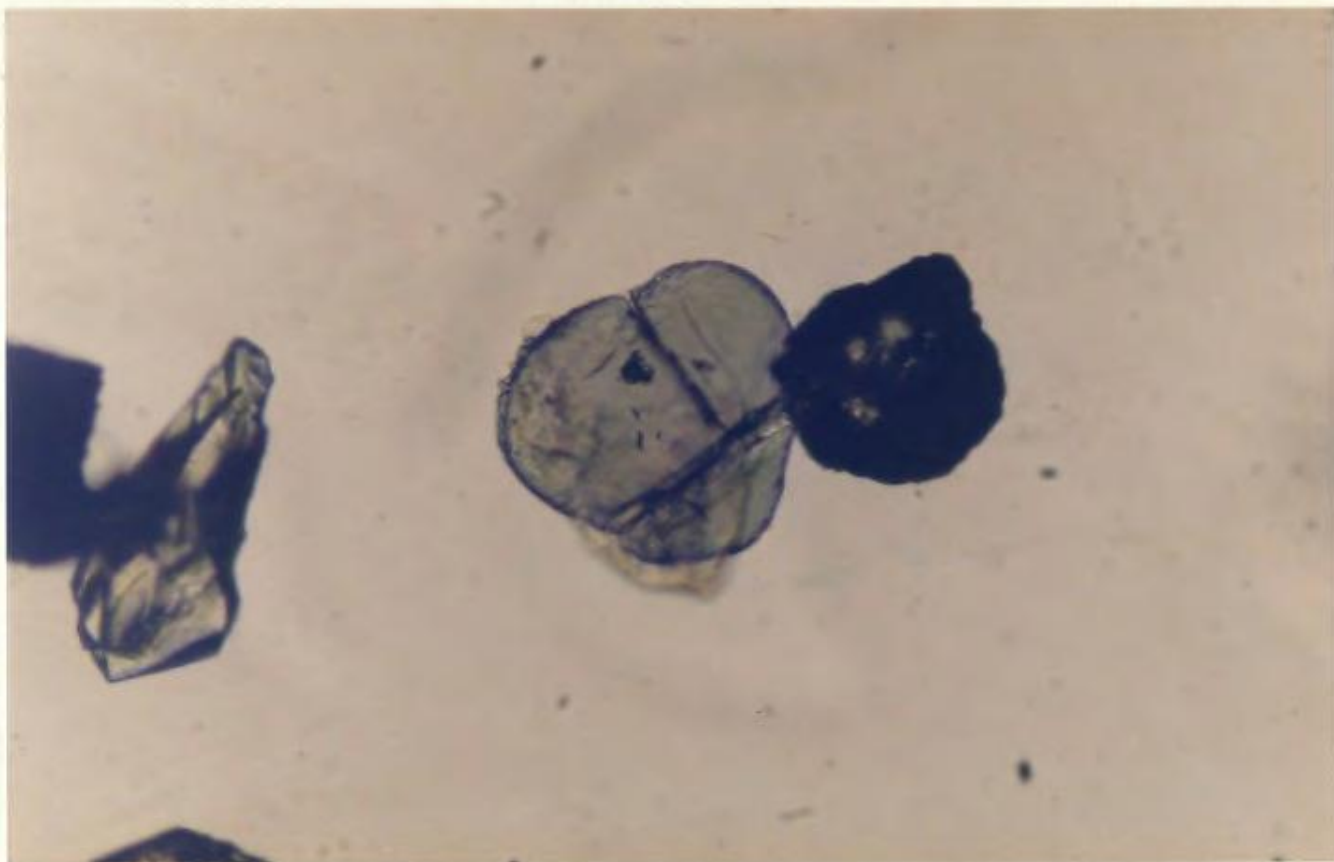


100 microns

Plate 4.41: Tourmaline. Cross-sectional (or basal) cut. Note characteristic 3-sided tourmaline morphology.

100 microns

Plate 4.42: Tourmaline. Well rounded basal (cross-sectional) grain.

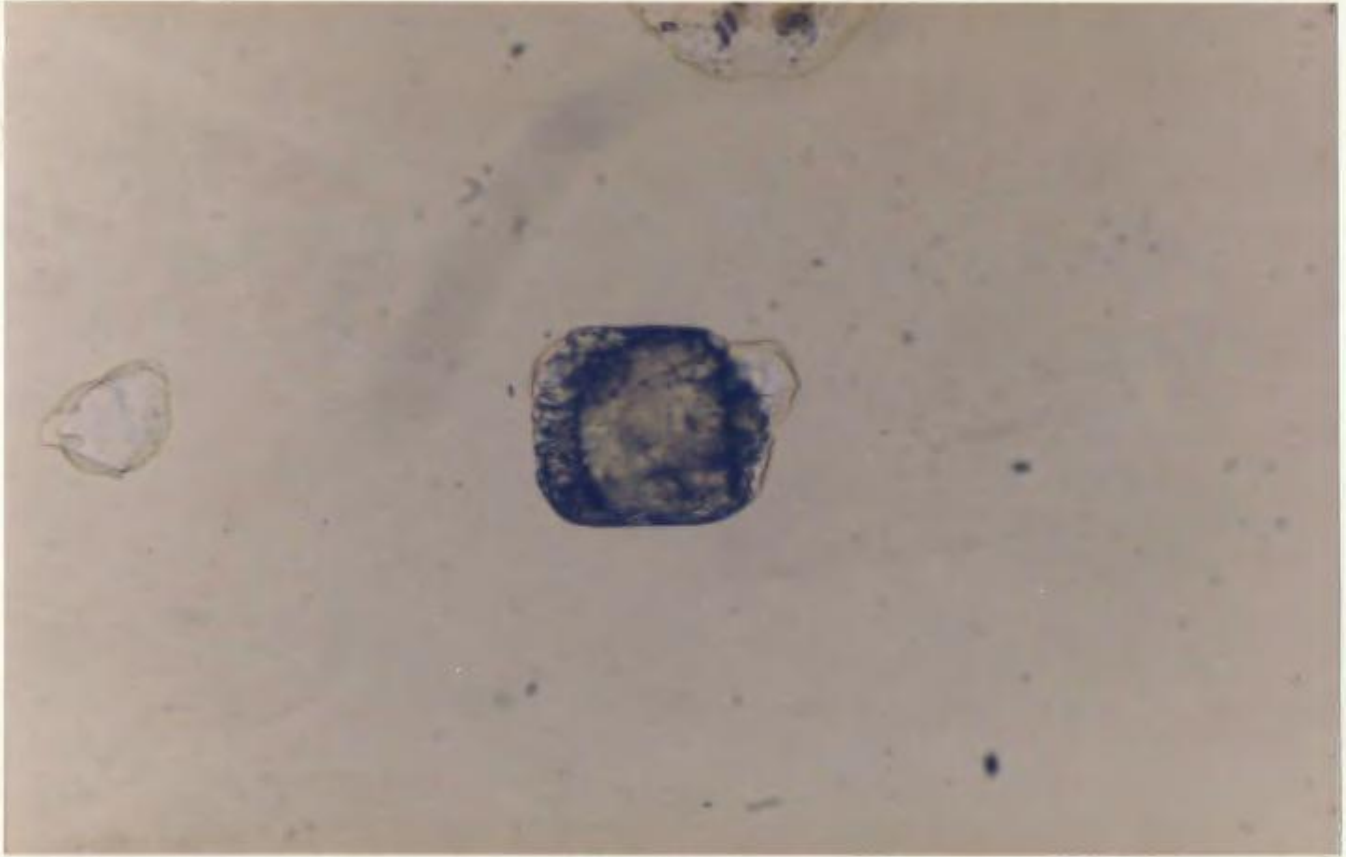


100 microns

Plate 4.43: Tourmaline. Sub-equant, sub-prismatic grain with over-growths.

50 microns

Plate 4.44: Zircon. Angular, prismatic grain with randomly distributed inclusion; slight zoning.

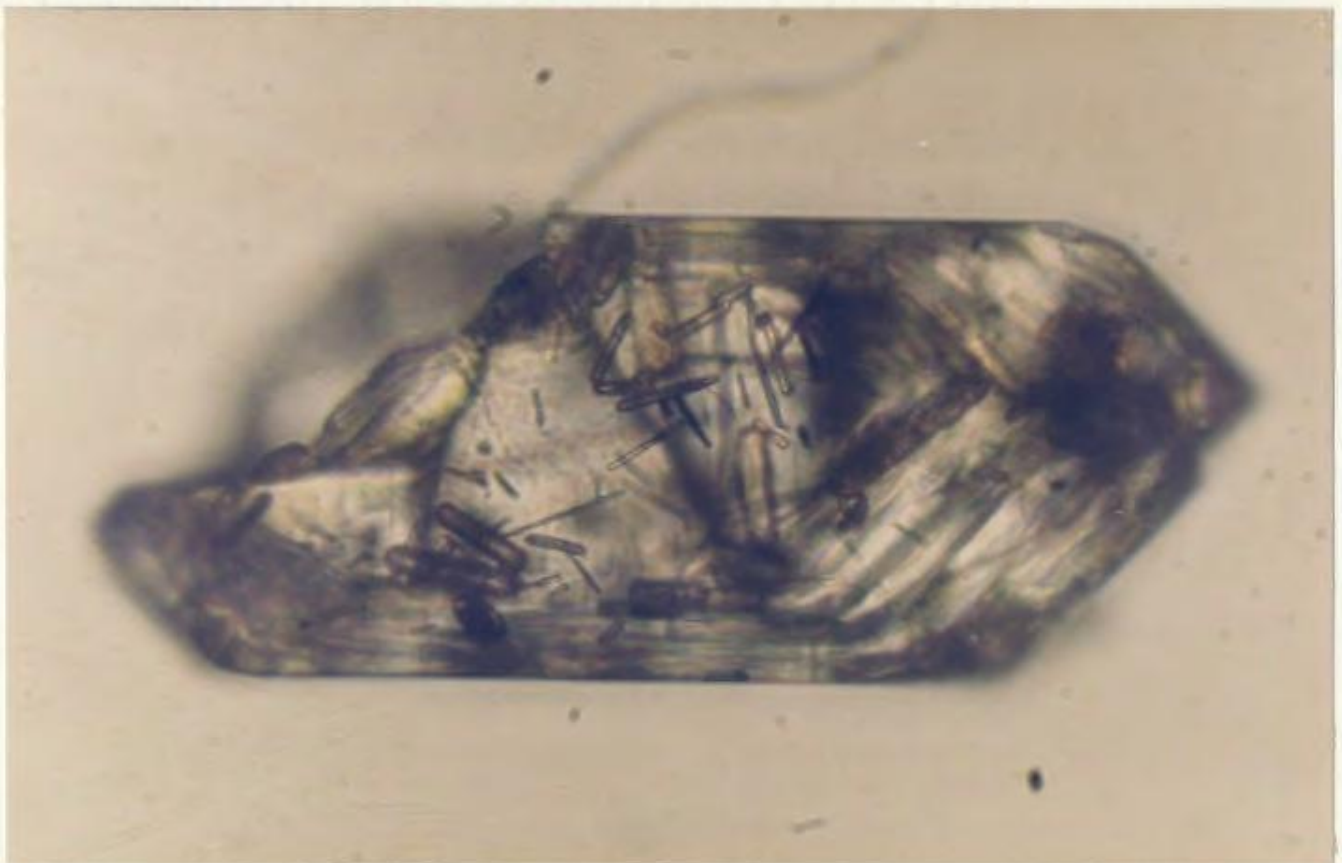
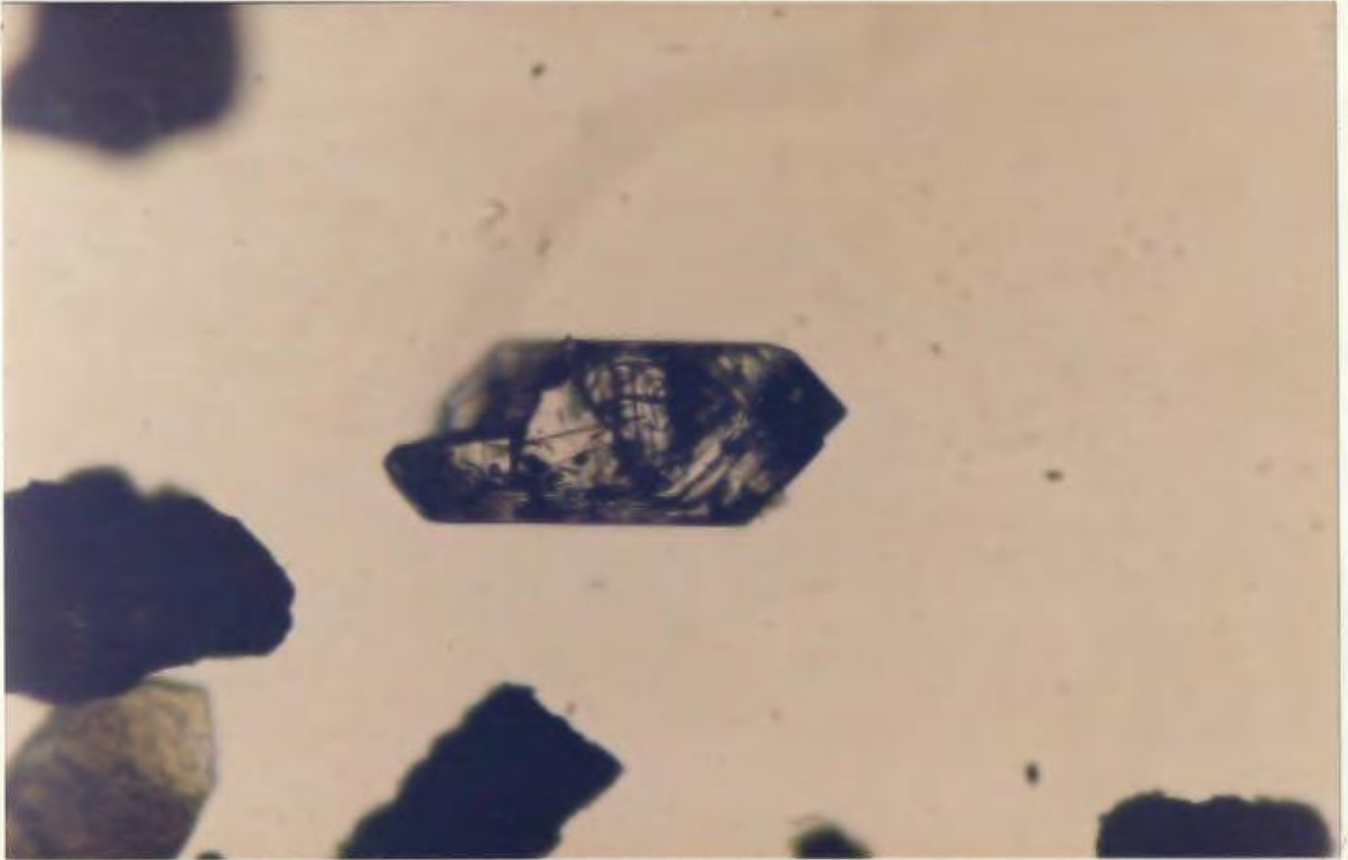


100 microns

Plate 4.45: Zircon. Prismatic grain with rutile needles and zoning.

50 microns

Plate 4.46: Zircon. Enlarged view of Plate 4.45.

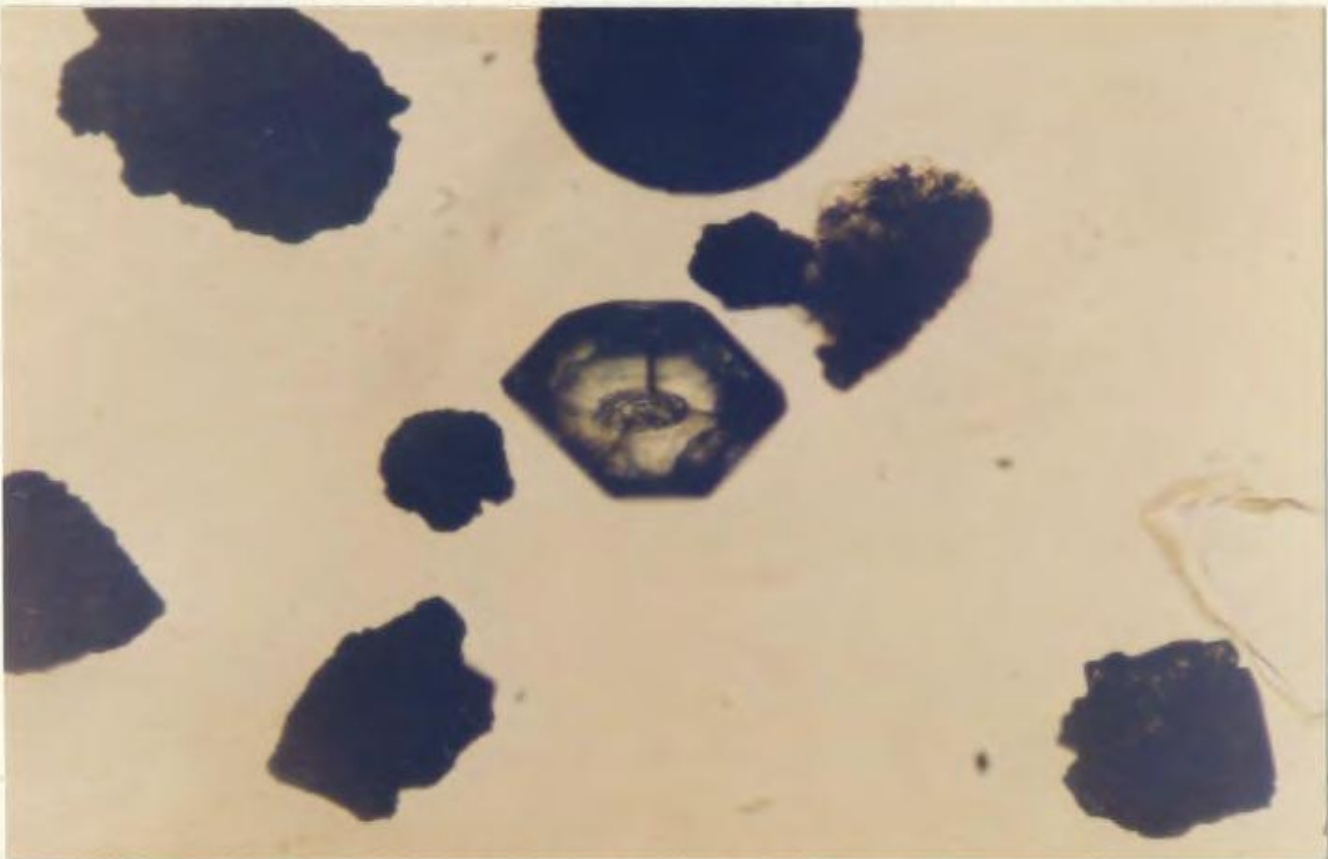


100 microns

Plate 4.47: Zircon. Sub-rounded, prismatic zircon with zoning.

100 microns

Plate 4.48: Zircon. Angular, prismatic, zoned grain.

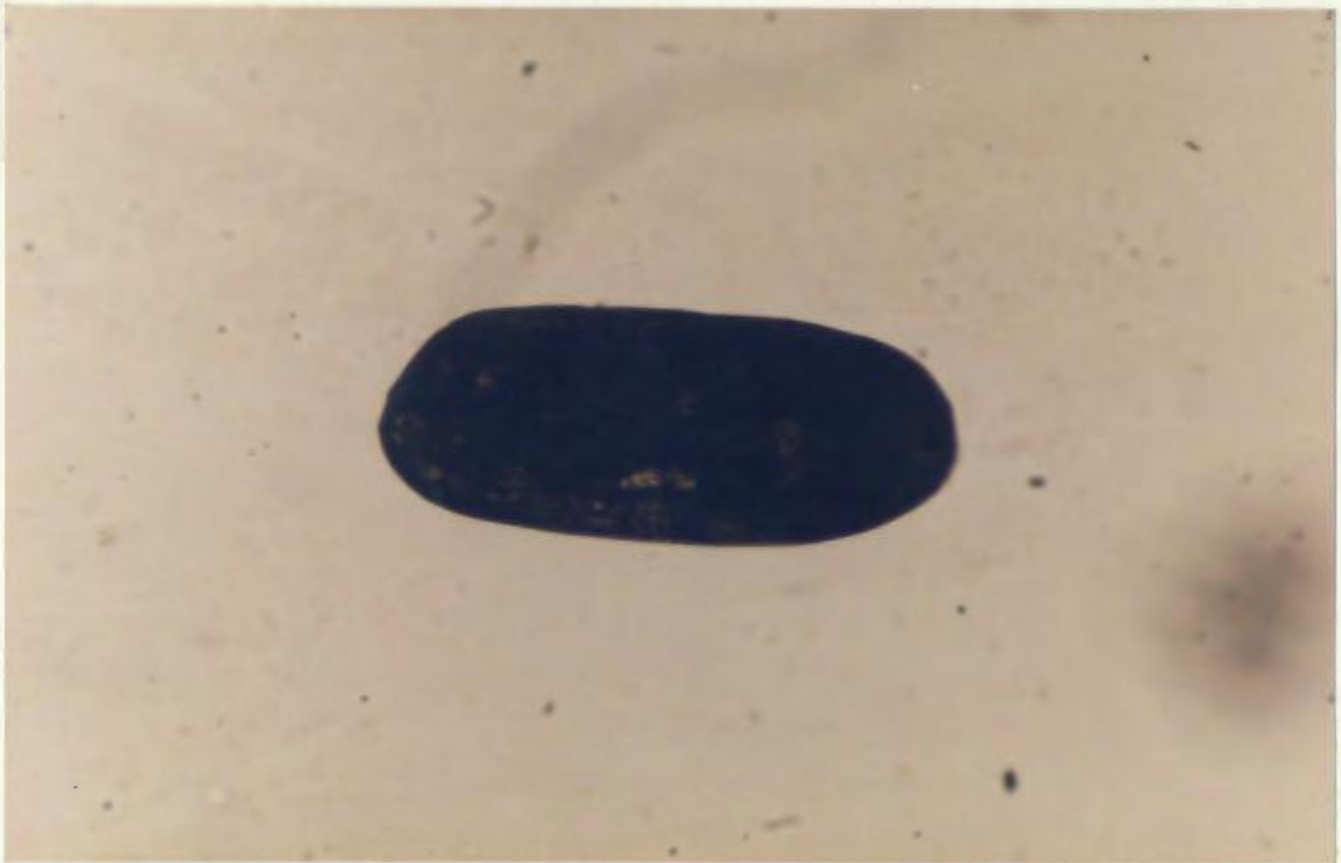
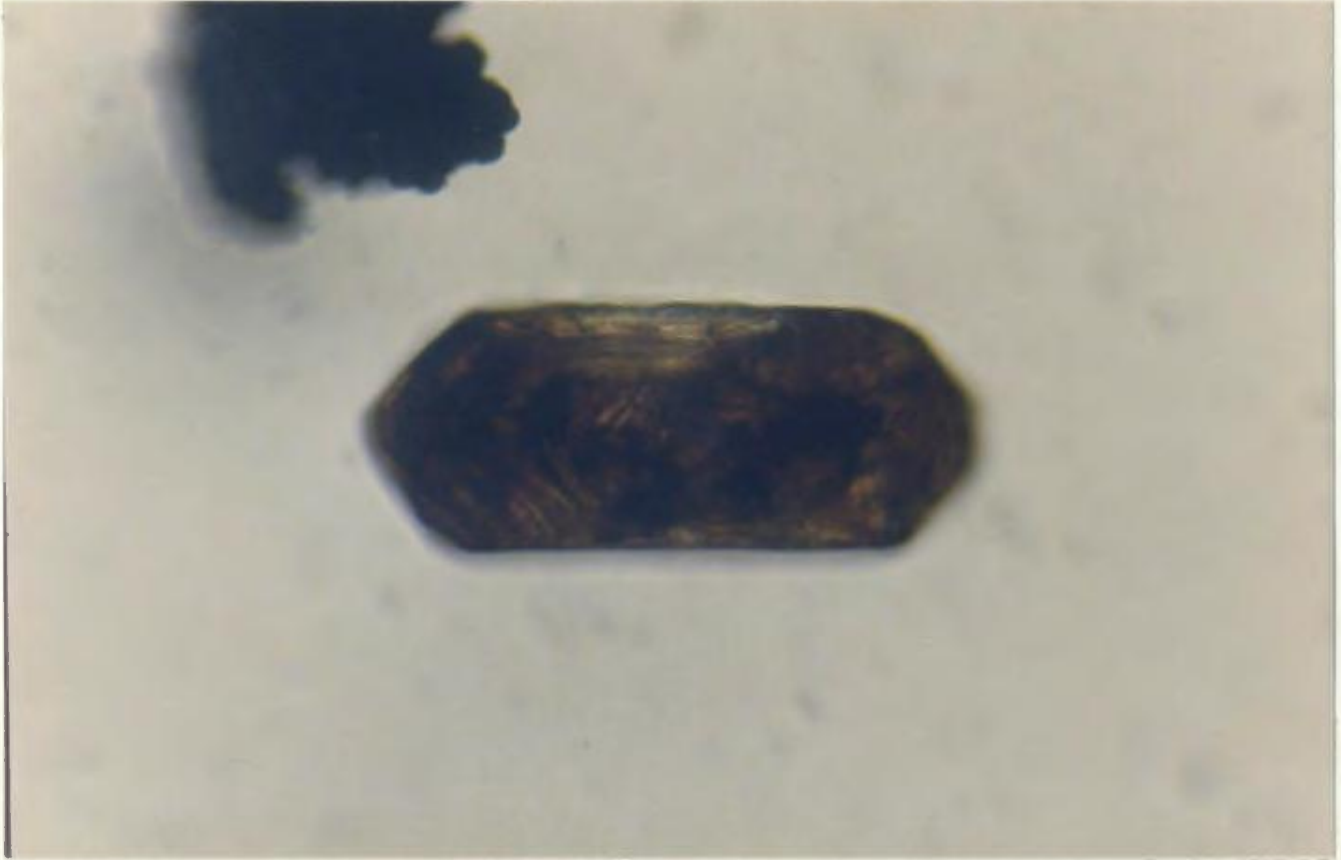


100 microns

Plate 4.49: Zircon. Zoned euhedral grain. Zoning between metamict and unaltered bands.

100 microns

Plate 4.50: Zircon. Metamict.

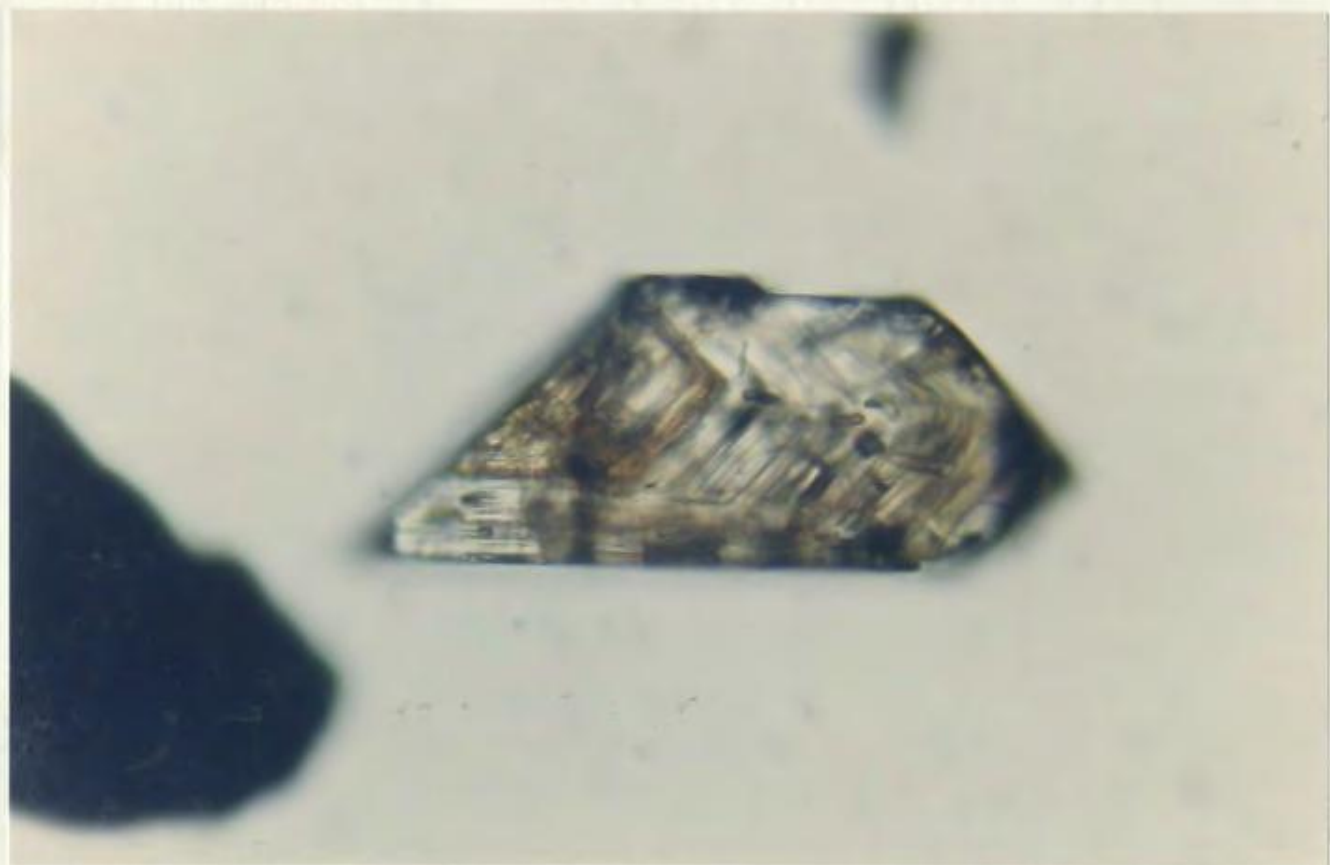
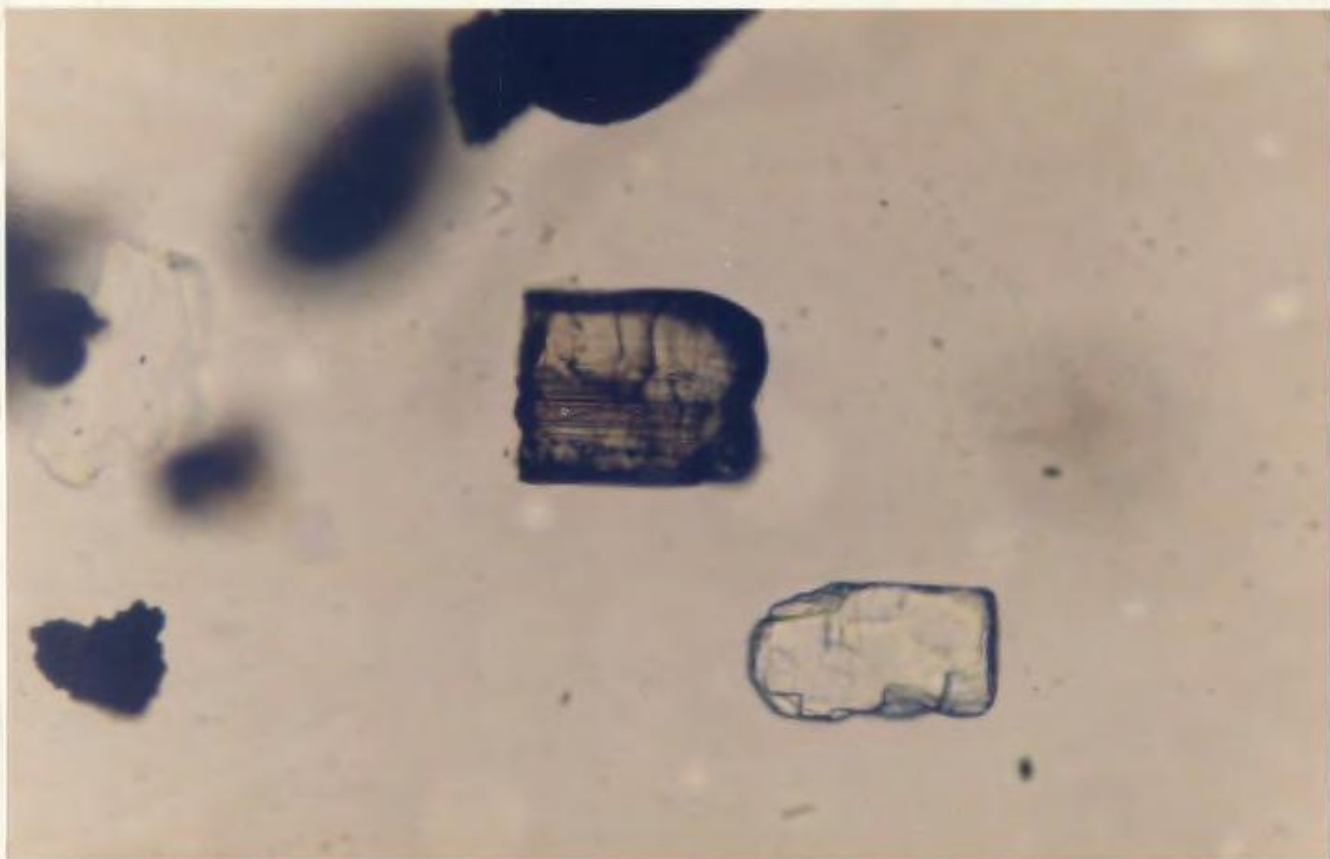


100 microns

Plate 4.51: Zircon. Broken prismatic zircon showing striations parallel to the C-axis.

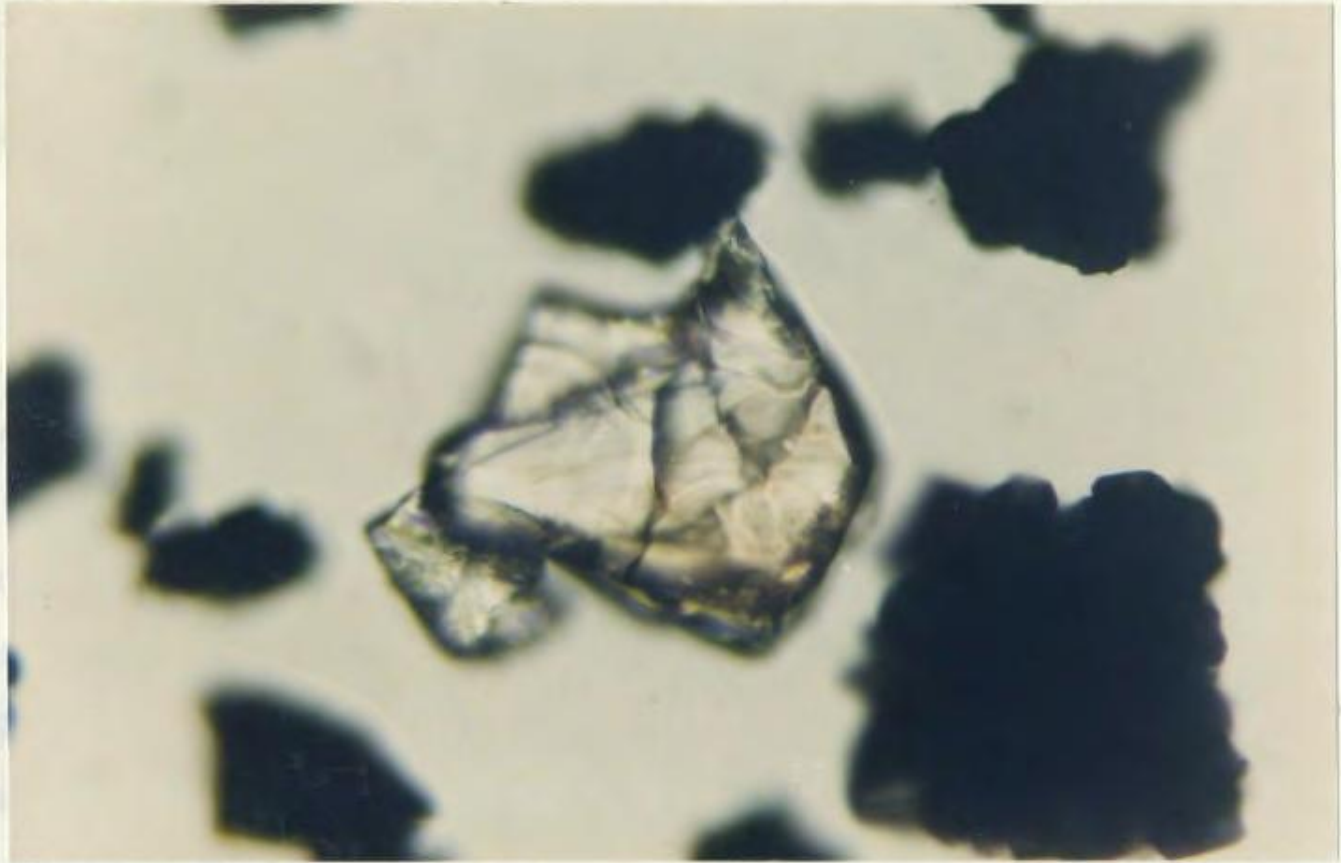
100 microns

Plate 4.52: Zircon. Broken euhedral zircon with striations parallel to the grain edge.



100 microns

Plate 4.53: Zircon. Colourless angular grain, devoid of inclusions.



... analysis, developed by Pearson
... is a multi-variate technique that may be applied to
... type of data and to any number of data points. It
... objects and associations existing between
... subjects and objects and is designed to convert the original
... information into a low dimensional array of principal
... components.

Factor analysis is performed using the
... technique. In each factor analysis, subjects
... relationships between variables while the factor analysis
... analysis studies relationships between subjects or variables.

CHAPTER 5

CORRESPONDENCE ANALYSIS

5.1 Introduction

To provide an unbiased and objective analysis of the heavy mineral data generated in this study, it was decided to apply factor analysis to the data set. Correspondence analysis was chosen to examine similarities and differences between the lower Tertiary sands on the Labrador Shelf.

Correspondence analysis, developed by Benzecri (1970), is a multi variate technique that may be applied to any type of data and to any number of data points. It detects associations and oppositions existing between subjects and objects and is designed to extract the maximum information from a two dimensional array of positive numbers.

Factor analysis is performed using two applications. R-mode factor analysis explores relationships between variables while Q-mode factor analysis studies relationships between objects or samples.

Correspondence analysis is a distribution free technique that combines the advantages of R- and Q-mode analysis, exploring the duality between them, and using weighting procedures to reduce scaling problems. Because of this duality between R-mode and Q-mode analysis (Gower, 1966; Klován and Imbrie, 1971), the eigenvalues of the R-mode matrix and Q-mode matrix are the same, therefore, only the eigenvector of the R-mode matrix needs to be extracted. This technique greatly reduces computing time and cost.

Scaling problems occur when comparing variables of different orders of magnitude. Principal component analysis uses standardization of variables to avoid this problem, however, the standardization is not symmetrical. In correspondence analysis a symmetrical transformation is applied to the original data matrix (David et al., 1974). This principal of distributional equivalence is one of the advantages of correspondence analysis in that it gives stability to the results (Teil, 1975). The main differences between principal component analysis and correspondence analysis are outlined by Teil (1975, p. 11).

It is beyond the scope of this thesis to discuss the mathematical theory behind correspondence analysis. The reader is, therefore, referred to Lebart et al. (1984), David and Beauchemin (1975), David et al. (1974) and Benzecri (1970). David and Beauchemin (1975) provide a

FORTRAN IV program for correspondence analysis.

Correspondence analysis for this study was accomplished in three steps. Firstly, analysis of the entire set of heavy mineral data was made. Subsequent steps involved analysis of parts of the original data set as determined by examining the results of step one.

5.2 Interpreting the Results of Correspondence Analysis

The results of correspondence analysis are displayed as two dimensional diagrams where the results of the R-mode and Q-mode analysis are plotted together. Visual inspection of the plot of sample points and variable points in the same plane yields information as follows:

- (1) groups of sample points are the result of the same process or belong to the same family;
- (2) nearby variable points show correlation between variables;
- (3) a group of sample points is characterized by the variable points close to that group (David et al., 1974).

To interpret the results of correspondence analysis, several pieces of information are required:

- (1) a listing of the original data and point identification,
- (2) factors in variable dimensional space and

sample dimensional space,

- (3) the percent of variation explained by each of the factors,
- (4) graphical plots of both sample points and variable points in the preferred plane or planes.

The results of the first step in the correspondence analysis procedure are found in Table 5.1 and displayed in Figure 5.1. The first two factors account for 55% of the variation with the first five factors explaining only 84% of the variation, suggesting that factors other than those indicated here are responsible for variations between heavy mineral samples. Factor 1 is amphibole (Am) and factor 2 is glauconite (Gl). The factor plot (Fig. 5.1) demonstrates the crowding effect caused by the high amphibole and glauconite values. Because of the overlapping of the values, interpretation was not possible. Examining the F_3 (kyanite) against F_4 (zircon) (Fig. 5.2) shows that amphibole and pyroxene are closely associated. A check of the raw data revealed that while pyroxene occurs in all wells in quantities from a trace to 6%, its largest occurrences (8.5 to 11.5%) are with amphibole (46.0 to 60.0%) in samples from the Skolp well.

Glauconite is an authigenic mineral with high

TABLE 5.1: Correspondence analysis on the entire heavy mineral suite, loadings of the first five factors with percentage of the total variance explained

| | F ₁ | F ₂ | F ₃ | F ₄ | F ₅ |
|-----------------------|----------------|----------------|----------------|----------------|----------------|
| GN | - 0.40 | 3.78 | 12.91 | -18.38 | - 0.90 |
| EP | 0.34 | 0.02 | - 0.75 | 7.49 | -53.58 |
| RU | - 0.04 | 0.29 | 0.01 | 2.04 | 3.32 |
| TM | - 0.13 | 1.43 | 6.23 | - 4.21 | 16.55 |
| ZI | - 0.53 | 0.12 | 0.09 | 50.87 | 15.00 |
| PY | 1.83 | - 0.38 | 0.01 | - 0.11 | 1.19 |
| AM | 61.33 | -30.42 | 0.04 | - 0.29 | 1.17 |
| ST | - 0.09 | 0.27 | 1.66 | - 0.45 | 0.34 |
| KY | - 0.12 | 0.82 | -72.16 | - 5.92 | 2.16 |
| AN | - 0.14 | 0.00 | 0.17 | 2.20 | - 0.16 |
| AP | - 0.03 | 0.21 | - 4.60 | 0.84 | 1.60 |
| SI | 0.00 | 0.00 | 0.02 | 0.33 | - 0.57 |
| GL | -34.99 | -61.86 | 0.01 | - 0.77 | 0.01 |
| MO | - 0.02 | - 0.17 | 0.64 | 5.63 | - 0.47 |
| DU | - 0.01 | 0.07 | 0.66 | 0.15 | 0.42 |
| SP | - 0.01 | 0.15 | 0.00 | 0.02 | 2.49 |
| CH | 0.00 | 0.02 | 0.03 | 0.29 | 0.07 |
| % variation explained | 28.41 | 26.73 | 11.41 | 9.05 | 8.23 |

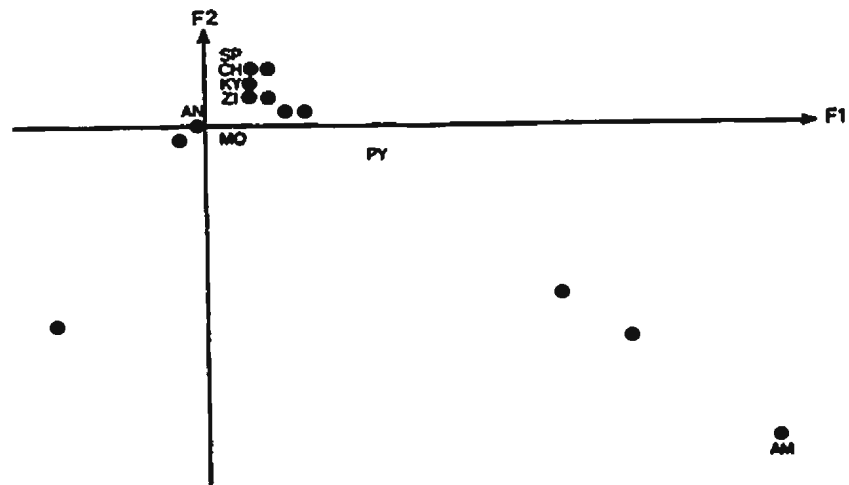


Figure 5.1 Paleocene and Eocene Correspondence Analysis of the entire heavy mineral suite

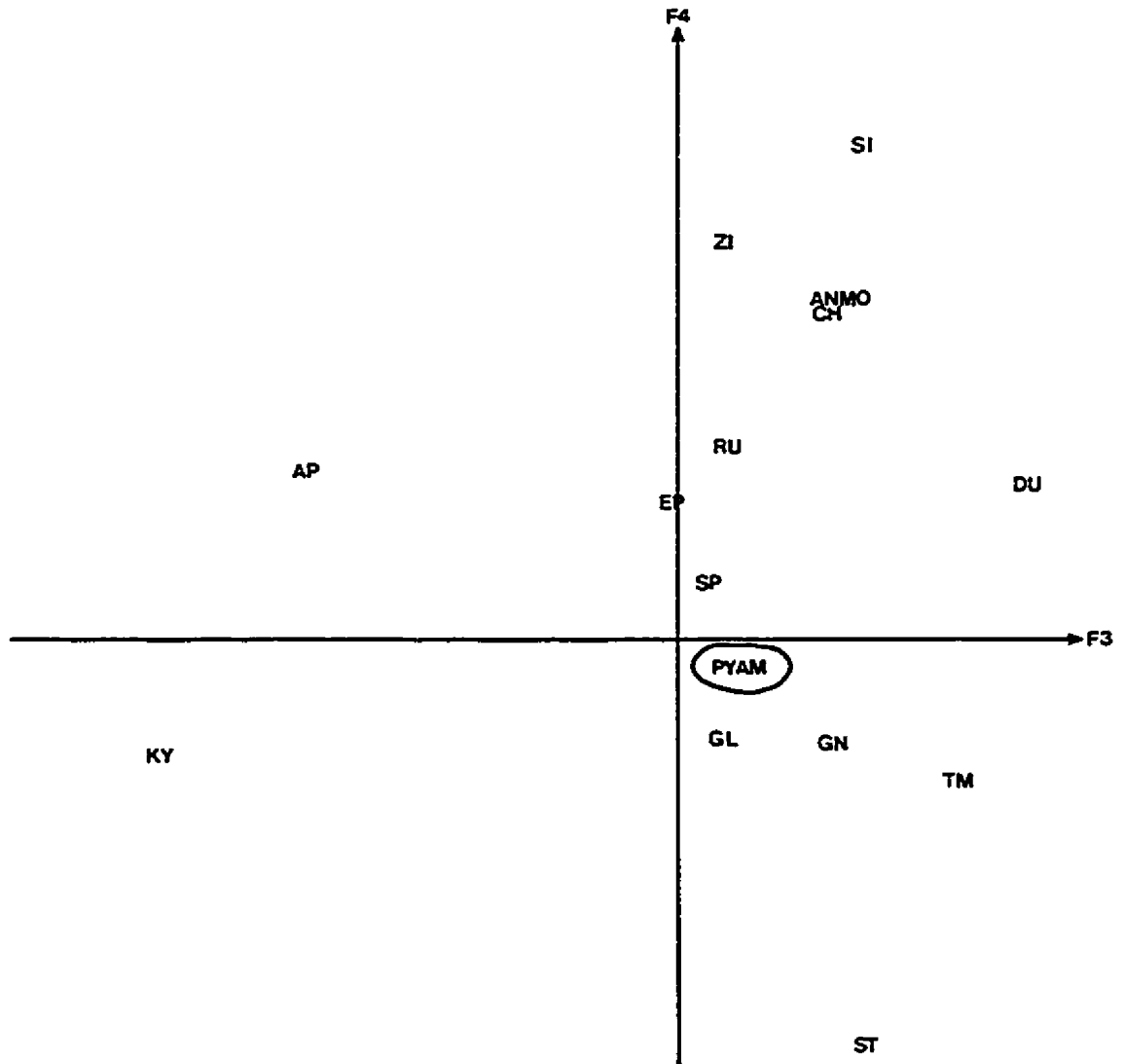


Figure 5.2 Paleocene and Eocene Correspondence Analysis showing the close association between amphibole and pyroxene

specific gravity and is related to sediment deposition rather than source rock and, therefore, should not be included in this heavy mineral analysis.

The minor heavy minerals explain little of the variation between the samples, so it was decided to exclude the minor minerals and glauconite and analyze only the major heavy minerals.

The results of the major heavy mineral analysis are given in Table 5.2 where the first two factors explained 61% of the variation, and the first five factors explained 95% of the variation. Figure 5.3 shows the association between amphibole and pyroxene, points 11, 12, 13 are samples from the Skolp well defining the Amphibole-Pyroxene subprovince.

There are indications of groupings among the remaining point cloud, associated with particular factors, viz., (1) kyanite; (2) rutile and zircon, and possibly epidote; and (3) garnet, staurolite and tourmaline.

Step three excluded pyroxene and amphibole from the major heavy mineral analysis. The results are shown in Table 5.3. The first two factors explain 58% of the variation; the first four factors explain 95%. The factor plot (Fig. 5.4) is very similar to Figure 5.3 but with little overlap of values in the point cloud.

Visual examination of the factor plot (Fig. 5.4:

TABLE 5.2: Correspondence analysis on the major heavy mineral (including Pyroxene and Amphibole)

| | F ₁ | F ₂ | F ₃ | F ₄ | F ₅ |
|-----------------------|----------------|----------------|----------------|----------------|----------------|
| GN | - 3.03 | -14.25 | 15.77 | 0.08 | -23.11 |
| EP | 0.01 | 1.71 | - 2.77 | 62.73 | 14.23 |
| RU | - 0.25 | - 0.05 | - 2.97 | - 2.49 | - 1.63 |
| TM | - 1.01 | - 8.02 | 1.84 | -17.45 | 52.13 |
| ZI | - 0.74 | 0.00 | -70.23 | - 7.20 | 3.85 |
| PY | 2.05 | - 0.05 | 0.03 | - 1.16 | - 0.02 |
| AM | 91.81 | - 0.12 | 0.08 | - 1.17 | 0.05 |
| ST | - 0.32 | - 1.83 | 0.30 | - 0.47 | 4.99 |
| KY | - 0.68 | 73.96 | 6.01 | - 7.25 | 0.00 |
| % variation explained | 43.64 | 17.59 | 14.86 | 12.73 | 6.22 |

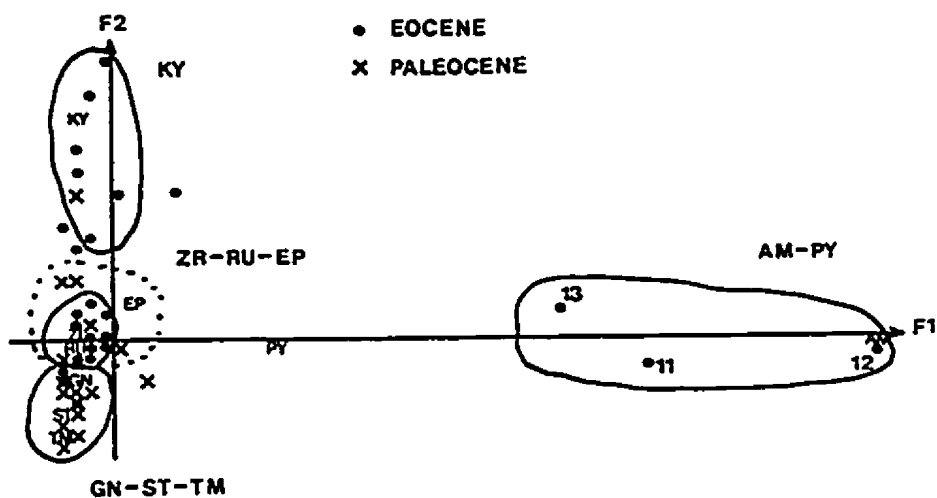


Figure 5.3 Paleocene and Eocene Correspondence Analysis of the major heavy mineral suite

TABLE 5.3: Correspondence analysis on the major heavy mineral (excluding Pyroxene and Amphibole)

| | F ₁ | F ₂ | F ₃ | F ₄ | F ₅ |
|-----------------------|----------------|----------------|----------------|----------------|----------------|
| GN | -15.43 | -15.53 | 0.24 | 23.11 | - 0.03 |
| EP | 2.55 | 6.70 | 59.09 | -12.40 | 0.00 |
| RU | - 0.08 | 2.23 | - 3.25 | - 1.72 | -66.92 |
| TM | - 8.95 | - 3.26 | -14.21 | -54.39 | 0.72 |
| ZI | 0.00 | 63.01 | -15.03 | 3.54 | 0.94 |
| ST | - 2.01 | - 0.42 | - 0.49 | - 4.83 | 6.49 |
| KY | 70.98 | - 8.84 | - 7.68 | - 0.01 | 0.03 |
| % variation explained | 31.56 | 26.59 | 24.35 | 11.05 | 3.64 |

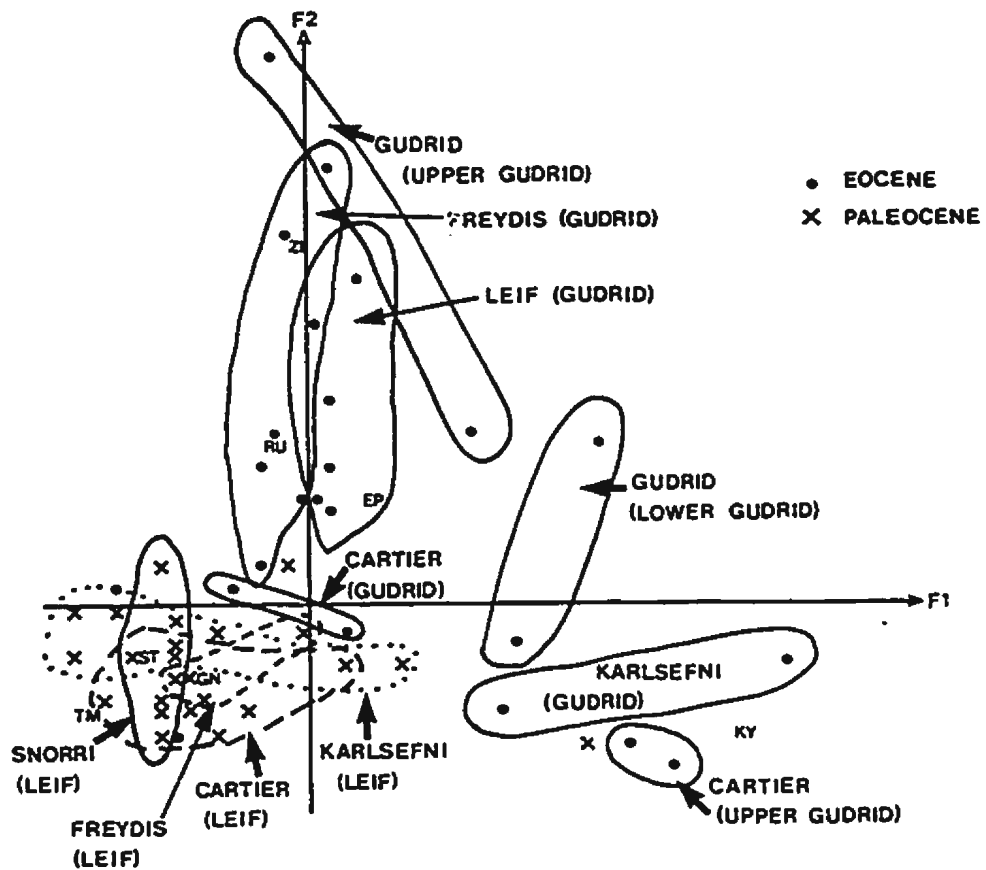


Figure 5.4 Paleocene and Eocene Correspondence Analysis of the major heavy mineral suite, excluding amphibole and pyroxene

F_2 against F_1) reveals segregation in the point cloud. The Paleocene-age Gudrid sand samples define two major groups: one group influenced by Zi-Ru-Ep (zircon-rutile-epidote) factors and the other by the Ky (kyanite) factor. Samples from the Leif and Freydis wells are closely related, plotting along the Zi-Ru-Ep (zircon-rutile-epidote) axis. The samples from the upper Gudrid sand of the Gudrid well have a very similar position on the plot, with a strong influence by kyanite. The lower Gudrid sand of the Cartier well plots towards rutile and epidote. The Paleocene at Karlsefni, the lower Gudrid sand at Gudrid, and the upper Gudrid sand at Cartier plot along the Ky (kyanite axis). The Eocene-age Leif sand samples, with the exception of one point, plot in clusters around the Gn-St-Tm (garnet-staurolite-tourmaline) factors.

The significance of these observations will be considered in detail in the discussion of provenance, Chapter 6.

CHAPTER 6

PROVENANCE

6.1 Introduction

The discussion of the provenance of the Lower Tertiary sands on the Labrador Shelf will be in three parts: firstly, the results of the light fraction and heavy mineral analyses (Chapters 3 and 4, respectively); secondly, the results of the correspondence analysis; and thirdly, the variations and similarities between samples and wells will be discussed in detail.

6.2 Mineralogy

The Paleocene and Eocene sandstones examined in this thesis are immature, as indicated by the low quartz-feldspar ratios (Table 3.1, p. 61) and fall within the arkose to subarkose zones on the QFL (quartz-feldspar-lithic fragments) plot (Fig. 3.1, p. 63).

The quartz-type study suggested a predominance of quartz from metamorphic sources. The diamond plot (Fig.

3.2, p. 64; after Basu et al., 1973) demonstrates that the sands were derived from middle- to upper-rank metamorphic grade rocks with some samples falling within the lower-rank metamorphic rocks area of the plot.

Cathodoluminescence studies of the quartz grains also indicate a predominance of metamorphic quartz, with lesser occurrences of quartz from plutonic rocks.

Both plutonic and schistose metamorphic lithic fragments are present, with plutonic rock fragments being more common. This contrasts with the dominance of metamorphic quartz indicated by the quartz studies. Preferential disaggregation of metamorphic lithic fragments would provide individual quartz grains with metamorphic characteristics, resulting in an apparent increase in the volume of plutonic lithic fragments.

The heavy minerals present in the studied samples suggest high-rank metamorphic rocks and sialic and mafic igneous rocks are present in the source area (see Table 4.1, p. 69). The presence of well rounded zircon and tourmaline suggest pre-existing sedimentary rocks were also present. The results of the heavy mineral analysis will be considered in detail in the discussion section (p. 163).

The calculated ZTR (zircon-tourmaline-rutile) indices are consistent with Hubert's (1962) index range for arkosic and subarkosic sands. If this index is an accurate

measure of maturity, it agrees with the degree of maturity indicated by the quartz-feldspar ratios.

Both the heavy and light minerals exhibited variability in grain rounding and sphericity. The rounding and sphericity of detrital grains can be the result of (1) distance of transport; (2) mineral hardness, (3) grain size availability in the source rock, or any combination of these factors. The last two of these factors require explanation. Mineral hardness appears to affect the degree of grain roundness in that harder minerals are susceptible to breakage, producing angular fragments, whereas softer minerals are more susceptible to abrasion, resulting in a greater likelihood of grains being rounded (Rubey, 1933). The size of minerals available in the source rock can affect roundness in that some minerals are present as larger crystals and are susceptible to physical breakup along cleavage, parting and fracture surfaces. Other mineral species occur as small crystals and polycyclic grains that are less susceptible to breakup and therefore are likely to be more rounded.

Chemically and mechanically unstable minerals are abundant in the heavy mineral suites, co-existing with stable minerals. Degredation of the heavy minerals appears to be minor. Amphibole and pyroxene display characteristic ragged terminations. Whether this is the result of

diagenetic alteration in the sediment or chemical alteration due to metamorphism is not known, however, the latter is suspected to be the cause. Ragged terminations are a diagnostic feature of amphibole and pyroxene in thin sections (Heinrich, 1965) and there is no adequate reason to attribute similar terminations in detrital grains to other causes. Occasional embayments in some minerals, such as garnet and staurolite, are likely dissolution features. The other heavy mineral species appear to have been essentially unaffected by diagenesis.

The feldspars in the light fraction of the lower Tertiary sands appear relatively fresh with little evidence of alteration. Clay mineralogy studies of the Labrador Sea wells (Hiscott, 1984) indicate: (1) Lower to Middle Cretaceous clays were dominated by kaolinite and derived from granitic rocks under humid, temperate weathering conditions; (2) Middle to Upper Cretaceous clays are dominated by smectite derived from weathering of local basalts; and (3) Paleogene clays are polymineralic and relatively homogeneous and are associated with a continent wide drainage basin.

6.3 Correspondence Analysis

Correspondence analysis provides an unbiased, statistical approach to the interpretation of the heavy

mineral data generated in this study. Ideally, the factors defined by correspondence analysis can be considered to be end-members representing particular source rock lithologies. The samples in this study can be viewed as mixtures, with each end-member contributing to the final composition of the sand.

The results of the correspondence analysis are found in Chapter 4 and will be discussed in detail herein. Examination of the point cloud distributions on the various factor plots reveals consistencies in the point groupings. The factors defined by the correspondence analysis are: (1) Amphibole factor, (2) Kyanite factor, (3) Zircon-Rutile factor, (4) Garnet-Staurolite-Tourmaline factor.

These factors, and the groupings of the wells, define heavy mineral provinces on the Labrador Shelf. The Paleocene samples plot along different factors, defining two heavy mineral provinces: the Kyanite Province and Zircon-Rutile-Epidote Province with the Amphibole-Pyroxene Subprovince, and the Zircon-Rutile-Kyanite mixed zone (Fig. 6.1). This mixed zone indicates a southward shift in the Kyanite/Zircon-Rutile-Epidote boundary from the lower Gudrid to the upper Gudrid sand member. The Eocene samples cluster around one factor, defining one heavy mineral province, Garnet-Staurolite-Tourmaline, for the entire Labrador Shelf (Fig. 6.2).

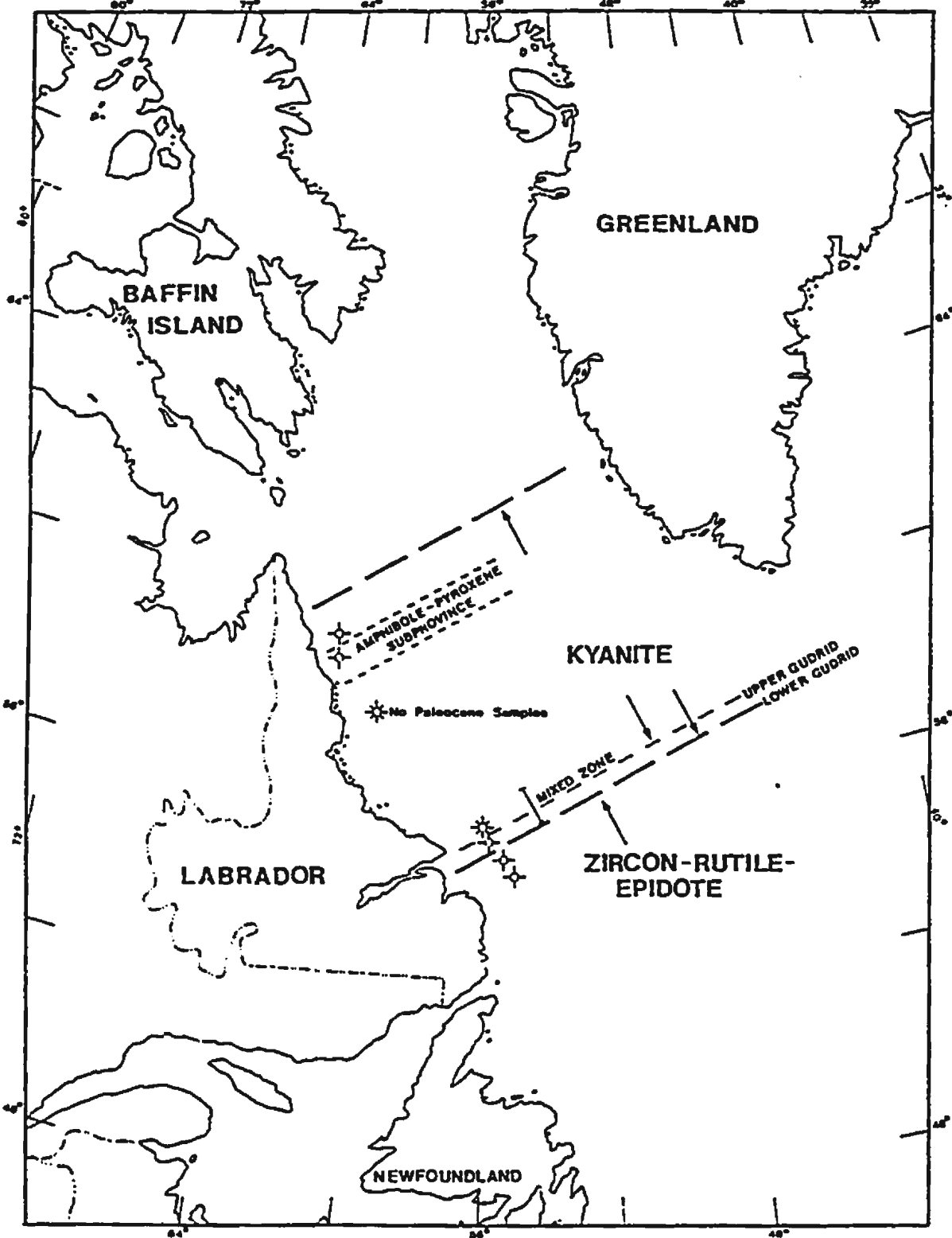


FIGURE 6.1 Paleocene heavy mineral provinces

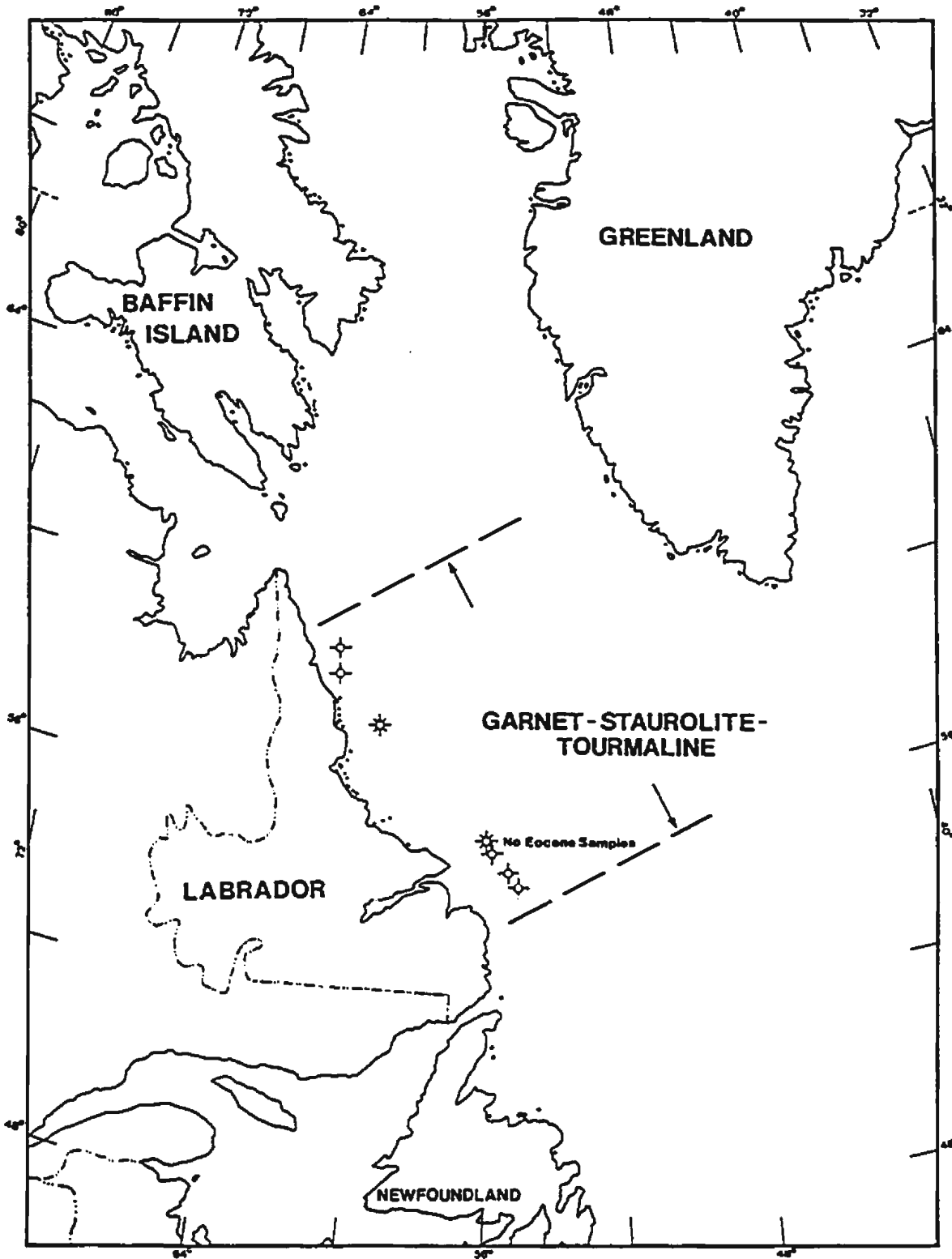


FIGURE 6.2 Eocene heavy mineral provinces

6.3.1 Amphibole Factor

Amphiboles and pyroxenes are present in igneous and metamorphic rocks. Amphiboles occur in granites, syenites, and diorites, and metamorphosed intermediate and basic igneous rocks that have reached epidote-amphibolite and amphibolite facies (Miyashiro, 1973). Pyroxene, in particular clinopyroxene, also occurs in the high temperature regime of the amphibolite facies. Changes from epidote-amphibolite to amphibolite facies with increasing temperature corresponds to a colour change in hornblende from blue-green through to brownish green and brown (Miyashiro, 1973). Although all these colour variations are recognized in the hornblende from the samples of the sediments on the Labrador Shelf, the dominant colour is green, consistent with derivation from an amphibolite facies source (Stockwell et al., 1970).

Amphibolite facies schists and gneisses are preferred as the dominant source for the amphibole and pyroxene. Amphibolite facies metamorphic terranes are common and widespread throughout the Canadian Shield.

The sudden and substantial increase in amphibole concentrations, from less than 4% elsewhere, to 65% in the Gudrid sands at Skolp will be addressed in section 6.4.1.2.

6.3.2 Kyanite Factor

Kyanite is characteristic of low temperature, medium to high pressure metamorphism of pelitic rocks. It occurs in association with staurolite, with or without sillimanite, and with almandine garnet in the epidote-amphibolite and amphibolite facies (Miyashiro, 1973).

Kyanite-rich rocks occur locally in association with the Grenville Front and in the Superior Province (Goodwin et al., 1970). Kyanite is also present in sillimanite-bearing gneisses. Although kyanite-bearing outcrops are not aerally extensive, these alumino-silicate-bearing gneisses are distributed throughout much of the Canadian Shield.

6.3.3 Zircon-Rutile Factor

Zircon and rutile are characteristic of acid igneous rocks. Zircon occurs in granites and diorites as well as intermediate syenites; rutile occurs in pneumatolized granites and alkali-anorthosites. Rutile is also common in high-grade metamorphic terranes (Force, 1980).

Zircon and rutile, along with tourmaline, are considered to be ultrastable heavy minerals. Their presence in the heavy mineral concentrations may indicate

that the sediments were derived from pre-existing sedimentary rocks. During the Proterozoic, a thick sand-shale sequence was thought to be widespread over much of the Canadian Shield (McMillan, 1973; Coleman, 1921), but these sediments were unlikely as a sediment source for the Tertiary sands as most of this supracrustal sequence had probably been stripped from the shield by late Mesozoic (Greene, 1974), leaving only isolated remnants. Derivation from pre-existing Mesozoic sedimentary rocks, however, cannot be ruled out.

The rounding of the ultrastable heavy minerals gives some support to earlier sedimentary sequences, however, the angularity of the other heavy minerals and the light minerals, the presence of abundant fresh feldspar, and the diversity of other less stable heavy minerals indicate dominant sediment input from rocks other than pre-existing sedimentary sources. Rounding of zircon grains has been recognized in pegmatites, granitic gneisses and granites (Vitanage, 1957) as well as in paragneisses, or gneisses derived from pre-existing sedimentary rocks (Heimlich et al., 1975). The common occurrence of metamict zircons indicates input from igneous sources while the clear, brilliant zircons suggest they have undergone recrystallization in a metamorphic environment (Wyatt, 1954). Zircon rounding cannot be used as a diagnostic

feature.

Because rutile and zircon commonly occur as accessory minerals in a wide variety of igneous rocks determining individual source rocks was not possible with any degree of confidence. TiO_2 -rich granites were recognized as a possible rutile source.

6.3.4 Epidote Factor

Epidote is indicative of crystalline metamorphic rocks, particularly metabasites and metamorphosed impure limestones. Epidote can occur in low to high pressure regimes of greenschist, epidote-amphibolite, and amphibolite facies (Miyashiro, 1973). In the greenschist facies epidote occurs with actinolite; in the amphibolite facies the amphibolite is hornblende.

The epidote factor most likely represents greenschist to amphibolite facies metabasites; metamorphosed impure limestones are rare on the Canadian Shield. Chlorite and actinolite were rarely noted, indicating a lack of sediment input from greenschist facies rocks; the widespread occurrence, albeit usually in trace amounts, of pyroxene (clinopyroxenes) and amphibole (hornblende, with the exception of samples from the Skolp well) in the heavy mineral fractions indicates amphibolites and granulites were sediment sources. Both amphibolite and

granulite facies metamorphic rocks cover extensive areas of Canadian Shield and are likely sources for the epidote.

Because of the clustering of the Zircon-Rutile factor and the Epidote factor, they have been grouped together as one heavy mineral province. It was not possible to separate these groupings to make two heavy mineral provinces.

6.3.5 Garnet-Staurolite-Tourmaline Factor

Garnet, staurolite, and tourmaline comprise the last factor. These minerals are associated, along with several other mineral species such as kyanite, andalusite, sillimanite, the micas, and rutile, occurring in rocks of regional metamorphic origins. Staurolite is indicative of crystalline schists, particularly epidote-amphibolite and amphibolite facies metapelitic rocks. It occurs with andalusite, sillimanite, and cordierite under low pressure conditions; and with kyanite, with or without sillimanite, under medium and high pressure conditions, respectively. Tourmaline occurs in acid igneous rocks, granites and their pegmatites, pneumatolytic granites, schists, gneisses, and phyllites. Garnet, depending on the particular variety present can be indicative of acid to ultrabasic igneous rocks, as well as a variety of metamorphosed rocks; almandine and spessartine are the two most commonly occurring garnet species.

Almandine is the common garnet in schists and gneisses, as well as in granites, rhyolites, and pegmatites; spessartine often occurs in granite pegmatites and metamorphosed manganese-bearing rocks.

The garnet-staurolite-tourmaline factor likely corresponds to a mix of lithologies. Garnet-bearing gneisses are widespread and may also provide a source for tourmaline. The rare brown-yellow tourmalines suggest metamorphosed limestones; marbles occur sporadically in part of the Canadian Shield. Staurolite is typical of amphibolite facies metapelites, and may also be present in sillimanite-bearing gneisses.

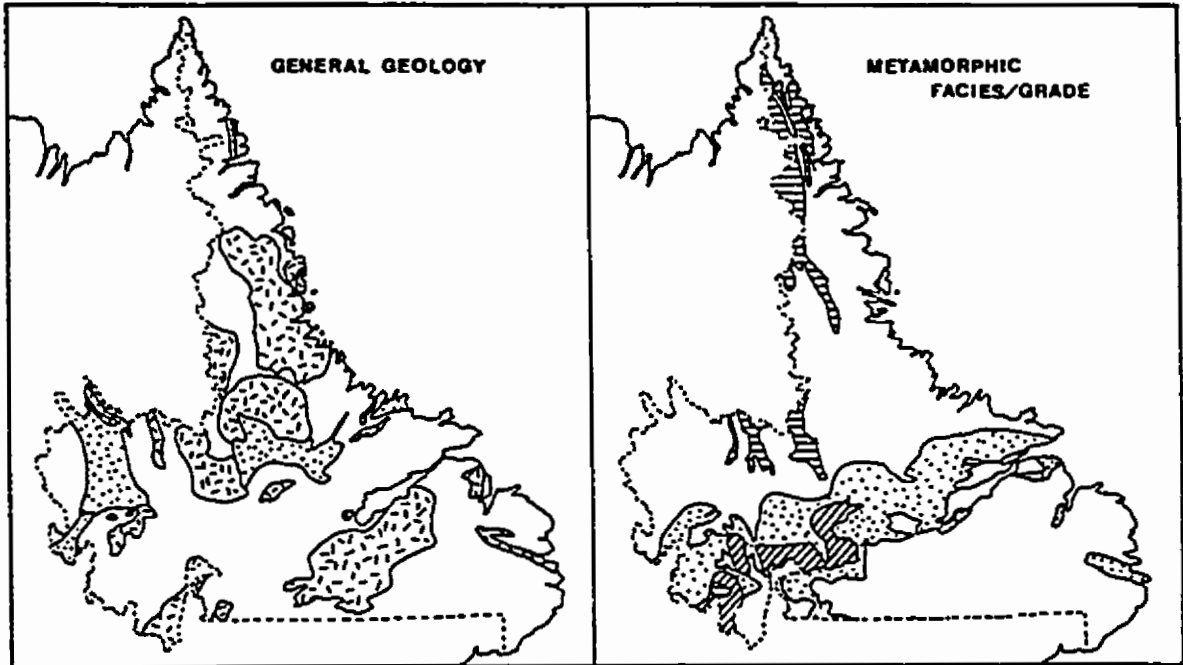
Examination of the heavy mineral data indicate that medium to high-grade (epidote-amphibolite, amphibolite, and granulite facies) metamorphic rocks were the dominant sources for much of the detritus supplied to the Tertiary sequence on the Labrador Shelf. Acid igneous rocks, which have been overprinted by varying metamorphic grades, and metapelites appear to support the recognized mineral associations. Mafic igneous rocks appear to be very minor source rocks. The dominance by metamorphic rocks is supported by the results of the light fraction analysis. The factors defined by the correspondence analysis also concur with these observations.

6.4 Discussion

The Canadian Shield is dominated by acid plutonic and gneissic complexes covering several hundred thousand square kilometres, and commonly overprinted by metamorphic facies ranging from greenschist to granulite facies, with amphibolite and granulite facies dominating (Fig. 6.3).

The sands from the Labrador Shelf have mineralogies that are indicative of the metamorphic character of the source rocks. Metapelitic (high alumino-silicate) rocks can be distinguished from metabasites. Some granitic source rocks can be defined. Pre-existing sedimentary rocks appear to be of local importance as source rocks.

The Tertiary sedimentary sequence on the Labrador Shelf is a sand-shale package, with shale being the dominant lithology. The predominance of the finer detrital components and the enormous volume of sediment deposited, suggests an equally enormous drainage basin supplying detritus. The thickness of the sediment wedge varies throughout the study area. Paleocene-age, sediment thickness in the Saglek Basin reached 5000m and 4000m in the Hopedale Basin. A similar pattern is repeated in the Eocene with sediments in the Saglek Basin reaching 3000m and in the Hopedale Basin only 2000m (Fig 6.4). The greater thickness of sediment at the "mouth" of Hudson



LEGENDS

- | | |
|---|--|
|  BASIC ROCKS & ANORTHOSITES |  AMPHIBOLITE |
|  SUPRACRUSTAL ROCKS & METAMORPHOSED EQUIVALENTS |  GRANULITE |
|  GRANITE & GRANITIC GNEISS |  SILLIMANITE GNEISS |
| |  PARAGNEISS |

FIGURE 6.3 Summary of geology and metamorphic facies of Labrador

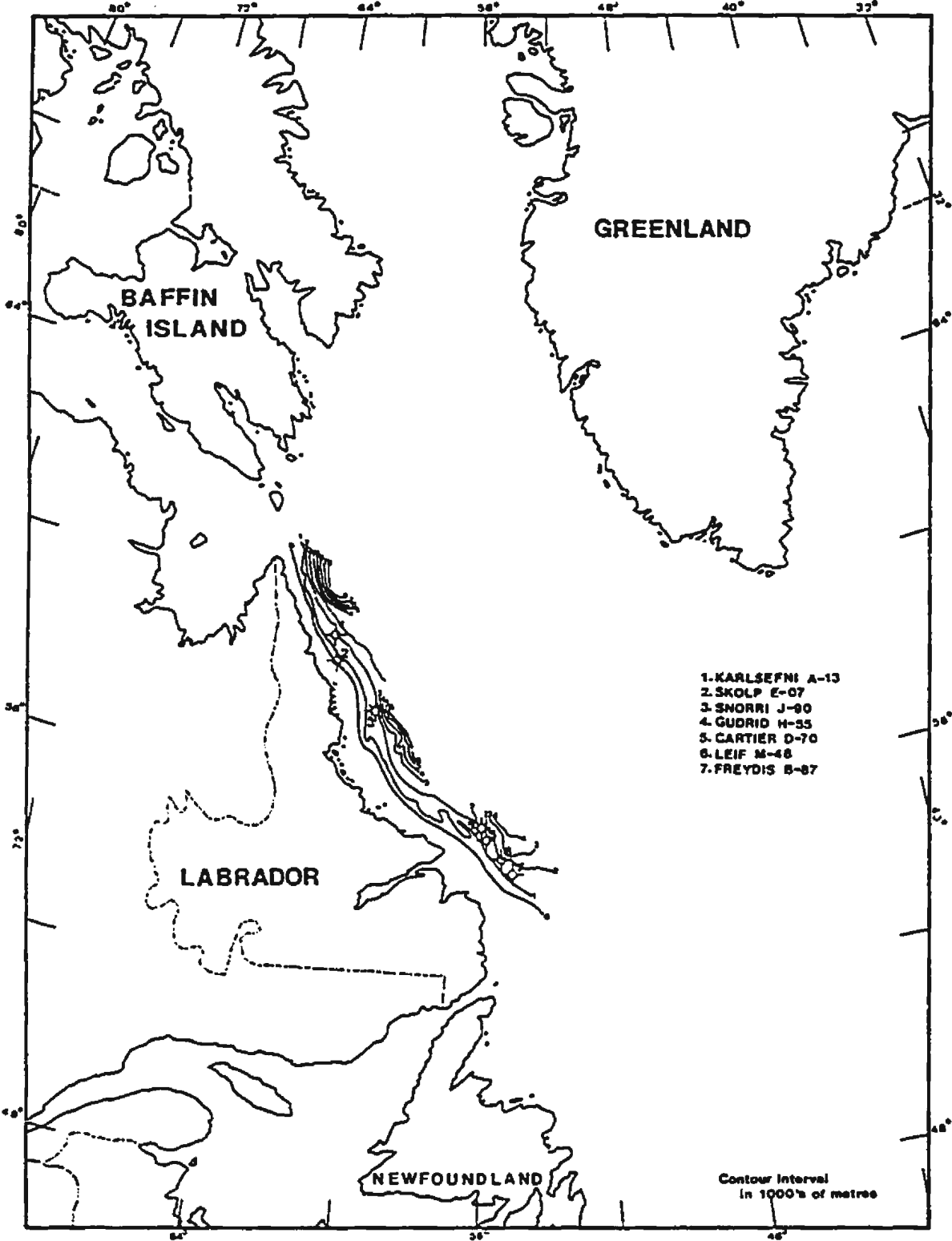


FIGURE 6.4 Isopach of Cartwright and Kenamu Formations

Strait, supports the interpretation of a super-river supplying detritus to the Labrador Sea during the lower Tertiary. The Okak Arch, separating the Saglek and Hopedale Basins, likely prevented Cretaceous and Paleocene sediments from being transported along shore into the Hopedale Basin. The effects of the Okak Arch were considerably lessened by Eocene time (as a result of sediment infill) and lateral sediment transport was more likely.

6.4.1 Paleocene Sands

The Paleocene Cartwright Formation and Gudrid sand member are present throughout the study area. Generally, the Gudrid sands are light brown to buff, medium grained quartzose sands and translucent to very light brown, coarse grained, arkosic, slightly kaolinitic sands; dolomite cement is present, particularly in the lower part of the sequence. Bouma cycle sand-shale turbidites have been recognized in cores from the Gudrid sand and, with the presence of detrital coal, glauconite, and abundant calcareous cement (McWhae et al., 1980) it has been suggested that these sands are part of a fan sequence downdip from coastal deltaic sands and peripheral bar deposits.

The Gudrid sand member samples were obtained from

the following wells (from north to south): Karlsefni A-13, Skolp E-07, Gudrid H-55, Cartier D-70, Leif M-48, and Freydis B-87.

6.4.1.1 Karlsefni

Heavy mineralogy suggests that the Gudrid sand in the Karlsefni well was derived from metapelitic source rocks that had reached the medium to high pressure regime of epidote-amphibolite to amphibolite facies metamorphism as indicated by the high (45-46%) concentrations of kyanite. Minor input from igneous plutonic sources was indicated by low rutile and zircon amounts accompanied by relatively low garnet abundances. The presence of epidote suggests metabasites were available as source rocks.

6.4.1.2 Skolp

At Skolp, the Gudrid sand is dominated by an amphibole-pyroxene combination, likely derived from a hornblende-rich amphibolite facies metabasite source. Epidote is associated with the amphibole. Garnet occurrences have an inverse relationship with the amphibole (ie. high garnet occurs with lower abundances of amphibole).

The Upper Cretaceous Freydis Member and Markland Formation at Skolp are dominated by abundant kyanite and

high concentrations of garnet, similar to Karlsefni, indicating a garnet-bearing metapelite that had reached amphibolite facies metamorphism.

6.4.1.3 Snorri

No Paleocene-age sand samples were obtained from Snorri.

6.4.1.4 Gudrid

At the Gudrid well, the Gudrid Members occur as a continuous sand with a disconformity between the lower and upper members; elsewhere in the area the Gudrid Member sands are separated by shales of the Cartwright Formation.

The sands from the Gudrid well are characterized by high abundances of zircon; rutile values are also higher than average. Garnet is noticeably less abundant, as is epidote. Both pyroxene and amphibole occur in minor, trace amounts. Kyanite is present, dividing the sand into lower and upper kyanite-rich zones separated by a middle kyanite-poor zone.

The kyanite occurrences suggest a metapelitic source rock (similar to that of Karlsefni and Skolp). The high concentration of zircons and rutile, coupled with low amounts of garnet, suggest that the already concentrated ultrastable minerals were released from pre-existing

sedimentary rocks and that acid igneous rocks likely were minor source rocks.

6.4.1.5 Cartier

The kyanite distribution in the Cartier well is similar to that of the Gudrid well. The sands are characterized by high kyanite in the upper and lower zones separated by a low kyanite zone. The lower kyanite-rich zone is also marked by high zircon abundances. Garnet concentrations increase downwards. Epidote values are similar throughout. Amphibole and pyroxene are present at the top of the Paleocene in trace quantities.

The kyanite indicates metapelites in the amphibolite facies, with associated garnet. Garnet, with zircon, also suggest acid plutonic/gneissic source rocks. The presence of amphibole, pyroxene, and epidote suggests a metabasite source, such as the layered gabbros, or perhaps the garnetiferous gabbroic gneiss, of the Makkovik Subprovince.

6.4.1.6 Leif

The Gudrid sands encountered at Leif revealed high zircon concentrations accompanied by high epidote, low garnet and low kyanite. Amphibole was not encountered and pyroxene occurred in trace amounts only. Rutile reached 5%

of the total heavy mineral content.

The elevated zircon content, with the low garnet content, and slightly elevated rutile likely indicate input from a local sedimentary source or a paragneissic source, masking any input from acid plutonic/gneissic sources. The epidote and pyroxene contents are indicative minor input from a metabasite source (see above).

6.4.1.7 Freydis

The Paleocene sands from Freydis are characterized by low kyanite concentrations and associated staurolite. The zircon abundances define upper and lower zircon-rich zones separated by a middle zircon-poor zone. Garnet and epidote have an inverse relationship in that as garnet decreases downward, epidote increases. Amphibole is not present and pyroxene occurs rarely, in trace amounts only. Rutile and tourmaline do not appear to be diagnostic.

The two "floods" of zircon may represent derivation from pre-existing sedimentary rocks or from paragneissic terranes, whereas the intermediate low zircon zone may be more indicative of sediments from acid plutonic sources. Tourmaline appears more closely associated with the low zircon zone, and may represent a pegmatitic or a pneumatolyzed granitic source. The relationship between garnet and epidote may represent a blending of sediments

from a metabasite source with sediments derived from granites or granitic gneisses.

Generally, the Gudrid Member samples showed marked differences in gross heavy mineralogy and position on the factor plots. The source rocks included a variety of metamorphic rocks (metapelites, metabasites, paragneisses and granitic gneisses) that had reached amphibolite and possibly granulite facies metamorphism, and acid and basic plutonic rocks.

6.4.2 Eocene Sands

The Eocene-age sand, the Leif Member, is developed at the top of the Kenamu Formation. It varies from a fine-grained white to light brown quartz sand, and silty sand, and marine silty shale, shale and siltstone, with thin dolomitic limestone beds. The lateral distribution of the Leif sand is not completely understood; it ranges from absent to 210m in thickness, while the remainder of the Kenamu Formation is present throughout the study area. Because of the clean, relatively thick nature of the Leif sand, it has been interpreted as a neritic, perhaps tidal deposit (McWhae et al., 1980) that formed close to the time the Labrador Sea ceased spreading. As a shallow marine or tidal deposit it would be subject to extensive reworking by tidal influences or long-shore drift.

During correspondence analysis the Eocene-age samples showed a marked clustering with respect to one factor on each of the projections, suggesting either a single source for the sand or a variety of sources subsequently mixed.

6.4.2.1 Karlsefni

Pronounced kyanite concentrations occur in the upper part of the Leif sand in the Karlsefni well. The lower part of the sand is characterized by lower kyanite and epidote abundances with higher tourmaline, abundant garnet, staurolite, and zircon. Rutile values are slightly elevated. Amphibole occurs in only one sample and pyroxene is present in only trace amounts.

Kyanite and staurolite indicate source rocks of pelitic schists and gneisses that have reached amphibolite facies metamorphism. The high zircon and garnet indicate input from acidic plutonic sources. Rutile is probably associated with the garnet and zircon sources.

6.4.2.2 Skolp

The samples of the Leif sand from the Skolp well are similar to the lower part of the Eocene sand encountered at Karlsefni, i.e., low kyanite, high garnet, staurolite and zircon, and likely have the same or a

similar source (see above).

6.4.2.3 Snorri

The samples from Snorri, with the exception of the upper-most sample, show a marked similarity throughout the sand, suggesting widespread sediment mixing. Other than abundant staurolite and the high zircon contents of the shallowest sample, the heavy minerals do not show any anomalous values.

Staurolite is characteristic of medium grade metamorphic rocks and may occur with kyanite, with or without sillimanite, in schists and gneisses. The common acid igneous plutonic/gneissic source appears to be most prevalent.

6.4.2.4 Gudrid

No samples of Eocene age were obtained from the Gudrid well.

6.4.2.5 Cartier

The heavy minerals from the Leif sand encountered at Cartier are the typical mix of metamorphic and acidic source rock indicators. Kyanite was low, as was staurolite. Both amphibole and pyroxene were present in trace amounts and epidote was variable. Garnet values were

high; both rutile and tourmaline appear non-diagnostic. Zircon has similar concentrations throughout the section.

These sediments were likely derived from an acid plutonic/gneissic source with minor input from mixed metamorphic source rocks.

6.4.2.6 Leif

The Eocene sands from the Leif well again display abundant kyanite and staurolite. Amphibole and pyroxene are present in trace amounts, epidote in relatively low concentrations. Garnet is abundant, as is zircon. Tourmaline and rutile are not diagnostic.

Metapelitic rocks, as indicated by kyanite and staurolite appear to dominate. Garnet is likely part of the metamorphic terrane, corresponding to a garnet schist or gneiss, as well as indicative of an acid igneous source with associated zircon. Zircon may also represent pre-existing sedimentary source rocks.

6.4.2.7 Freydis

Garnet is the dominant heavy mineral from the Leif sand in the Freydis well. Rutile, tourmaline and zircon all have similar concentrations; amphibole and pyroxene occur in trace amounts. Kyanite and staurolite occur together in minor concentrations. Epidote does not appear

diagnostic.

These sands were likely derived from garnetiferous kyanite-bearing schists or gneisses. Acidic plutonics or perhaps pre-existing sedimentary rocks are suggested by the zircon, tourmaline and rutile concentrations.

The Eocene-age Leif sand samples from all the wells examined showed marked similarities in gross heavy mineralogy, position on the factor plots, and with respect to interpreted source rocks. In view of the depositional environment of the Leif sand, this was expected.

Interpreted as a neritic, perhaps tidal deposit, these sands have been influenced by many factors in the depositional regime (shallow continental shelf) as well as transported detritus in the erosional regime (onshore Canadian Shield).

By Eocene time the drainage basins on the Canadian Shield had stabilized, becoming mature terranes of low relief (McMillan, 1973; Hiscott, 1974; Balkwill et al., 1990). Sediment mixing occurred in the fluvial systems. In the marine environment the sands were under the influence of longshore currents and lateral sediment migration, resulting in extensive sediment mixing and homogenization.

Overall, little can be said concerning the definition of sources of the Eocene-age sands, other than

the sands were likely derived from garnetiferous schists and/or gneisses with variable input from kyanite-bearing metamorphic rocks and acid plutonic rocks and/or gneisses.

CHAPTER 7

CONCLUSIONS

1. The samples examined in this study were taken from the Paleocene and Eocene sand intervals encountered in seven boreholes on the Labrador Shelf. These sands are part of the Lower Tertiary sedimentary sequence that underlies the continental margins off Labrador and Baffin Island. This sedimentary sequence formed in response to updoming, rifting and sea-floor spreading.
2. Grain studies of the heavy mineral and light mineral fractions show that the sands are texturally and mineralogically immature suggesting rapid erosion with moderate transportation distances from source areas and little post-depositional diagenetic alteration.
3. The enormous volume of Tertiary sediments implies that drainage basins at that time covered an enormous geographic area, including much of North America east of the Canadian Cordillera and southeast of the Arctic Archipelago.

4. The principal source rocks for the Paleocene and Eocene sediments were amphibolite facies metamorphic rocks, especially garnet-, hornblende-, and kyanite-rich schists and/or gneisses, and acidic plutonic rocks, particularly granites and/or granite gneisses. Basic plutonic rocks were minor contributors. Low grade metamorphic (greenschist) facies and pre-existing sedimentary rocks were rarely indicated as sediment sources.
5. Paleogeography, lithology, and sedimentology indicate that the environments of deposition are different for the two sands in this study. The Paleocene-age Gudrid sands are developed as seaward-facing fan deltas while the Eocene-age Leif sand is a shoreface and coastal sand deposit. These differences in depositional environment are reflected in the results of the correspondence analysis.
6. The results of correspondence analysis of the data generated in this study reveal differences between the Paleocene sands and Eocene sands. On the factor plots the Paleocene-age Gudrid sands exhibited separation between wells and clustering of the samples from the individual wells suggesting that these sands retained some of the heterogeneity recognized in the Cretaceous sands. By Eocene time, the Leif sands, on the factor

plots, exhibited severe overlap of all the wells and a clustering towards one factor, the garnet-staurolite-tourmaline factor. This pronounced clustering indicates mixing of the sediments, during fluvial transportation and during lateral transport while in the marine environment.

7. Transportation of the sediments were generally perpendicular to the axis of the Labrador Sea. Lateral transport played an important role in sediment mixing during the Eocene.

- Ambrose, J.W., 1964, Exhumed paleoplains of the Precambrian Shield of North America: American Journal of Science, V. 262, p. 817-857.
- Andrews, J.T., Guennel, G.K., Wray, J.L. and Ives, J.D., 1972, An early Tertiary outcrop in North-Central Baffin Island, Northwest Territories, Canada: Canadian Journal of Earth Sciences, V. 9, p. 233-238.
- Austin, G.H., 1973, Regional geology of eastern Canada offshore: American Association of Petroleum Geologists, Bulletin v. 57, p. 1250-1275.
- Balkwill, H.R., 1987, Labrador Basin: Structural and Stratigraphic Style, in Beaumont, C. and Tankard, A.J., eds., Sedimentary Basins and Basin-Forming Margins: Canadian Society of Petroleum Geologists, Memoir 12, p. 17-43.
- Balkwill, H.R., McMillan, N.J., MacLean, B., Williams, G.L., and Srivastava, S.P., 1990, Geology of the Labrador Shelf, Baffin Bay, and Davis Strait, Chapter 7 in Keen, M.J. and Williams, G.L., eds., Geology of the Continental Margin of Eastern Canada: Geological Survey of Canada, Geology of Canada, no. 2, p. 293-348.
- Basu, A., Young, S.W., Suttner, L.J., James, W.C., and Mack, G.H., 1975, Re-evaluation of the use of undulatory extinction and polycrystallinity of detrital quartz for provenance interpretation: Journal of Sedimentary Petrology, v. 45, p. 873-882.
- Beh, R.L., 1975, Evolution and geology of western Baffin Island and Davis Strait, Canada, in Yorath, C.J., Parker, L.R. and Glass, D.I., eds., Canada's Continental Margins and Offshore Petroleum Exploration: Canadian Society of Petroleum Geologists, Memoir 4, p. 453-476.
- Bell, J.S., co-ordinator, 1989, Frontier Science Program, East Coast Basin Atlas Service, Labrador Sea: Geological Survey of Canada, Atlantic Geoscience Centre, Dartmouth, Nova Scotia, 112p.
- Benzecri, J.P., 1970, Distance distributionnelle et metrique du chideux en analyse factorielle des correspondances: Laboratoire de Statistique Mathematique, Universite de Paris 6. 3e edition.

- Berkhout, A.W.J., 1973, Gravity in the Prince of Wales, Somerset, and Northern Baffin Islands Region, in Aitken, J.D. and Glass, D.J., eds., Canadian Arctic Geology: Geological Association of Canada-Canadian Society of Petroleum Geologists, p. 63-79.
- Bird, J.B., 1967, The Physiography of Arctic Canada: Baltimore, Johns Hopkins Press, 336p.
- Blais, R.A., 1959, L'origine des minerais Cretaces du gisement de fer de Redmond, Labrador: Naturaliste Canadien, v. 86, p. 265-299.
- Bluemle, J.P., 1972, Pleistocene drainage development in North Dakota: Geological Society of America, Bulletin, v. 83, p. 2189-2193.
- Bourne, J.H., 1978, Metamorphism in the eastern and southwestern portions of the Grenville Province, in Metamorphism in the Canadian Shield: Geological Survey of Canada, Paper 78-10, p. 315-328.
- Bridgwater, D., Escher, A., Jackson, G.D., Taylor, F.C. and Windley, B.F., 1973, Development of the Precambrian Shield in west Greenland, Labrador, and Baffin Island: American Association of Petroleum Geologists, Memoir 19, p. 99-116.
- Carver, R.E., 1971, Heavy-mineral separation, in Carver, R.E., ed., Procedures in Sedimentary Petrology, New York, Wiley-Interscience, p. 427-452.
- Christie, A.M., 1952, Geology of the northern coast of Labrador from Grenfell Sound to Port Manvers, Newfoundland: Geological Survey of Canada, Paper 52-22, 16p.
- Clarke, D.B. and Upton, B.G.J., 1971, Tertiary basalts of Baffin Island: field relations and tectonic setting: Canadian Journal of Earth Sciences, v. 8, p. 248-258.
- Cooke, H.C., 1929, Studies of the physiography of the Canadian Shield; 1 mature valleys of the Labrador Peninsula: Royal Society of Canada Transactions, v. 23, sec. iv, p. 19-120.

- Cramez, C., 1977, Geophysical Setting of the Labrador Sea. Aquitaine Company of Canada, unpublished report, 37p.
- Cumming, L.M., 1968, Rivers of the Hudson Bay Lowlands, in Hood, P.J., ed., Earth Science Symposium on Hudson Bay: Geological Survey of Canada, Paper 68-53, p. 144-168.
- Currie, K.L., 1968, Mistastin Lake, Labrador: a new Canadian crater: Nature, v. 220, p. 776-777.
- _____, 1969, Geology of the Mistastin Lake structure, Labrador: Geological Survey of Canada, Paper 69-1A, p. 138-139.
- Cutt, B.J., and Laving, J.G., 1977, Tectonic elements and geological history of south Labrador and Newfoundland continental shelves, Eastern Canada: Canadian Society of Petroleum Geologists, Bulletin, v.25, p. 1037-1053.
- David, M. and Beauchemin, Y., 1975. The correspondence analysis method and a FORTRAN IV program. Geocom Program 10.
- David, M., Campiglio, C. and Darling, R., 1974, Progresses in R- and Q-mode analysis: Correspondence Analysis and its application to the study of geological processes: Canadian Journal of Earth Sciences, v. 11, p. 131-146.
- Deer, W.A., Howie, R.A. and Zussman, J., 1975, An Introduction to the Rock-Forming Minerals: London, Longman Group Ltd., 528p.
- Douglas, R.J.W. (ed), 1970, Geology and Economic Minerals of Canada: Geological Survey of Canada, Economic Geology Report 1, 838p.
- Eastcan Exploration Ltd., 1975a, Well History Report, Eastcan et al., Leif M-48: released to Open File August, 1975 by Department of Energy, Mines and Resources, Ottawa.
- _____, 1975b, Well History Report, Eastcan et al., Gudrid H-55: released to Open File October, 1976 by Department of Energy, Mines and Resources, Ottawa.

- _____, 1976a, Well History Report, Eastcan et al.,
Snorri J-90: released to Open File September, 1977
by Department of Energy, Mines and Resources,
Ottawa.
- _____, 1976b, Well History Report, Eastcan et al.,
Cartier D-70: released to Open File October, 1977
by Department of Energy, Mines and Resources,
Ottawa.
- _____, 1976c, Well History Report, Eastcan et al.,
Freydis B-87: released to Open File August, 1977
by Department of Energy, Mines and Resources,
Ottawa.
- _____, 1978a, Well History Report, Eastcan et al.,
Karlsefni A-13: released to Open File October,
1978 by Department of Energy, Mines and Resources,
Ottawa.
- Embleton, C. and King, C.A.M., 1971, Glacial and Periglacial
Geomorphology: Toronto, MacMillan of Canada, 608p.
- Fahrig, W.F., 1967, Shabogomo Lake map area (23G E 1/2)
Newfoundland, Labrador and Quebec: Geological
Survey of Canada, Memoir 354.
- Folk, R.L., 1974, Petrology of Sedimentary Rocks: Austin
Hemphill Publishing Co., 170p.
- Force, E.L., 1980, The provenance of rutile: *Journal of
Sedimentary Petrology*, v. 50, p. 485-488.
- Frarey, M.J., 1961, Menihok Lakes, Quebec and Newfoundland:
Geological Survey of Canada, Map 1087A.
- Galehouse, J.S., 1971, Point counting, in Carver, R.E., ed.,
Procedures in Sedimentary Petrology, New York,
Wiley-Interscience, p. 385-407.
- Gower, J.C., 1966, Some distance properties of latent root
and vector methods used in multivariate analysis:
Biometrika, v. 53, p. 325-338.
- Grant, A.C., 1972, The continental margin off Labrador and
eastern Newfoundland - morphology and geology:
Canadian Journal of Earth Sciences, v. 9, p.
1394-1430.

- _____, 1975, Geophysical results from the continental margin off southern Baffin Island, in Yorath, C.J., Parker, E.R. and Glass, D.J. eds., Canada's Continental Margins and Offshore Petroleum Exploration: Canadian Society of Petroleum Geologists, Memoir 4, p. 411-431.
- _____, 1980, Problems with plate tectonics: the Labrador Sea: Canadian Society of Petroleum Geologists, Bulletin, v. 28, p. 258-278.
- _____, 1982, Problems with plate tectonic models for Baffin Bay-Narcs Strait; evidence from the Labrador Sea, in Dawes, P.R. and Kerr, J.W., eds., Nares Strait and the Drift of Greenland; a conflict in plate tectonics, Meddelelser om Gronland, Geoscience 8, p. 313-326.
- Greene, B.A., 1974, An outline of the geology of Labrador: Mineral Division, Department of Mines and Energy, Newfoundland, Information Circular 15, 64p.
- Heinrich, E.W., 1965, Microscopic Identification of Minerals: New York, McGraw-Hill Book Co., 414p.
- Henderson, G., Rosenkrantz, A. and Schiener, E.T., 1976, Cretaceous-Tertiary sedimentary rocks of West Greenland, in Escher, H. and Watt, W.S., eds., Geology of Greenland: Geological Survey of Greenland, Copenhagen, p. 340-362.
- Higgs, R., 1977, Provenance of Mesozoic-Cenozoic siliclastic sediments of the Labrador and West Greenland continental margins: M.Sc. Thesis, University of Calgary, Calgary, 169p.
- Hinz, K., Schulter, H-U., Grant, A.C., Srivastava, S.P. Umpleby, D.C., and Woodside, J., 1979, Geophysical transects of the Labrador Sea: Labrador to southwest Greenland: Tectonophysics, v. 59, p. 151-183.
- Hiscott, R.N., 1984, Clay Mineralogy and Clay-Mineral Provenance of Cretaceous and Paleogene Strata, Labrador and Baffin Shelves: Bulletin of Canadian Petroleum Geology, vol. 32, p. 272-280.

- Hubert, J.F., 1962, A zircon-tourmaline-rutile maturity index and the interdependence of the composition of heavy mineral assemblages with the gross composition and texture of sandstone: *Journal of Sedimentary Petrology*, v. 32, p. 440-450.
- _____, 1971, Analysis of heavy-mineral assemblages, in Carver, R.E., ed., Procedures in Sedimentary Petrology, New York, Wiley-Interscience, p. 453-478.
- Ives, J.D., 1957, Glaciation of the Torngat Mountains, Northern Labrador: *Arctic*, v. 10, p. 67-87.
- Keen, C.E., 1979, Thermal history and subsidence of rifted continental margins - evidence from wells off Nova Scotia and Labrador shelves: *Canadian Journal of Earth Sciences*, v. 16, p. 505-522.
- _____ and Hyndman, R.D., 1979, Geophysical review of the continental margins of eastern and western Canada: *Canadian Journal of Earth Sciences*, v. 16, p. 712-747.
- Kerr, J. Wm, 1967, A submerged continental remnant beneath the Labrador Sea: *Earth and Planetary Science Letters*, v. 2, p. 283-289.
- _____, 1981, Evolution of the Canadian Arctic Islands - a Transition between the Atlantic and Arctic Oceans, in Nairn, A.E.M., Churkin, M. Jr., and Stelhi, F.G., eds., *The Ocean Basins and Margins*, vol. 5, *The Arctic Ocean*: New York, Plenum Publishing Corporation, p. 105-199.
- King, A.F. and McMillan, N.J., 1975, A mid-Mesozoic breccia from the coast of Labrador: *Canadian Journal of Earth Sciences*, v. 12, p. 44-51.
- Klose, G.W., Malterre, E., McMillan, N.J., and Zinkin, C.G., 1982, Petroleum exploration, offshore Baffin Island, northern Labrador Sea, Canada, in Embry, A.F. and Balkwill, H.R., eds., *Arctic Geology and Geophysics*: *Canadian Society of Petroleum Geologists, Memoir 8*, p. 233-244.
- Klovan, J.E. and Imbrie, J., 1971, An algorithm and FORTRAN IV Program for large scale Q-mode analysis: *Mathematical Geology* 3, p. 61-67.

Knight, I. and Morgan, W.C., 1977, Stratigraphic subdivision of the Aphebian Ramah Group, northern Labrador: Geological Survey of Canada, Paper 77-15, 31p.

_____, 1981, The Aphebian Ramah Group, Northern Labrador, in Campbell, F.H.A., ed., Proterozoic Basins of Canada: Geological Survey of Canada, Paper 81-10, p. 313-330.

Kristofferson, Y., 1978, Sea-floor spreading and the early opening of the North Atlantic: Earth and Planetary Science letters, v. 38, p. 273-290.

_____, and Talwani, M., 1977, Extinct triple junction south of Greenland and the Tertiary motion of Greenland relative to North America: Geological Society of America, Bulletin, v. 88, p. 1037-1049.

Larsen, E.S. and Berman, H., 1934, The microscopic determination of the non-opaque minerals (2nd ed.): United States Geological Society, Bulletin, no. 848, 266p.

Laughton, A.S., 1971, South Labrador Sea and the evolution of the North Atlantic: Nature, v. 232, p. 612.

_____, 1972, The southern Labrador Sea - a key to the Mesozoic and early Tertiary evolution of the North Atlantic (DSDP leg 12), in Initial Reports of Deep Sea Drilling Project 12, U.S. Government Printing Office, Washington, D.C., p. 1155-1179.

Lebart, L., Morineau, A. and Warwick, K., 1984, Multivariate Descriptive Statistical Analysis, Correspondence Analysis and Related Techniques for Large Matrices: New York, John Wiley and Sons, 231p.

Le Pichon, X., Hyndman, R.D. and Pautot, G., 1971, Geophysical study of the opening of the Labrador Sea: Journal of Geophysical Research, v. 76, p. 4724-4743.

Martin, R., 1973, Geological history of Baffin Bay - continental drift before sea-floor spreading and the exploration for hydrocarbons, in Hood, P.J., ed., Earth Science Symposium on Offshore Eastern Canada: Geological Survey of Canada, Paper 71-23, p. 599-620.

- Mason, B. and Berry, L.G., 1968, Elements in Mineralogy: San Francisco, W.H. Freeman and Company, 550p.
- McMillan, N.J., 1973b, Shelves of Labrador Sea and Baffin Bay, Canada: Canadian Society of Petroleum Geologists, Memoir 1, p. 473-517.
- McWhae, J.R.H. and Michel, W.F.E., 1975, Stratigraphy of Bjarni H-81 and Leif M-48, Labrador Shelf: Canadian Society of Petroleum Geologists, Bulletin, v. 23, p. 361-382.
- _____, Elie, R., Laughton, K.C. and Gunther, P.R., 1980, Stratigraphy and petroleum prospects of the Labrador Shelf: Canadian Society of Petroleum Geologists, Bulletin, v. 28, p. 460-488.
- Meneley, R.A., 1986, Oil and gas fields in the east coast and arctic basins of Canada, in Halbouty, M.T., ed., Future Petroleum Provinces of the World: American Association of Petroleum Geologists, Memoir 40, p. 143-176.
- Miall, A.D., Balkwill, H.R., Hopkins, W.S.Jr., 1980, Cretaceous and Tertiary sediments of Eclipse Trough, Bylot Island Area, Arctic Canada, and their regional setting: Geological Survey of Canada, Paper 79-23, 20p.
- Milner, H.B., 1962, Sedimentary Petrography, vol. II - Principles and Applications, 4th edition: London, George Allen & Unwin Ltd., 715p.
- Miyashiro, A., 1975, Metamorphism and Metamorphic Belts: London, George Allen & Unwin Ltd., 492p.
- Morgan, W.C., 1975, Geology of the Precambrian Ramah Group and basement rocks in the Nachvak Fiord-Saglek Fiord area, North Labrador: Geological Survey of Canada, Paper 74-54, 42p.
- _____, 1979, Nachvak Fiord-Ramah Bay, Newfoundland-Quebec: Geological Survey of Canada, Map 1469A.
- Muller, G., 1967, Sedimentary petrology, Part I, Methods in Sedimentary Petrology, translated by Hans-Ulrich Schmincke, Hafner Publishing Co., 283p.

- Pelletier, B.R., 1968, Submarine physiography, bottom sediments and models of sediment transport, in Hood, P.J., ed., Earth Science Symposium on Hudson Bay: Geological Survey of Canada, Paper 68-53, p. 100-135.
- Pettijohn, F.J., Potter, P.E. and Siever, R., 1972, Sand and Sandstone: New York, Springer-Verlag, 618p.
- Potter, P.E., 1955, The petrology and origin of the Lafayette gravel, Part 1, mineralogy and petrology: Journal of Geology, vol. 63, p. 1-38.
- Poulsen, V., 1966, An occurrence of Lower Paleozoic rocks within the Precambrian terrain near Sukkertoppen: Geological Survey of Greenland, Report 11, p. 26.
- Powers, M.C., 1953, A New Roundness Scale for Sedimentary Particles: Journal of Sedimentary Petrology, vol. 23, p. 117-119.
- Price, R.A. and Douglas, R.J.W. (eds.), 1972, Variations on Tectonic Styles in Canada: Geological Association of Canada, Special Paper 11, 688p.
- Rahmani, R.A. and Lerbekmo, J.F., 1975, Heavy-mineral analysis of Upper Cretaceous and Paleocene sandstones in Alberta and adjacent areas of Saskatchewan: Geological Association of Canada, Special Paper 13, p. 607-632.
- Rashid, M.A., Purcell, L.P. and Hardy, I.A., 1980, Source rock potential for oil and gas of the east Newfoundland and Labrador areas, Canadian Society of Petroleum Geologists, Memoir 6, p. 589-608.
- Rittenhouse, G., 1943, Transportation and deposition of heavy minerals: Geological Society of America, Bulletin, v. 54, p. 1725-1780.
- Roots, W.D. and Srivastava, S.P., 1984, Origin of the marine magnetic quiet zones in the Labrador and Greenland Seas: Marine Geophysical Research, v. 6, p. 395-408.
- Royden, L. and Keen, C.E., 1980, Rifting process and thermal evolution of the continental margin of eastern Canada determined from subsidence curves: Earth and Planetary Science letters, v. 51, p. 343-361.

- Rubey, W.W., 1933, The size-distribution of heavy minerals within a water-laid sandstone: *Journal of Sedimentary Petrology*, v. 3, p. 3-29.
- Russell, D., 1941, Tables for the identification of detrital minerals III anisotropic "heavy" minerals. Report of the Committee on Sedimentation 1940-1941 National Research Council.
- Ryan, A.B., Martineau, Y., Korstgaard, J., and Lee, D., 1984, The Archean-Proterozoic Boundary in Northern Labrador: Report 2 in: *Current Research, Newfoundland Department of Mines and Energy, Mineral Development Division, Report 84-1*, p. 545-551.
- Schneider, E.D., 1972, Sedimentary evolution of rifted continental margins: *Geological Society of America, Memoir 132*, p. 109-118.
- Schuchert, C. and Dunbar, C.O., 1934, Stratigraphy of Western Newfoundland: *Geological Association of America, Memoir 1*, 123p.
- Srivastava, S.P., 1978, Evolution of the Labrador Sea and its bearing on the evolution of the North Atlantic: *Geophysical Journal of the Royal Astronomical Society*, v. 52, p. 313-357.
- _____, 1985, Evolution of the Labrador Sea and its implications to the motion of Greenland along Nares Strait: *Tectonophysics*, v. 114, p. 29-53.
- _____, Falconer, R.K.H and MacLean, B., 1981, Labrador Sea, Davis Strait, Baffin Bay: geology and geophysics - a review, in Kerr, J. Wm. and Fergusson, A.J., eds., *Geology of the North Atlantic Borderlands: Canadian Society of Petroleum Geologists, Memoir 7*, p. 333-398.
- Stevenson, I.M., 1970, Rigolet and Groswater Bay map areas, Newfoundland (Labrador): *Geological Survey of Canada, Paper 69-48*.
- Stockwell, C.H., McGlynn, J.C., Emslie, R.F., Sandford, B.V., Norris, A.W., Donaldson, J.A., Fahrig, W.F. and Currie, K.L., 1970, Geology of the Canadian Shield, in Douglas, R.J.W., ed., *Geology and Economic Minerals of Canada: Geological Survey of Canada, Economic Geology Report 1*, p. 43-150.

- Taylor, F.C., 1981, Precambrian Geology of the Canadian North Atlantic Borderlands in Kerr, J. Wm and Fergusson, A.J., eds., Geology of the North Atlantic Borderlands: Canadian Society of Petroleum Geologists, Memoir 7, p. 11-30.
- _____, and Dence, M.R., 1969, A probable meteorite origin for Mistastin Lake, Labrador: Canadian Journal of Earth Sciences, v. 6, p. 38-45.
- Teil, H., 1975, Correspondence factor analysis: an outline of its method: Journal of Mathematical Geology, v. 7, No. 1, p. 3-12.
- Total Eastcan Ltd., 1980, Well History Report, Total Eastcan Skolp E-07: released to Open File, 1980 by Department of Energy, Mines and Resources, Ottawa.
- Umpleby, D.C., 1979, Geology of the Labrador Shelf: Geological Survey of Canada, Paper 79-13, 34p.
- van Andel, T.H., 1959, Reflections on the interpretation of heavy mineral analyses: Journal of Sedimentary Petrology, v. 29, p. 153-163.
- van der Linden, W.J.M., 1975, Crustal attenuation and sea-floor spreading in the Labrador Sea: Earth and Planetary Science Letters, v. 27, p. 409-423.
- Vitanage, P.W., 1957, Studies of zircon types in Ceylon Pre-Cambrian complex: Journal of Geology, v. 65, p. 117-138.
- Vogt, P.R., Avery, O.E., Morgan, W.J., Johnson, G.L., Schneider, E.D., and Higgs, R.H., 1969, Morphology, magnetic anomalies and evolution of the Northeast Atlantic and Labrador Sea, Part III - Evolution: EOS Transactions of the American Geophysical Union, vol. 50, p. 189.
- Wade, J.A., Grant, A.C., Sanford, B.V., and Barss, M.S., 1977, Basement structures, eastern Canada and adjacent areas: Geological Survey of Canada, Map 1400A (1:200,000).
- Wardle, R.J. and Bailey, D.G., 1981, Early Proterozoic sequences in Labrador, in Campbell, F.H.A., ed., Proterozoic Basins of Canada: Geological Survey of Canada, Paper 81-10, p. 331-358.

- Williams, H. and Stevens, R.K., 1969, Geology of Belle Isle-northern extremity of the deformed Appalachian miogeosynclinal belt: Canadian Journal of Earth Sciences, v. 6, p. 1145-1157.
-
- _____, 1974, The ancient continental margin of eastern North America, in Burke, C.A. and Drake, C.L., eds., The Geology of Continental Margins, New York, Springer-Verlag, p. 781-796.
- Wilson, J.T. and Clarke, D.B., 1965, Geological expedition to Capes Dyer and Searle, Baffin Island, Canada: Nature, v. 205, p. 349-350.
- Wyatt, M., 1954, Zircons as provenance indicators: American Mineralogist, v. 39, p. 983-990.
- Ziegler, P.A., 1969, The Development of Sedimentary Basins in Western and Arctic Canada: Alberta Society of Petroleum Geologists, 29p.
- Zinkernagel, U., 1978, Cathodoluminescence of quartz and its application to sandstone petrology, in Fuchtbauer, H., Lisitzyn, A.P., Milliman, J.D., and Seibold, E., eds., Contributions to Sedimentology, No. 8, 69p.

APPENDIX 1 - Laboratory Techniques

(1) HEAVY MINERAL SEPARATION

Apparatus

- nalgene tubes (with dimples made approximately 2.5cm from base)
- tube holder
- centrifuge
- scintered glass funnels
- ashless filter papers
- vacuum pump
- vacuum flask
- dewar (for liquid nitrogen)
- 3-tube holder (for dewar)

Chemicals

- tetrabromoethane
- acetone or methanol solvent
- liquid nitrogen

Technique

1. Fill Nalgene tubes with 2gms of sample cover and label (ball point pen on masking tape, wrapped around the tube, withstood effects of the solvent).
2. Fill the tube with 50ml. of tetrabromoethane and cap tightly.
3. Centrifuge each sample for 20 minutes at 3500rpm.
4. Partially submerge the centrifuged samples in liquid nitrogen until frozen. Using the solvent, thaw the portion of the tetrabromoethane containing the light fraction if necessary, pouring the heavy liquid, solvent and minerals onto a filter paper lined scintered glass funnel. Continue this procedure until all light fractions have been poured off.
5. Repeat step 4 thawing the plug containing the heavy minerals (pouring off all the light fractions then repeating with the heavy fractions reduces contamination). The plug containing the heavy minerals may be left to thaw naturally if time permits.

(2) CLEANING HEAVY LIQUID

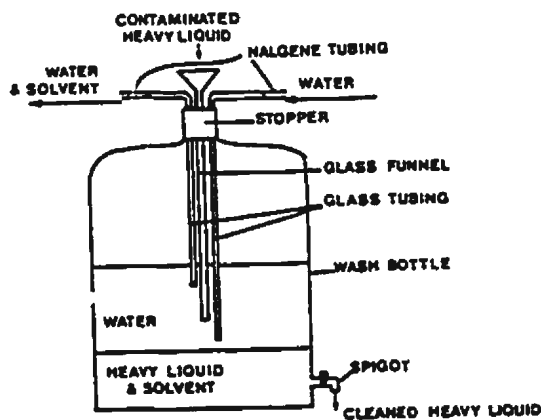
Apparatus

- wash bottle
- stopper
- spigot
- nalgene tubing
- glass tubes
- glass funnel
- water supply
- sink (to dispose of water and solvent)

Technique

1. Set up apparatus as shown in figure.
2. Fill the wash bottle with water.
3. Pour contaminated tetrabromoethane (+ acetone or methanol) in funnel, being certain to keep the level of the heavy liquid below the end of the funnel and a layer of water on top of the heavy liquid.
4. Turn on input water tap and regulate input to match output so that heavy liquid is not forced back up the funnel. If the level of the input tube is kept close to the surface of the heavy liquid, some agitation of the heavy liquid is assured.
5. Test specific gravity of the clean tetrabromoethane prior to use to assure its cleanliness.

Note: If methanol is used as the solvent, when the contaminated heavy liquid comes in contact with water, the liquid becomes white and milky. When the liquid is clear, the heavy liquid is cleaned.



(3) IRON OXIDE STAIN REMOVAL

Apparatus

- 50ml beakers
- Braun sonic disaggregator
- pipettes
- vacuum flask
- scintered glass funnels
- ashless filter papers
- ring stand

Chemicals

- stannous chloride Sn_2Cl
- HCL (10ml concentrated)
- distilled water

Formula

- $\text{SN}_2\text{Cl} + \text{H}_2\text{O} + \text{HCL}$

Technique

1. Soak samples in stannous chloride solution for 12 hours.
2. Add enough distilled water to make 20ml.
3. Place beaker on ring stand with tip of disaggregator probe at 2.5 - 3cm into the liquid.
4. Run disaggregator for 3 minutes initially, continuing in 1 minute intervals until grains are clean.
5. Repeated rinsing and pipetting of the cleaning solution, taking care not to pipette the sample itself, was used to remove the precipitate formed during cleaning.
6. Finally, the sample was poured into a filter paper lined scintered glass funnel and thoroughly washed, and left to dry.

This procedure was followed for both heavy and light fractions.

APPENDIX 2 - Weights of Entire Heavy Mineral Suites
and Magnetics of Samples Studied

| | Weight of Entire Sample (in grams) | Weight of Magnetics (in grams) |
|------------------|---|--------------------------------------|
| <u>Karlsefni</u> | | |
| 2188 | 0.0596 | 0.0032 |
| 2211 | 0.0353 | 0.0034 |
| 2235 | 0.0289 | 0.0020 |
| 2299 | 0.0445 | 0.0028 |
| 2336 | 0.0195 | 0.0005 |
| 2374 | 0.0144 | 0.0122 |
| 2400 | 0.0065 | 0.0016 |
| 4128 | 0.1152 | 0.0092 |
| 4139 | 0.0138 | 0.0019 |
| <u>Skolp</u> | | |
| 600 | 0.0886 | 0.0119 |
| 750 | 0.0168 | 0.0017 |
| 900 | 0.1748 | 0.0203 |
| 950 | 0.2597 | 0.0180 |
| 1000 | 0.1078 | 0.0146 |
| 1300 | 0.0032 | 0.0002 |
| 1700 | 0.0339 | 0.0005 |
| 1850 | 0.0056 | 0.0004 |
| 2200 | 0.0346 | 0.0034 |
| 2750 | 0.0018 | 0.0006 |
| 2950 | 0.0115 | 0.0013 |
| <u>Snorri</u> | | |
| 1789 | 0.0046 | 0.0032 |
| 1832 | 0.0207 | 0.0026 |
| 1850 | 0.0196 | 0.0111 |
| 1868 | 0.0278 | 0.0109 |
| 1887 | 0.0055 | 0.0002 |
| <u>Gudrid</u> | | |
| 2178 | 0.1167 | 0.0144 |
| 2230 | 0.0553 | 0.0551 |
| 2318 | 0.0515 | 0.0054 |
| 2355 | 0.0390 | 0.0111 |

Appendix 2 - Weights of Entire Heavy Mineral Suites
and Magnetics of Samples Studied - cont'd

| | Weight of Entire Sample (in grams) | Weight of Magnetics (in grams) |
|----------------|---|--------------------------------------|
| <u>Cartier</u> | | |
| 1256 | | |
| 1274 | 0.0405 | 0.0037 |
| 1286 | 0.1106 | 0.0032 |
| 1305 | 0.0157 | 0.0024 |
| 1323 | 0.0600 | 0.0104 |
| 1353 | 0.0251 | 0.0040 |
| 1710 | 0.1750 | 0.0246 |
| 1774 | 0.0952 | 0.0075 |
| 1817 | 0.2310 | 0.1043 |
| 1847 | 0.0439 | 0.0140 |
| 1859 | 0.0199 | 0.0135 |
| <u>Leif</u> | | |
| 1259 | 0.0923 | 0.0045 |
| 1270 | 0.0623 | 0.0034 |
| 1286 | 0.0230 | 0.0025 |
| 1673 | 0.0230 | 0.0025 |
| 1682 | 0.0709 | 0.0575 |
| 1691 | 0.1596 | 0.0192 |
| <u>Freydis</u> | | |
| 908 | 0.0200 | 0.0042 |
| 930 | 0.0451 | 0.0052 |
| 969 | 0.0136 | 0.0026 |
| 994 | 0.0145 | 0.0021 |
| 1411 | 0.0405 | 0.0129 |
| 1436 | 0.0536 | 0.0140 |
| 1445 | 0.0810 | 0.0118 |
| 1463 | 0.0576 | 0.0083 |
| 1475 | 0.0658 | 0.0102 |
| 1500 | 0.0493 | 0.0150 |

18

18

18

